HIGHWAY RESEARCH RECORD

Number 4

Highway Safety

5 Reports

Presented at the
42nd ANNUAL MEETING
January 7-11, 1963

HIGHWAY RESEARCH BOARD
of the
Division of Engineering and Industrial Research
National Academy of Sciences—
National Research Council
Washington, D. C.
1963

Department of Traffic and Operations

Fred W. Hurd, Chairman
Director, Bureau of Highway Traffic
Yale University, New Haven, Connecticut

COMMITTEE ON HIGHWAY SAFETY RESEARCH

Charles W. Prisk, Chairman
Deputy Director, Office of Highway Safety
U. S. Bureau of Public Roads, Washington, D. C.

Earl Allgaier, Research Engineer, Traffic Engineering and Safety Department, American Automobile Association, Washington, D. C.
John E. Baerwald, Professor of Traffic Engineering, University of Illinois, Urbana
J. Stannard Baker, Director of Research and Development, Northwestern University, Traffic Institute, Evanston, Illinois
Robert Brenner, Engineer-Statistician, Department of Engineering, University of California, Los Angeles
Siegfried M. Breuning, Civil Engineering Department, Michigan State University, East Lansing
Leon Brody, Director of Research, Center for Safety Education, New York University, New York, New York
Basil R. Creighton, Assistant to Executive Director, American Association of Motor Vehicle Administrators, Washington, D. C.
A. Beecher Greenman, Chas. H. Sells, Inc., Babylon, Long Island, New York
Charles J. Keese, Civil Engineering Department, Texas Transportation Institute, Texas A & M College, College Station
John C. Kohl, Assistant Administrator, Office of Transportation, Housing and Home Finance Agency, Washington, D. C.
C. F. McCormack, Alan M. Voorhees & Associates, Washington, D. C.
J. P. Mills, Jr., Traffic and Planning Engineer, Virginia Department of Highways, Richmond
G. D. Sontheimer, Director of Safety, American Trucking Associations, Washington, D. C.
Kenneth A. Stonex, Assistant Engineer-in-Charge, Technical Liaison Section, Engineering Staff, General Motors Corporation, GM Technical Center, Warren, Michigan
S. S. Taylor, General Manager, Department of Traffic, Los Angeles, California
Wilbur M. White, Highway Safety Service, Hillsboro, Ohio
John L. Whitelaw, Librarian, Highway Traffic Safety Center, Michigan State University, East Lansing
Ross G. Wilcox, Highway Engineer, Portland Cement Association, Chicago, Illinois

Contents

Correlates of 30-MPH Intersection Collisions

DERWYN M. SEVERY, Research Engineer, Institute of Transportation and Traffic Engineering, University of California, Los Angeles

Two automobile intersection collision experiments were conducted under identical crash conditions to evaluate data reproducibility and provide a basis for studying performance differences accompanying changes in important subvariables. Studies were made of collision performance as a function of whether the cars had been involved in a previous, more severe impact. Comparison of vehicle dynamics, skid and debris patterns, damage patterns, and cost to repair is provided. Average coefficients of friction operating during specific postcontact spin-out trajectories of vehicles were calculated, and related findings discussed. In addition, the difference between laminated and tempered side-window glass for the struck car was evaluated for this particular collision exposure.

Triaxial accelerometers, mounted in the heads and chests of anthropometric dummies, safety belt tensiometers and high-speed photography provided the principal sources of recorded data. An IBM 7090 computer facilitated data reduction. The relative performances of lap belt vs combination shoulder and lap belts were studied for simulated adult motorists; child and infant dummies were used to evaluate special restraining devices.

• DURING a two-year period 14 intersection-type collision experiments were conducted for the purpose of obtaining detailed information on the dynamic interaction between motorist and vehicle structure (Fig. 1). This series of collisions represented 28 car-damage exposures for the six available 1960 Plymouth four-door sedans. It was necessary, therefore, to repair these cars following each collision. Three positions of impact and four speeds of impact were selected to represent intersection collision configurations (Fig. 2). The 30-mph collision into the center doorpost (Experiment 57) was selected for a repeat study for correlation purposes. The relation these experiments, X-57 and X-62, bear to the entire Series II experiments is shown in the figure; the X-57, X-62 impact configuration is shown cross-hatched.

(Experiment 57, or X-57, refers to one of 64 full-scale collision experiments conducted at UCLA during the years between 1949 and 1963. These experiments have been numbered consecutively, starting with Experiment 1 conducted in 1949. The correlate Experiments 57 and 62, reported by this paper, were conducted in 1961 and 1962, respectively.)

At the conclusion of the Series II experiments, X-62 was conducted to obtain data that could be used to establish the correlation of collision dynamics thus obtained with similar data from X-57. This comparison provided data from two 30-mph center-side impact experiments of identical collision configuration, but involving cars having different histories of prior impacts. The striking car for Experiment 57 had not been used previously as a striking car and had been struck at its left front side in a previous 20-mph experiment. The struck car for Experiment 57 had been used as a striking car in a 20-mph rear-side collision and as a struck car in both front-side and rear-side collisions at 10 mph. The procedure of conducting a series of experiments at one speed (for example, 20 mph) and then scheduling each of these cars once again, following re-

Paper sponsored by Committee on Highway Safety Research.

pairs, to a 30-mph impact was based on the postulation that the effect of an earlier low-speed impact on the car's collision performance at a higher speed would be negligible. Both cars used for the 30-mph correlate Experiment 62 had been repaired, following exposure to an earlier 40-mph collision. In addition, these cars had previously been used for 10-, 20-, and 30-mph collisions but, of course, had been repaired following each of these experiments.

This review of collision histories establishes that the prior exposures for the cars used in Experiment 57 were minor compared with the prior exposures of the cars used

Figure 1. Intersection collision.

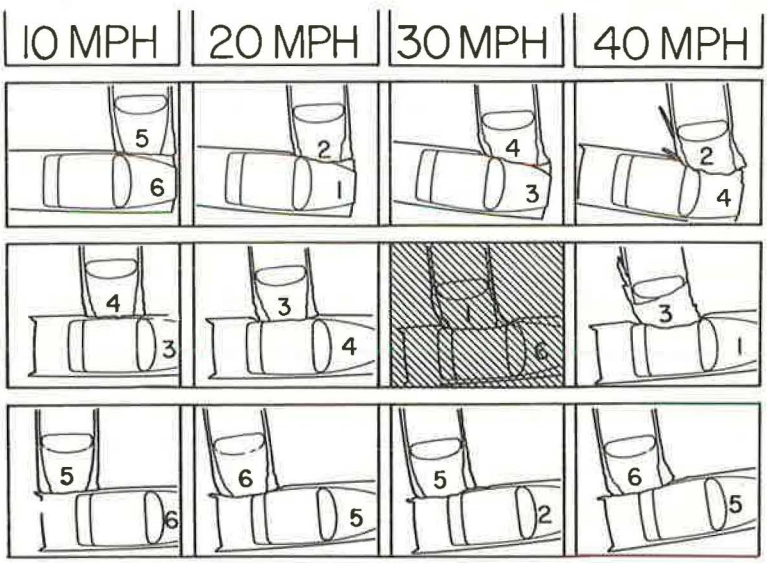

Figure 2. Automobile assignment schedule (correlate Experiments 57 and 62 cross-hatched).

in Experiment 62. The comparative data to be presented from these two experiments show that for right-angle collisions up to 40 mph, a car's collision performance is essentially unimpaired by damage sustained from previous collisions, providing quality repair work has been performed.

Perhaps more important than determining the validity of using repaired vehicles in the Series II experiments was the opportunity that the correlate experiment provided for evaluating other factors. Many occupant environmental conditions could be modified for this correlate experiment without compromising the basic purpose of the experiments.

EQUIPMENT AND FACILITIES

Although described in detail by prior publications (1, 2), a brief explanation of physical facilities and equipment required for these experiments will assist in understanding the discussions of findings to follow. A decommissioned airstrip at the U.S. Naval Station, Long Beach, Calif., was made available by the Navy for UCLA's collision research. On the airstrip's level asphalt surface, an aluminum monorail guide track system was anchored to provide directional control for the crash vehicles. Other operational systems described elsewhere (1, 2) were incorporated, permitting side-impact collision experiments to be conducted under completely controllable and yet absolutely realistic conditions. A mobile electronics laboratory, a mobile machine shop, and an operations van provide on-the-scene research support facilities. The Chrysler Corporation donated the six 1960 Plymouth four-door sedans used as collision cars, two station wagons serving as mobile instrumentation recording vehicles, and a Chrysler Model 300 G as a tow vehicle for accelerating the crash cars to their impact positions. Other equipment and facilities required for this research were provided in part by the University of California and, in substantial measure, by a research grant from the U.S. Public Health Service.

PROCEDURES AND INSTRUMENTATION

A detailed explanation of experimental procedures and instrumentation systems is provided in prior publications (1, 2); however, a brief explanation will assist to a better understanding of the discussion of the findings. A tow car is connected to each of the two crash cars by a steel cable passing around sheaves (Fig. 3). The length of the cable to each crash car is adjusted to assure their proper position at the time of collision. The crash cars receive directional control from their slipper-shoe connection with the monorail guide track they straddle as they are pulled toward the position of impact. Both constraints—the towing and directional control—are released prior to impact. High-speed cameras and other photographic devices are positioned as shown by the black squares in Figure 2; their individual specifications are given in Table 1. In addition, each car and its occupants are instrumented with transducers whose outputs are transmitted to an instrument recording car by way of a 100-ft electrical cable. Each instrument car carried an 18-channel recording oscillograph and remote controls for starting cameras located on the crash cars and to operate the crash car's emergency braking system.

An operation plan is developed for each series of collision experiments and carries an appendix that describes in detail the various phases of preparation necessary before an experiment can be conducted. Only by meticulously adhering to the details prescribed for each technical division of the project is it possible to conduct these complex operations without hazard of loss of critical data. Comprehensive photographic coverage provides essential positional correlation for the oscillographic data. In addition, these 30 photographic devices record observations not provided by other instrumentation, and therefore, are also primary sources of data.

ANALYSIS AND FINDINGS

Force and Acceleration Data

The intersection collision is among the most complex of collision exposures. This is because of the multivariant conditions that exist. The principal variables requiring

consideration are speed, angle of impact, eccentricities of impact, and the structural properties and weight of the vehicles involved. All these variables were held constant for the correlate collisions presented in this paper for the purposes previously described. Triaxial accelerometers were used to provide resultant acceleration data for the car and occupants.

Figures 4 and 5 show time after impact, in seconds, on the abscissa located to the right of the struck car diagram. The transducer patterns are drawn to scale in correspondence with this time axis and with peak values shown to enable the value of any ordinant position to be computed. In addition, the seated positions of the adult, child, and infant dummies are shown for each car.

Figures 4 and 5 show the striking car for both Experiments 57 and 62 registered a 10G peak acceleration; the struck car for Experiment 57 registered 16G compared with 17G for the struck car of Experiment 62. This close correlation supports the value of

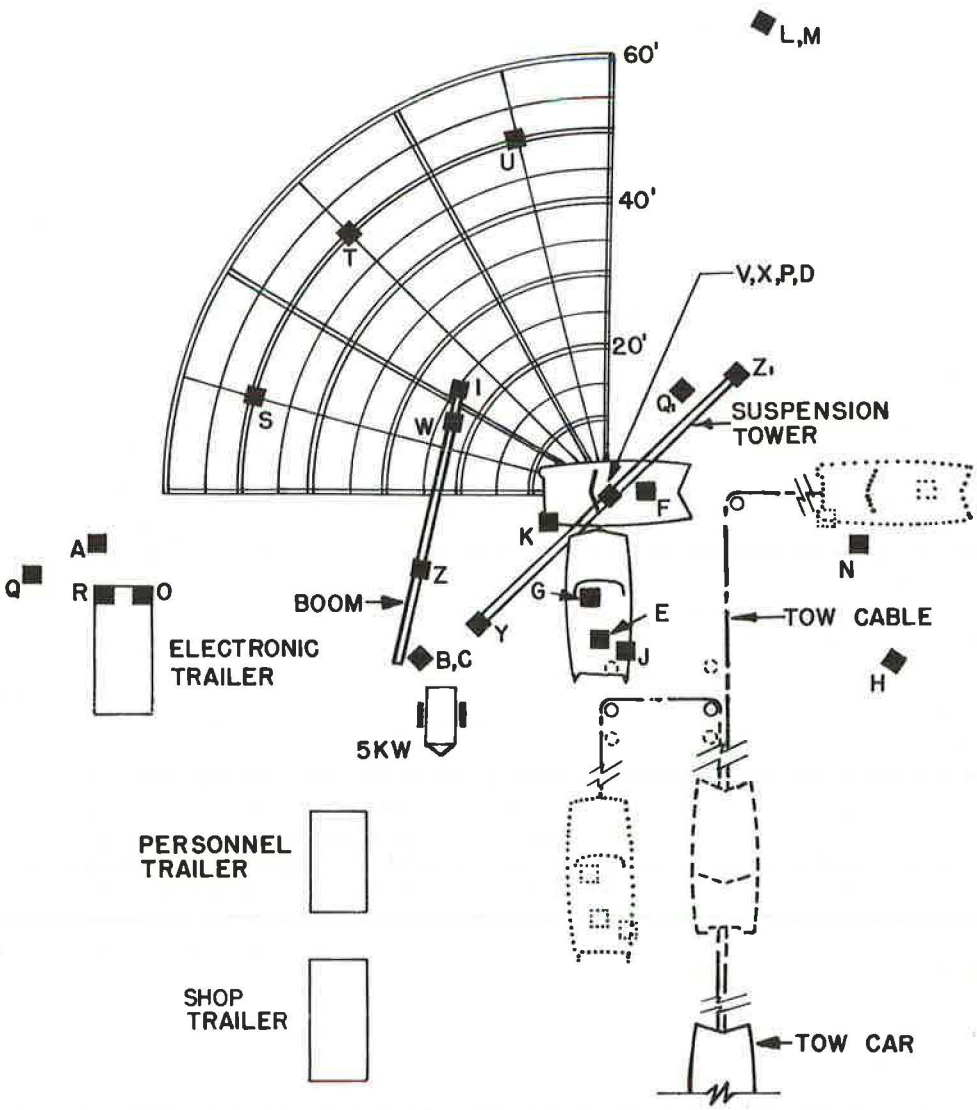

Figure 3. Vehicle control and photographic systems.

TABLE 1

INSTRUMENTATION

Device	Purpose	Location	Specifications
Camera:			
High-speed	Displacement/time for automobile and dummy kinematic data	Cameras A, B, C, and D (Fig. 3)	Eastman I & II and Fastax WF-3, 16-mm Kodak Ektachrome ER 7257, 600-1,000 frames per sec (f/s)
Moderately high-speed	Displacement/time for automobile and dummy kinematic data	Cameras E, F, G, J, K, L, M, N, and O (Fig. 3)	8-Photosonics 1B, Traid, and 1-Urban Engr. Co. GSAP MBH 200-16, high G tolerance 200 f/s, 16-mm Kodak Ektachrome 7257
Standard	General and backup photographic coverage	Cameras P, Q, R, S, T, U, V, and W (Fig. 3)	1-K-200 with 170° lens at 64 f/s; 2 Bolex, Zoom lens at 24 f/s; 4 GSAPS wide angle lens at 64 f/s; 1 Cine Special, 1-in. lens at 64 f/s; all 16-mm Ektachrome 7255
Special	Larger format; sequentials photographs of collision events	Camera H on 20-ft tower. Camera I on 40-ft boom tower (Fig. 3)	Hulcher Model 102, 20 f/s 70-mm Super Anscochrome (Camera rotated 90° to permit cine-reduction) Camera I, Bell & Howell Eyemo, 48 f/s Ektachrome ER 5257; both cameras have rotating shutters
Still	Precision-timed photographs	Cameras X, Y, Z, Z_1 (Fig. 3)	Super Speed Graflex 4 × 5 Ektachrome 1/1,000-sec electronically controlled to fire at precalculated millisec after contact
Calibrated references	A calibrated and fixed reference during impact	Near impact center	¼-by 6-by 96-in. plywood, vertical 4-ft posts and ropes calibrated yellow and black alternate 1-ft increments, positioned both vertically and horizontally
Reference targets	Precision photographic references for micromotion analysis	On points of interest for both car and occupants.	5-by 2-in. diamond-shaped yellow and black targets
Electrical accelerometer	Sensing of acceleration	For both vehicles triaxial accelerometers at right side station-9 frame; driver's and passenger's chests, driver's head	B & F LF 50-50 and LF 50-100; Statham A 38 a-60-350 and AE-100-350
Seat belt tensiometer	Sensing belt loads	Between floor pan anchorage and belt webbing for lap belt and between passenger shoulder and door post anchorage for passenger shoulder belt	See (1) for dual--type strain gage description
Recording oscillograph	Amplitude-time records of transducer signals	Carried by instrument recording vehicle	18-channel Consolidated Electrodynamics oscillograph, type 5-114 P2 with related converter and power supply
Electronic delay timers	Precision timing for still photography	Electric pressure pads near impact center	200- and 500-millisec time delay devices built by ITTE
Photographic oscillographic synchronization unit	Zero time (vehicle contact); flash bulb for film and pulse for oscillograph	Pressure switches between car contacting surfaces and flash bulb photocell on car hoods	See (1)
Pulse generator	Timing for hi-speed cameras	Between camera and power source	Wallensak, 100 and 1,000 cps
Auxiliary timer	Backup timing	Near impact center in view of all cameras	Rotating yellow and black drum; constant-speed 1,740-rpm motor
Wheel revolution counter	Car speed data	Right rear wheel of both vehicles	Induction pickup for oscillograph
Tire-skidmark tracer	Identification of which tires generated skids	On each tire-rib, ¼ in. from road surface	Artist-type oil paint deposits
Deflection recorders	Measurements of differential motion of body and door latch components	Approximately 20 positions on doors and door latches	2½-in. bronze stylus arm bracket on car body, door on latch with stylus spring loaded against carbon-blackened polished chrome or glass plate, secured to adjacent member
Polar coordinate grid	Position data for vehicles from point of impact to positions of rest	On asphalt surface at test site	Yellow traffic marker paint on asphalt (Fig. 3)

carefully controlled collision experiments and establishes that prior collision exposure of a car will not significantly alter its collision performance, provided it has been properly repaired.

Not all the positions monitored by instrumentation in Experiment 57 were exactly repeated in Experiment 62. For example, in Experiment 57 the front seat passenger of the striking car was instrumented for chest acceleration and combination shoulder strap and lap belt load. In Experiment 62, this same dummy was instrumented for lap belt force data only. His triaxial chest transducers were transferred to the three-year-old child standing behind him in order to provide initial acceleration data for children undergoing this type of exposure. A similar repositioning of transducers from the chest of the passenger for the struck car in Experiment 57 was made for Experiment 62 to provide the three-year-old in the struck car with chest transducer instrumentation.

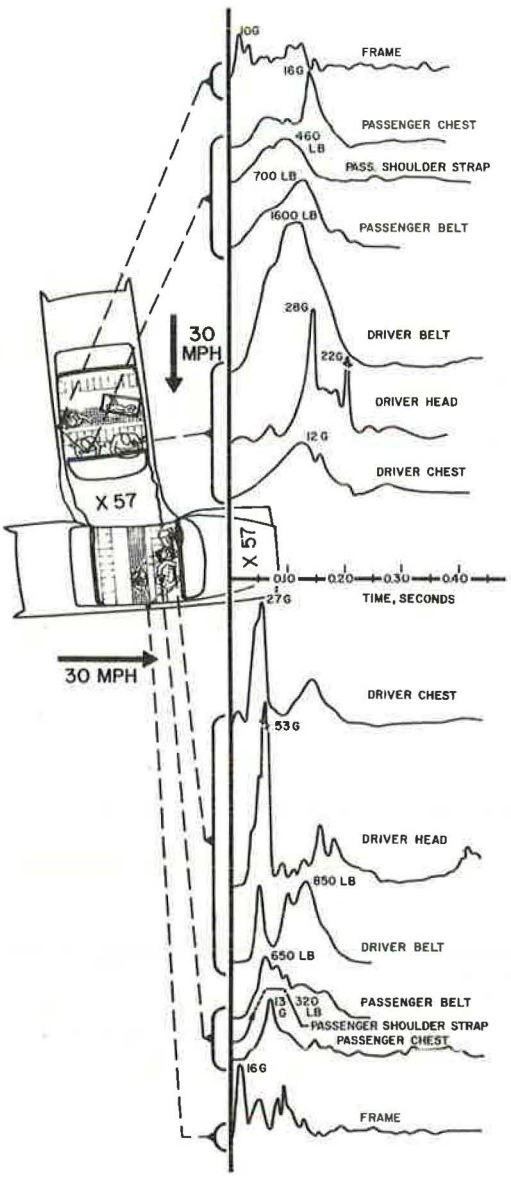

Figure 4. Transducer patterns, X-57, center-side impact, 30 mph.

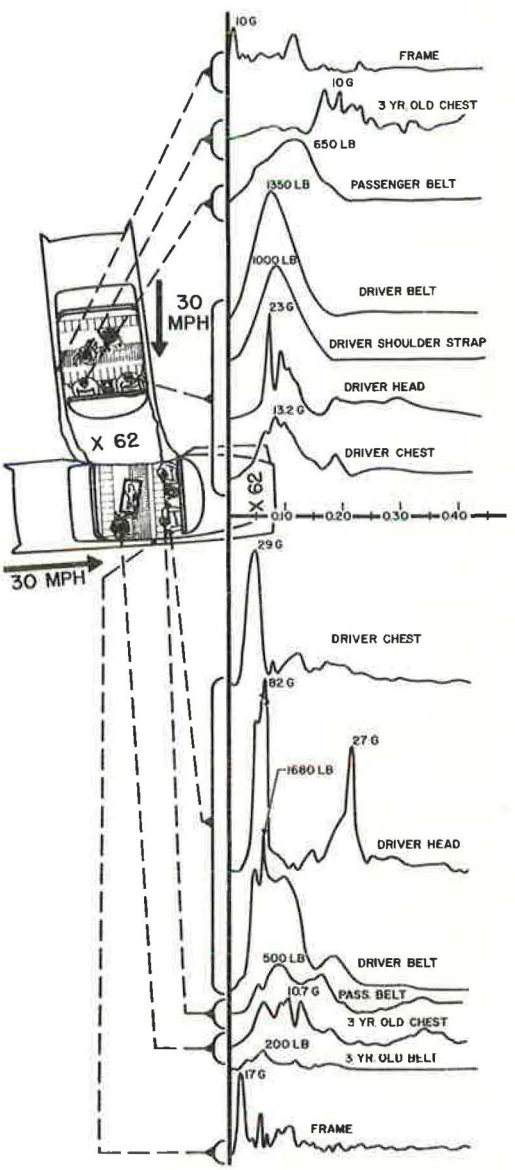

Figure 5. Transducer patterns, X-62, center-side impact, 30 mph.

TABLE 2

ANTHROPOMETRIC DUMMY SPECIFICATIONS

Dummy	Seated Position	Height (in.)	Gross Weight (lb)	Joint Articulation	Manufacturer
Adult drivers[a]	Left front	72	200	Principal	Sierra Engineering Model 157
Adult passengers[a]	Right front	68	170	Principal	Sierra Engineering Models 292 & 185
Children	Rear seat	35	37	Five only[b]	UCLA-ITTE
Infants	Rear seats	26	12	Five only[b]	UCLA-ITTE

[a]Drivers were interchanged from striking to struck car to accommodate use of special head camera installed in one of these driver's heads. Their identical specifications permitted this interchange without introducing any bias. Corresponding passenger dummy was transferred in each instance.

[b]Five joints: arms at shoulder girdle, legs at pelvic girdle, and a single neck joint. Joints have limited action of conventional toy doll. A three-year-old child anthropometric dummy having trauma sensitivity is currently being manufactured to UCLA-ITTE specifications.

Safety belt tensiometer loads, per se, are not particularly significant unless the heights and weights of the restrained anthropometric dummies are likewise provided. Table 2 assists in judging the relative significance of the various belt forces discussed in this paper. The exact meaning of these tensiometer peak load values is not clear without further explanation of what this instrumentation measures. Belt tensiometer data represent the forces at belt anchor points on the car structure. Furthermore, the lap belt tensiometer values represent the total tension on the two anchor points, or loop-load, whereas the passenger shoulder strap tensiometer values represent the tension at the single shoulder anchor point at the center doorpost and is not a measure of the chest loop-load. The lap belt tensiometer peak values may be expected to increase in a rather uniform manner, with respect to increases in impact velocity, because they tend to compensate for the effects of lateral body loading components. This occurs because the tensiometer toward which the body is thrown may show reduced tension whereas the other unit, for this same body displacement, would show a correspondingly increased value.

The passenger shoulder strap tensiometer values should not be regarded as absolute upper torso restraint forces but rather as approximate values having reasonably good correlation with the variables of speed and impact configuration, because of the following interactions:

1. During collision, changes in the motorist inertia force vector as a function of time causes a continuous misalignment, both vertically and horizontally, between the shoulder strap and the direction of the motorist's inertia force.
2. Variability of the strap-to-motorist-body frictional forces are recorded by the tensiometer at the strap anchor point as though they were true restraint force variations.
3. The slip-link feature of the combination belt under study permits shoulder strap anchorage forces to be a function of lap belt forces.

The passenger shoulder strap tensiometer readings are valid only with respect to the tensile force acting at the doorpost anchorage, although they do provide a useful indication of the relative severity of collisions.

Driver Exposures

The driver dummies for all four car exposures were provided with head and chest

triaxial accelerometers and safety belt tensiometer instrumentation. Inasmuch as the car's collision performance remained substantially the same, despite a prior divergent history of collision, driver interaction with the car's interior provided valid comparative data. Furthermore, to obtain greater usefulness from this correlate experiment, it was desirable to evaluate additional dependent variables. The restraining devices for the front-seat adult dummies of the striking car were interchanged. In Experiment 57 the driver of the striking car wore a lap belt only, whereas in X-62 this same driver wore a combination shoulder strap and lap belt. The driver's head deceleration resulting from his head striking the steering wheel in X-57 registered 28G, in contrast with 23G for X-62. The added restraint of the shoulder strap in X-62 accounted for the reduced head acceleration. The driver stressed this shoulder strap to a registered 1,000 lb during the impact, while his lap belt simultaneously reached a peak of 1,350 lb. A slip-link feature of this combination belt provides for automatic adjustment during impact for variations in chest and hip restraint force magnitudes.

Driver Dummy Interaction with Tempered and Laminated Side Glass

The resistance of safety glass to breakage depends on a variety of factors, identified by another paper (3). A brief review of these factors will assist in understanding the findings to follow. The stresses applied to glass during impact depend on the mass, contact geometry, velocity, and resilience of the impacting object as well as on the type and thickness of glass, ambient temperature, glass edge constraint, and other physical factors of this nature. When the impacting object is a human head, a difficult problem arises when attempting to select impact performance specifications for safety glass that will provide uniform rather than selective protection from injury. As the strength of glass—either tempered or laminated—is increased it tends to reduce the frequency of breakage, thus improving occupant protection from being ejected, protection from roof collapse during upset and perhaps most important, to reduce exposure to laceration. However, as the strength of glass increases, so does the frequency of brain concussions and skull fractures.

Although subject to several qualifications to follow, briefly stated, laminated glass as used in automobiles has a relatively high resistance to impact by small, sharp objects, whereas tempered glass has a relatively high resistance to impact by blunt objects. The following qualifications are appropriate to this statement:

1. The statement is true if resistance to impact means resistance to glass fracture. Laminated glass may fracture with the appearance of a single localized crack, or with a simple pattern of several cracks or it may fracture with total breakage accompanied with varying amounts of fragment dispersal. Tempered glass fracture extends almost instantaneously throughout the entire sheet and is generally accompanied by a complete dispersal of glass fragment.
2. The resistance that tempered glass exerts against a striking object terminates on fracturing. For laminated glass, this resistance continues to function following fracture until the plastic interlayer is ruptured.
3. Resistance to impact by tempered and laminated safety glass is a function of changes in glass continuity induced by the impact. For one range of impacts, laminated glass would be cracked substantially but tempered glass would be unbroken. For another range of impacts, laminated glass, although cracked and possibly punctured, would still function as a more or less cohesive surface but the tempered glass would be completely shattered out. And for still another range of impacts, both types of glass would be entirely or mostly broken out, although not necessarily with the same degree of hazard.
4. Resistance to impact by glass is a function of thickness and whenever comparisons between tempered and laminated glass are being made in this paper, their respective thicknesses may be assumed equal unless specified otherwise. Accordingly, resistance to impact may carry different interpretations, depending on the nature of the impact and the type of glass. With respect to nature of impact, the UCLA-ITTE project determined three causes for side-window breakage during intersection collisions:

   (a) Abrupt lateral acceleration of the window frame and glass into the motorist's head;

(b) Comparable action into the motorist's shoulder by the window sill, sufficient to break window glass; and
(c) Encroachment by the striking car into the struck car side below its window level, or direct contact with its window.

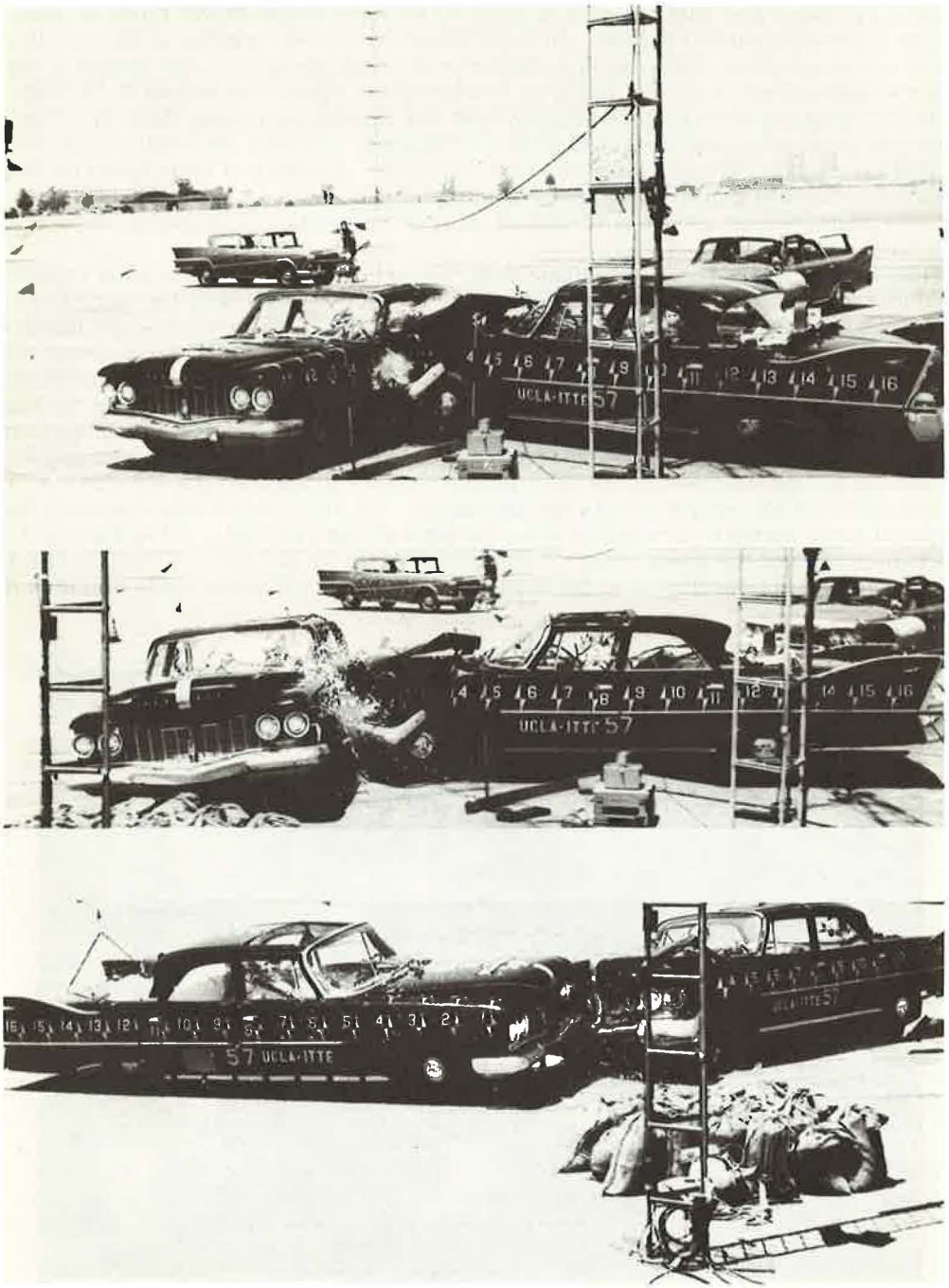

Figure 6. Experiment 57.

The correlate Experiments 57 and 62 demonstrated the head impact action described by item 1, accompanied to some extent by the interaction described by 2. With respect to item 3, inasmuch as the striking car impacted the driver's door, this mechanism for side-window glass fracture also operated, but as will be shown, with varying influence on the struck car driver's head blow—according to whether tempered or laminated glass was installed. Concerning item 4, the nominal thickness of the glass was $\frac{1}{4}$ in.

The driver of the struck car for both X-57 and X-62 wore a lap belt only. This condition of restraint was held constant in order to evaluate two different types of side-window glass adjacent to his head. In X-57 the left front side-window of the struck car was of tempered glass, whereas in X-62 it was of laminated glass. The impact of the driver's head shattered out the left front window of the struck car during X-57 (Fig. 6): the laminated glass was fractured during X-62 but remained in place (Fig. 7). The tempered glass accounted for a 53G peak acceleration, whereas the laminated glass accounted for an 82G peak acceleration (Figs. 4 and 5). Analysis of high-speed motion picture film showed that in both instances the head struck the side-window glass and that this glass was not additionally backed up by direct contact of opposing striking car structure.

The explanation for these anomalous data, wherein the resistance to blunt impact by tempered glass was less than the resistance by laminated glass of the same thickness, may be found by referring to the three causes of side-window breakage mentioned earlier. Inasmuch as both heads were seen by high-speed photography impacting the side glass, this action was quite understandably assumed to be the cause of the glass fracture. However, the other two factors, the motorist's shoulder stressing the base of the window and the striking car encroachment below the window were also operating and with considerable force. It appears that these stress concentrations increased sufficiently during the onset of the head impact with the glass to crack the glass with results different for tempered than for laminated. All head impact resistance by the tempered glass abruptly terminated when the edge stress reached a value sufficient to crack the glass and the glass ruptured completely from its mounts. A similar crack or series of cracks developing in the laminated glass will not appreciably diminish its

Figure 7. Experiment 62.

resistance to head impact because the cohesive properties of the plastic interlayer continue to function following initial cracking.

This explanation is supported independently by laboratory studies conducted at UCLA by the ITTE collision research project in which identical 1960 Plymouth doors were mounted with the same door hinge and latch restraints and their side glass impacted with a 9-lb simulated human head. Under these controlled conditions, and without the edge stress concentrations identified with full-scale collision studies, the impact velocity that produced a peak acceleration of 83G for laminated glass produced a peak acceleration of 130G for tempered glass of the same thickness.

These laboratory studies were conducted using a mass and impact velocity, for the simulated human head, comparable to the anthropometric dummy head mass and velocity, in which the side window was accelerated to impact the dummy's head during the full-scale collision experiments. The poor correlation between head impacts of 53G, for the full-scale crash, and 130G for the laboratory study, provides additional data indicating the sensitivity of tempered glass to coincidental edge stressing during collision. This observation is strengthened by the fact that high edge stressing was positively identified as accompanying head impact during the full-scale collisions and the laboratory studies were controlled to exclude edge stressing during head impact.

Additionally, the close correlation between the head impact peak acceleration of 82G obtained by full-scale crash tests and the head impact of 83G obtained by laboratory tests demonstrated the relative insensitivity of laminated glass to coincidental edge stressing during impact.

Driver Lap Belt Forces

The driver's chest for the struck car of X-57 and 62 registered 27 and 29G, respectively. The drivers of the struck car, X-57 and X-62, wore lap belts only. Poor driver seat belt correlation was obtained considering an 850-lb force was recorded for the driver of X-57 as compared with 1,680 lb for the driver in X-62. The explanation for this gross deviation may be found in an earlier publication (2) which states that seat belt force for this exposure is not a realistic source of data. The driver is pinned against the side of the car because of the abrupt acceleration the car received from the striking car; to the extent that the driver's belt in Experiment 57 was not as snug as it was in Experiment 62, the reading would be correspondingly less because a very slight translation by the driver's hips to his left will be abruptly checked by the intrusion of the striking car. Additionally, the intrusion of the striking car may produce seat belt displacements in the direction of advance of the striking car that are being recorded but have little bearing on real inertial forces of the dummy. Finally, the striking car in X-62 may have developed direct mechanical interaction with the tensiometer, one of which was located where the striking car intrusion was greatest.

Adult Dummy Restraint

Strong transverse forces are applied to motorists during intersection collisions. The purpose of including the combination shoulder and lap belt restraint configuration in the Series II intersection collision experiments was to provide an evaluation of the possible added advantage of a diagonal chest strap in reducing upper torso movement during impact. As reported in a prior publication covering 12 intersection collision experiments (2), the combination chest and lap strap provided effective restraint from these transverse forces in the majority of exposures. For the correlate Experiment 62, the diagonal chest strap of the front seat passenger of the struck car was eliminated so that this exposure could be studied for a dummy during collision wearing a lap belt only. Figure 4 shows the combination belt for the front seat passenger, struck car, registered 650-lb lap load and 320-lb shoulder belt load. This may be compared with the 500 lb for the lap belt load for the identical exposure in Experiment 62, wherein the dummy wore only a lap belt (Fig. 5). In X-57, one of the two lap belt anchorages is also the anchorage for the shoulder strap. Its tensiometer, therefore, records part of the chest strap load. In addition, examination of high-speed motion picture film provided additional information. Under the comparable collision conditions of Experi-

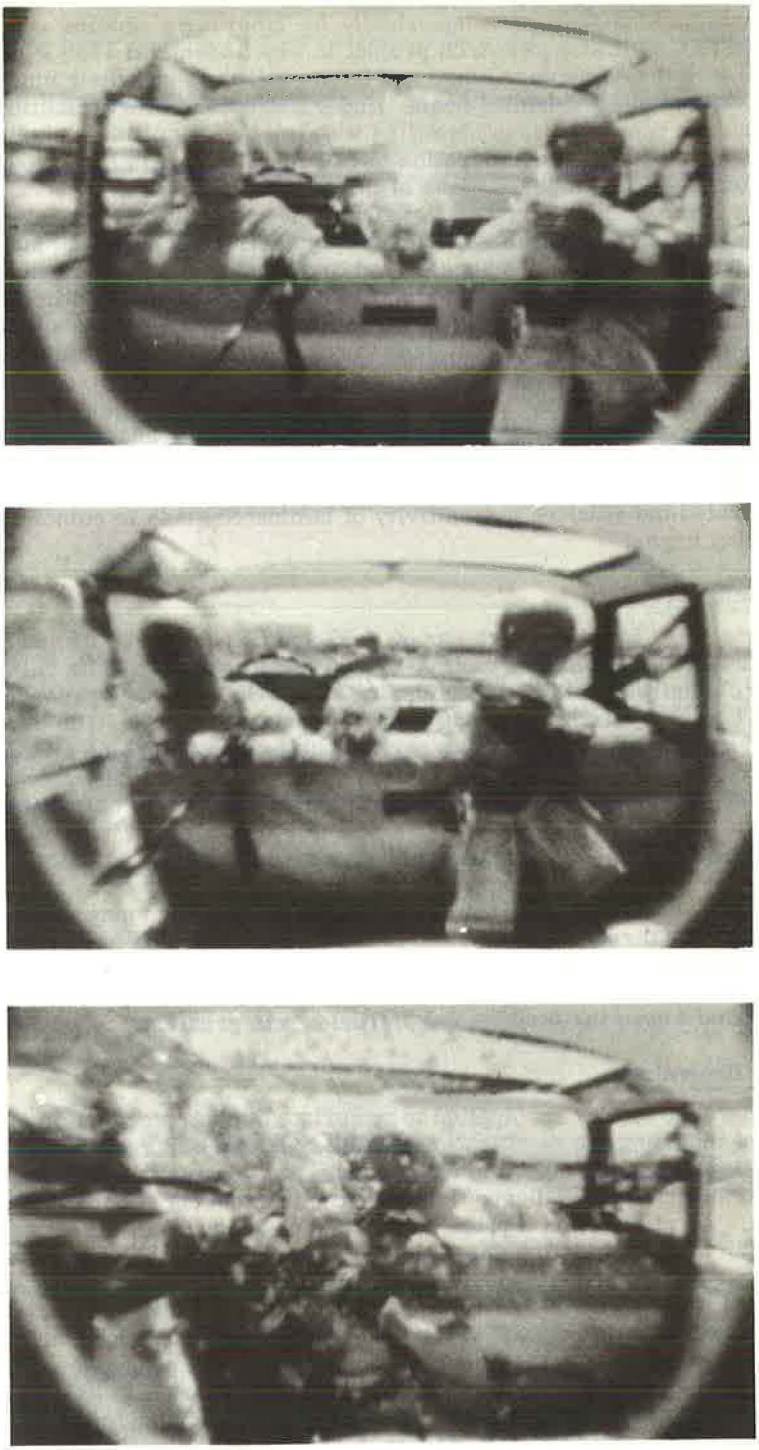

Figure 8. Inside struck car, X-57.

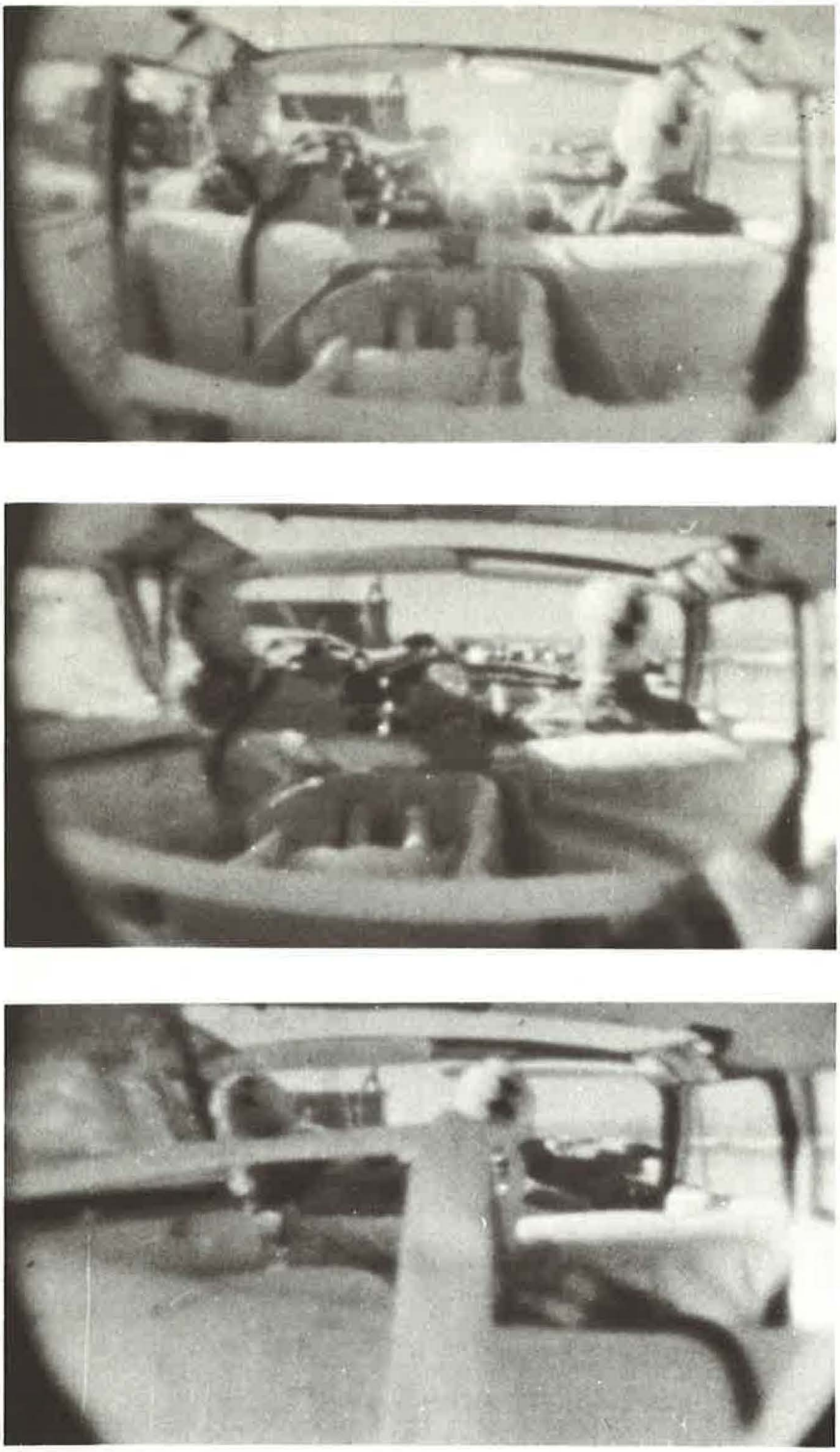

Figure 9. Inside struck car, X-62.

ment 62, the upper torso was permitted a greater lateral movement sufficient to strike the occupant seated to this dummy's left and this form of upper torso "restraint" is not presented as an added lap belt loading.

This discussion has concerned the movement of the right front seat passenger of the struck car illustrated in the sequence Figure 8 (X-57) and the companion Figure 9 (X-62). The shoulder cross-strap shown in Figure 8 for the front seat passenger passes from upper right shoulder to lower left hip and, therefore, does not offer as positive an upper torso restraint for impacts directed to the left side of the car, as for impacts directed at the right side. To the extent that the struck car is moving forward when impacted at its side, the contact at the side by the striking car decelerates the struck car; the inertial forces of the right front seat passenger develop forward movement of the dummy's hips (relative to the car interior) that function to tighten, through the slip-link, the diagonal chest strap. As a consequence of this slip-link feature, in the majority of the UCLA intersection collisions directed toward the belt side affording reduced protection, the dummy appeared to be rather well restrained by the cross-strap during the collision. The right front seat occupant's sideward movement for the two 30-mph correlate experiments shown in Figures 8 and 9 (struck car) was approximately the same for the dummy with a diagonal strap and lap belt as for the dummy with only the lap belt. Some allowance should be made, however, for the reduced degree of spinal articulation common to anthropometric dummies, as compared with their human counterpart.

In X-62, this right front seat passenger would subsequently have been ejected had he not been wearing a lap belt (Fig. 10). Under this same exposure condition a human might have had his head and shoulders partially ejected even though wearing a lap belt, and this is hazardous particularly if the car subsequently overturned or struck another object. The shoulder cross-strap is useful in reducing this tendency for the upper torso to be thrown outside an open door. The installation shown in Figure 8 is higher than shoulder height. It was found that severe neck lacerations can result when this strap functions to restrain upper torso ejection with the upper anchorage point substantially above shoulder height. Accordingly, the upper anchorage point for this strap should not be above shoulder height.

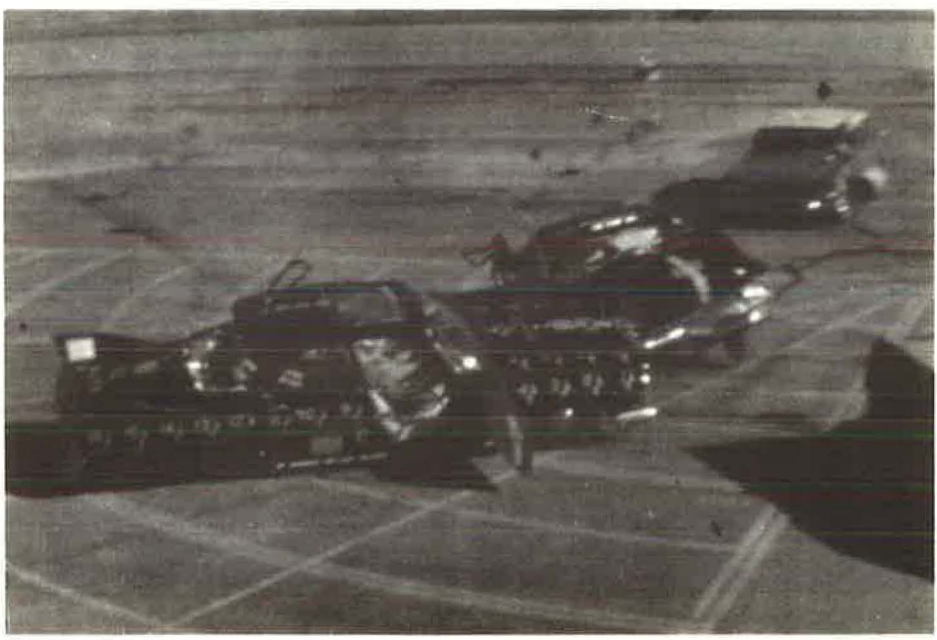

Figure 10. Door latch failure.

Child Motorist

Simulated children were included in this correlate experiment to provide additional information on the relative exposure hazards of children in various seated positions and postures with various means of restraints. In Experiment 62 the instrumented three-year-olds registered a 10G chest deceleration when riding in the striking car and a 10.7G chest deceleration when riding in the struck car (Fig. 5). However, the three-year-old in the struck car is secured by a lap belt that registered 200-lb loading, whereas the three-year-old in the striking car was unrestrained. The exposure positions are generally more severe for occupants in the struck car. The unrestrained child that was subjected to a 10G peak chest deceleration will frequently receive serious head injuries, for this exposure. The Figure 8 sequence, X-57, shows the probable extreme abuse a child experiences during impact when standing behind the front seat in the struck car. Under identical collision exposure conditions for X-62, except with this child dummy sitting on a cushion and restrained by an adult-type lap belt, the child was observed riding out the impact in an uneventful manner.

In the same Experiment 62, referring this time to the striking car, a similar three-year-old child dummy was equally as effectively protected by the adult-type lap belt; although the rear seat back tore loose and contributed to the forces the dummy sustained (Fig. 11). When the three-year-old is standing on the right side, behind the front seat in the striking car, the exposure is substantially less than the comparable position for the struck car, because the striking car is abruptly jerked to its left, tending to pin the child against the right side of the car in a not-too-abusive manner. This description assumes that the right rear door remains closed under the high-collision tension-failure forces that are augmented by human body inertia forces collectively acting to open the door. Had the struck car been traveling in the opposite direction, the child would have been thrown violently across the front seat back to her left much in the manner experienced by the child shown in the Figure 8 sequence.

Infant Motorists

Six-month-old simulated infants were included in these correlate experiments, one to each car. In the prior series of 12 intersection collisions, it was found that a bassinet whose long axis paralleled the long axis of the car, positioned behind the center of the front seat back and appropriately anchored, provided the best location. In Experiment 62, this location was repeated and the findings confirmed these prior observations. Of special interest, X-62 emphasized the importance of providing a protective covering (such as a net) for the bassinet. The bassinet anchorage held but the bassinet was forced substantially to the left as a result of the impact at the left side of the car. Impact forces were sufficient to throw the simulated infant from her bassinet. The three-year-old sitting in the rear seat to the right of the bassinet was restrained by a lap belt and, therefore, did not interact adversely with the bassinet as had been observed in prior collision experiments where the three-year-old was not restrained.

The infant standing in the center of the front seat of this struck car was provided with harness-type restraint and may be seen in Figure 9 riding out the crash in a rather uneventful manner, except for the abusive force applied subsequently by the adult sitting to her right (Fig. 12). An identical simulated six-month-old with the same harness restraint was seated between the two front seat motorists of the striking car and was observed equally as effectively restrained and was not so severely contacted by these front seat motorists.

The harness worn by these infants demonstrated the value of a well-designed protective restraint. This harness has been commercially available for several years and consists of straps that restrain the chest and shoulders interconnected with straps that restrain the hips and pelvis. The harness is restrained by a vertically positioned attachment strap that loops the entire car seat back and is anchored to the car floor below and to the rear of the attachment strap. This anchorage of the attachment strap limits forward movement of the seat unit and transmits the infant restraint forces to the car floor pan. A slip-loop feature permits the infant to stand, sit, or lie down on the seat. Even with this freedom of movement, the infant remains effectively restrained against collision forces acting in practically any direction.

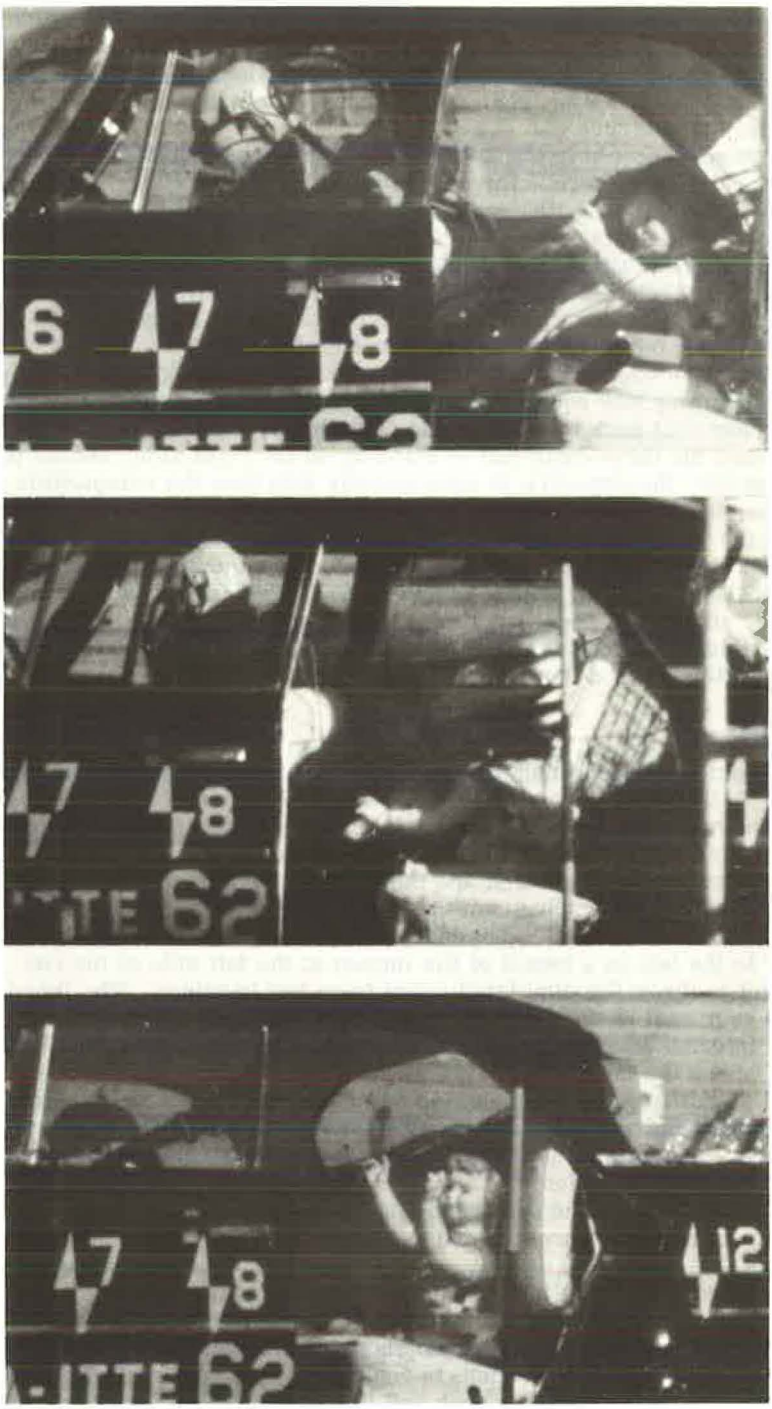

Figure 11. Lap belt protecting 3-yr-old.

Safety belts that transmit forces primarily to the viscera or adjacent areas of the body midway between the pelvic and shoulder girdles are unacceptable as motorist restraints. Manufacture of such devices should not be permitted because they increase rather than diminish the chances of injury during collision by directing collision forces to the more vulnerable portions of the body, a feature diammetrically opposed to the basic principle of protective restraining devices. Although these deficiencies are obvious, such devices are still being manufactured and sold to the public.

In X-57 (struck car) this same front seat center position for the infant was evaluated by having her seated in a bail-type car seat. A detailed discussion of this unsatisfactory seat performance during impact may be found elsewhere (2). Briefly, it was found that the bail fasteners readily detach during impact, permitting seat and child to strike the car interior. Should the bails not detach, adverse forces are applied by the chrome tubing to the infant's viscera. The infant for this seated position is exposed to the crushing forces of adult front seat motorists unavoidably thrown against the infant during impact. The rear seat, center position, is safest seat position for infants and children. Protective restraints can be applied for this seat position that do not restrict the child's need for some freedom of movement and that additionally permit the child to see the passing view outside the car. The driver remains undisturbed from his important task and the child is restrained in the position of greatest protection from collision forces, regardless of direction. From these preliminary findings, therefore, the harness restraint as previously described permitting the infant to stand or lie down is a satisfactory restraint and is the safest of infant restraint systems evaluated to date.

The striking car rear seat, for X-57, carried a bassinet resting on the seat. During impact the rather high acceleration forces to the striking car's left threw the bassinet from the seat to its right; however, the infant remained within the semi-protective confines of the bassinet. The tie down straps furnished with most bassinets, when properly anchored, greatly increase infant protection during collision.

Figure 12. Impact forcing door open.

Belt Elongation

Instrumentation was applied to all restraining harnesses used in Experiment 62 for the purpose of measuring safety belt fabric permanent set, or elongation. Measurements were recorded to the nearest $\frac{1}{16}$ in. and no permanent set was observed for these collision exposures. This observation can be explained by referring to Figure 4. The forces applied to the safety restraints did not approach the loop strength limits prescribed for these belts. Further, the restraining

webbing used in these automobile collision experiments was about one-half the strength specified for webbing in military aircraft. Even so, the forces it sustained were not sufficient to develop measurable elongation. Furthermore, a comparison of the motorist acceleration exposure levels for the 30-mph correlate experiments with those substantially higher levels established by Stapp, et al., as survivable, leads to the following conclusion: properly restrained, the 30-mph intersection collision is a survivable crash, except possibly for motorists sitting next to the impacted side of the struck car. This statement is not in any way intended to suggest that the 30-mph intersection collision is not a serious accident, but rather to assert that even considering the severity, these crashes are survivable for motorists wearing properly designed, installed, and applied safety belts.

Transducer Data Process

Using manual procedures, data reduction of a single collision experiment, instrumented in the comprehensive manner depicted by this paper, would require one full year of an engineer's time. Each successive experiment tends to be more thoroughly instrumented thereby increasing the data reduction task. To reduce the time required, an attempt was made to take advantage of high-speed computer processes. Previous attempts at UCLA had been unsuccessful because a program able to assimilate correctly the input data of the irregularly shaped curves recorded from transducers during collision had not been devised. A new approach to this problem by highly qualified specialists in computer programing at ITTE-UCLA provided a successful breakthrough. This technique is described in detail elsewhere (2) and is briefly summarized here.

Because of the asymmetrical nature of the intersection collision, impact-acceleration forces may occur in any direction. Bi-directional accelerometers were placed in clusters of three along mutually perpendicular axes to provide X, Y, Z axes sensing positive and negative accelerations. The resultant acceleration values were calculated by the IBM 7090 computer from acceleration values taken at selected common times. In addition to these resultant acceleration values, the directions of these resultants were also indicated; these acceleration vectors referred to the positions that the component transducers occupied, relative to the anthropometric dummy or car structure to which they were attached. The actual orientation of a given cluster of accelerometers at a specific instant during an impact could be determined by reference to one or more of the high-speed motion picture films, synchronized with the transducer data.

The transducers positioned within the car and within dummies were connected by a 100-ft multi-conductor cable to an 18-channel oscillograph carried by the instrument recording car that followed the crash car to the impact area. A flash bulb mounted on the crash car provided a visual signal as well as an electrical pulse indicating zero time for the motion picture and recording oscillograph systems. Appropriate sensitivity calibrations of transducers were made just before and immediately following the collision experiment.

Each oscillograph curve was traced on a separate sheet of vellum to permit inclusion of calibration time lines, scale factors, critical point notations, and other data that would tend to deface the original oscillograph record. The process of extracting the square root of the sum of the squares for the many triaxial data points, of applying the various channel scaling factors and of regraphing to a common scale, was a laborious task quite appropriate for the digital computer. The points to be plotted by the computer were indicated by pencil notation on the vellum graph. These points were spaced irregularly to avoid excluding peaks. This procedure enabled input data to be transferred in a perfunctory manner without loss to final accuracy. A Benson-Lehner "Oscar" curve-reading machine was used to translate the indicated points from the vellum curve onto punched cards. Special techniques were used to correct for deficiencies that are inherent with this machine. For example, each curve was read once by two separate "Oscar" operators who independently prepared punched cards for each transducer curve. Both sets of cards were compared and if found to be in reasonable agreement, both sets were used by the computer. The program provided for the following computer output:

1. A print-out of each curve in tabular and graphical form;

2. Similar print-outs of accelerometer resultants;
3. A print-out of the input data for control purposes; and
4. Information about the accuracy of each computation.

The program that was developed used a sequence of overlapping parabolic curves for computer presentation of the accelerometer durve. This procedure enabled the computer faithfully to follow the sharp peaks occurring at irregularly spaced intervals that are characteristic of accelerometer patterns generated during collisions. Correlation checks were made at all distinct phases of the entire data process as well as by independent techniques, such as comparing computer curves with those produced by hand solutions. Excellent correlation was obtained (2).

COLLISION PERFORMANCE

Vehicle Collision Dynamics

As would be expected, the two cars for these correlate experiments followed approximately the same collision sequence of events, generating about the same car-to-car deformations, approximately the same changes in directions and spin-out patterns as well as reaching about the same positions of rest. These observations are in part identifiable in Figures 6 and 10 for X-57 and 62, respectively.

The simulated motorists inside these cars appeared to respond the same for the two experiments, except for the variations imposed by different types of safety restraints and by the changes in the type of side-window glass they struck. That is, the primary movements of the dummies during collision, as viewed by high-speed photography, closely correlated for corresponding seating positions of X-57 and X-62. However, the type of interior surface encountered (for example, laminated vs tempered side glass) made a difference in dummy transducer readings.

Differences in collision dynamics for X-57 and X-62 may be observed by comparing Figures 13 and 14. Minor variations in corresponding car movements are evident and these differences are more apparent by comparing positions of rest for striking and struck cars.

The changes in direction and the displacements that the cars underwent as they collided and spun out to their positions of rest (Figs. 13 and 14) are given in Table 3.

Figures 15 and 16 provide further opportunity to determine the differences in positions of rest and also indicate the corresponding skid patterns leading to these positions of rest for Experiments 57 and 62. For the Series II intersection collision experiments the crash car brakes were not applied at impact; following impact, brakes were applied only in those instances where a crash car was heading for a tower anchorage or the car moved about 100 ft from the position of impact. No crash car emergency braking was required for X-57 or X-62; the skid patterns shown in Figures 15 and 16 are the result of the collision forces changing car headings. These skid marks may be termed "deviation" skids in those instances where abrupt changes in direction are evident at and next to the position of impact as a direct result of collision forces; "brush" and "centrifugal" skids where such marks are generated by the arcing or spinning car after leaving the position of impact as a secondary result of collision forces. Brush and centrifugal tire-skid marks can be laid down by vehicles attempting turning maneuvers at driving speeds higher than normal for the maneuver but deviation skid marks require a collision for their generation. Deviation skid marks are useful, therefore, in identifying the vehicle position on the roadway at the time of impact. In addition to deviation skid marks, car rim flanges, undersides of bumpers, or fractured bumper supports, and underbody sill metal or frames occasionally are forced into the pavement leaving gouge marks. Correlation of these pavement gouges with abraded metal components found on the wrecked vehicle often provide an objective basis for establishing the position of the car when those pavement gouges were generated. Pavement gouges may be made by the damaged vehicle at the position of impact or on its way to its position of rest, or both. A deviation skid mark is made only during collision: (a) as a result of the tire being abruptly stopped or nearly stopped by intruding structure of the opposing vehicle as the wheel is crushed rearward and frequently sideways, or (b) as a result of

TABLE 3

POLAR DISPLACEMENTS OF CAR CENTER OF MASS FOR 30-MPH CENTER SIDE IMPACT

Experiment	Polar Displacement			
	Striking Car		Struck Car	
	Deg	Ft	Deg	Ft
57	23	33	24	39
62	34	28	31	42

a side impact when the brakes have been previously locked up. The deviation rubber mark on the pavement is blackest when the distressed tire has been overridden by the other colliding vehicle because this places additional load on that tire. In such instances, the deviation skid may also be referred to as a distressed skid mark.

The high load carrying tires (those on the outside of the turn or spin) generate brush skids and their patterns for corresponding wheels of X-57 and X-62 followed the same general positioning relative to the impact axes; three corresponding skid patterns coincided within 1 ft of each other and the remaining two sets of patterns differed by an amount not exceeding $2\frac{1}{2}$ ft.

Non-braked brush skids are generated by tires on the advancing side of the arc that the center of mass of the car is following. This statement allows for the fact that, as a car spins out along a given trajectory, tires on the right or left side may alternately mark and then not mark the pavement according to whether they are on the advancing side of the arc or on the trailing side of the arc, respectively. The tires on the trailing side may carry a car load insufficient to generate observable rubber brush marks on the pavement. At times, these tires are entirely off the pavement (Fig. 6).

In X-62, the striking car rolled backwards 2 ft after it stopped broadside skidding. This caused the position of rest to be offset slightly from the terminal positions of skids. The dispersal of collision debris covered approximately the same area for both experiments and these data were presented for X-57 elsewhere (2, Fig. 8).

Coefficients of Friction During Post-Contact Spin-Out Trajectories

On approaching a curve in the road, a driver turns his steering wheel to establish a front wheel deflection that builds up the yawing velocity to a steady state (for constant car speed and constant road radius of curvature, superelevation, and coefficient of friction). (There is a significant lapse-distance between the point where steering wheel turning is initiated and the point where the car body starts to track the turn. As an example, at 35 mph this may be 30 ft and will vary depending on such factors as highway and vehicle design.) If the radius of curvature is too small (that is, the curve is too sharp for the car's approach speed), the minimum radius of turn the car can negotiate for that speed will exceed the geographic radius of curvature of the road; in a sustained curve, the car will drift lanes and leave the pavement. Any attempt to counteract this plight by turning the steering wheel to a larger front wheel deflection will disrupt the steady state yawing velocity and, thereafter, the yawing velocity will continue to increase as the car spins out of its turn.

It is generally conceded that tire-to-road side force during a turning maneuver may approach the value attainable for car deceleration by impending or locked-wheel skids in a straight forward direction. This judgment is based on the assumption that the transverse resistance the road surface offers to tire side-slip is about the same as the linear resistance the tire encounters for braked skid conditions in a forward direction; the calculated values of both resistive forces of friction are based on the same laws of motion and friction. Implicit in this judgment is the assumption, however, that only the tire is in contact with the road surface and does not include the more extreme con-

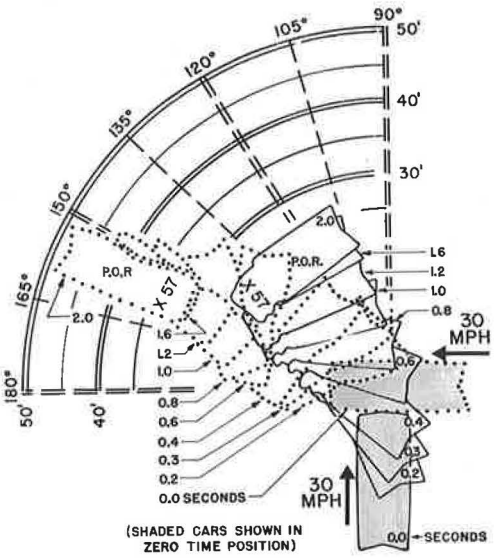

Figure 13. Collision dynamics, X-57, center-side impact, 30 mph.

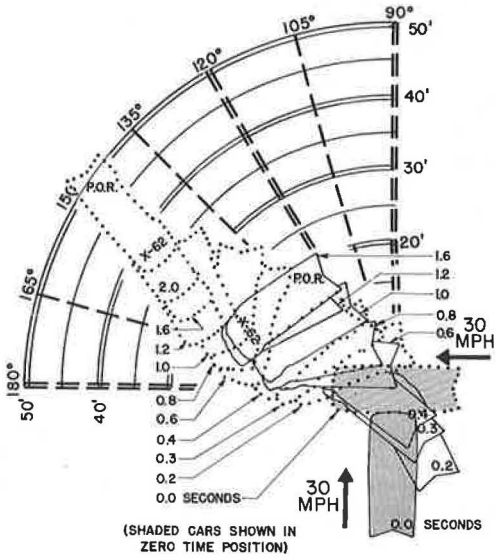

Figure 14. Collision dynamics, X-62, center-side impact, 30 mph.

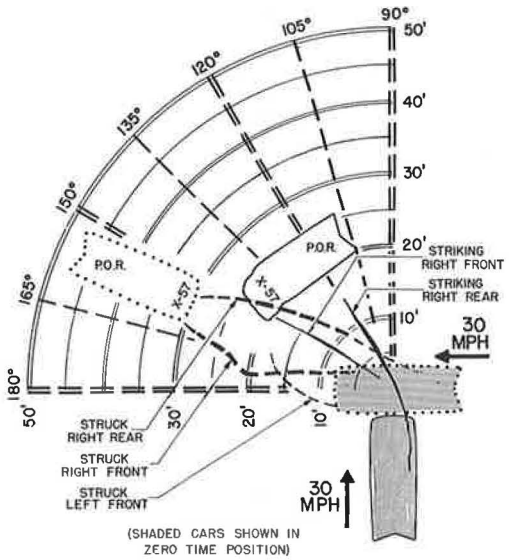

Figure 15. Position of impact, skid marks, and positions of rest, X-57.

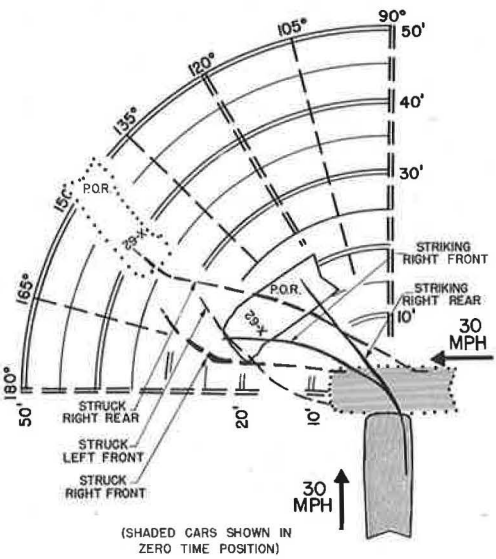

Figure 16. Position of impact, skid marks, and positions of rest, X-62.

ditions that bring into road contact not only the tire but also its rim and at times the car's sill. Also implicit is the assumption that the tire and wheel suspension dynamics provide as effective a tire-to-road gripping continuity for side-slip action as for straight ahead wheel skid action. The motions of a skidding automobile are treated rather comprehensively by Radt and Milliken (4).

Calculations were made to estimate the effective coefficient of friction for a colliding car undergoing post-contact spin-out starting with the instant the car broke contact with the opposing car and continuing to the car's position of rest. These coefficients of friction were calculated for a uniform, level, clean and dry asphalt surface that had a four-wheel locked skid coefficient of friction over the same speed range of 0.75. However, before mentioning findings, a further discussion of principal variables operating during spin-out will assist with an interpretation of data.

As the two cars contact each other during an intersection collision, each car's direction is modified so that it has a new heading and trajectory by the time contact is broken. The heading, or direction the car is pointing at any instant after contact may or may not be the same as the trajectory or direction the car is moving. In a broad-skid, the car is heading at a right angle to the direction it is moving. If the car spins out from impact to its position of rest, it may pass through both a broad-skid, or full brush-skid heading, and subsequently through a no brush-skid heading as it moves towards its position of rest. When the car is in a broad-side skid the effective coefficient of friction may exceed the locked wheel skid coefficient of friction. This will depend, however, on the extent of rim-gouging, which may occur even though the tires remain fully inflated, and also whether the car body-sill contacts the pavement.

Such car-metal-to-road contact will generate sparks and occasionally pavement scrape marks will be visible following the collision. This contact more often is evident, however, not by studying the road surface for scrapes but by inspecting the car rim flanges and body-sill areas for pavement abrasions. During spin-out, as the car's heading comes into alignment with the direction (or the reverse direction) the car is moving, the effective coefficient of friction diminishes substantially. Crippled wheel suspension, collapsed frame structure, or driver braking may singularly or in combination act to prevent this coefficient from approaching zero.

In some of the Series II intersection collisions, the car spun and then rolled on its wheels an additional distance before coming to rest. In others, the car started a spin at impact approaching a broadside skid as it came to rest. Cars in a third group had their headings altered by impact but continued thereafter to roll towards their positions of rest. Speed at impact, position of impact, and to a lesser extent, the respective types of cars involved are the principal independent variables operating to modify collision dynamics.

(The Series II cars were 1960 vintage and their low center of gravity and wide tread prevented upset. Cars of 1950 vintage were used in the Series I experiments and for an impact configuration, identical to X-57, and X-62, both striking and struck cars were overturned. However, corresponding positions of rest were similar, even though the older cars had undergone collision upset en route to their positions of rest.)

Examples of specific values of average effective coefficients of friction (f) for cars primarily undergoing broadside skidding are f = 0.7 for the struck car of X-57; f = 0.6 for the struck car of X-58; f = 0.9 for the striking car of X-61.

Damage Patterns and Costs to Repair

For the same make, model, and year car involved in the same type of 30-mph intersection collision on two occasions (X-57 and X-62), it is not surprising that the same damage patterns were produced for the striking cars and the struck cars of these experiments. That is to say that the location, extent, and nature of damage for these corresponding cars did not provide differences identifiable subjectively. To measure the amount the striking car crushed into the struck car during impact, a frame of reference for each of these cars had to be selected that was not also undergoing observable distortion. The high-speed motion picture films obtained from tower cameras provided the data; preliminary analysis of these films led to the selection of the windshield base

chrome trim as reference for the striking car and the right side door horizontal chrome trim as position reference for the struck car.

Maximum mutual compression is a measure of the change in distance from collision contact to maximum intrusion for the striking car's windshield as it crushes towards the non-impacted side of the struck car. In Experiment 57, this amounted to 1.9 ft; for X-62, 2.0 ft. Minor differences in intrusion for the struck car of X-62 may be explained as follows: in Experiment 61, the struck car had sustained damage that required section welding of the sill below the left side doorpost to prepare it for use in Experiment 62. Forces generated in X-62 were sufficient to break both the doorpost-to-sill weld and the rocker-section weld. Slightly greater intrusion by the striking car into the rear passenger compartment resulted for X-62 as contrasted with its correlate Experiment 57. Where section welding is required to repair a damaged vehicle, these welded sections should be strengthened or helium arc-welded to restore the original passenger compartment integrity. The collision damage sustained by cars provides a good indication of the relative speeds of the cars at the instant of impact. However, impact damage must be considered with respect to other factors such as the relative weights of the cars, their impact configuration, secondary or tertiary collisions, and the like. Controlled collision experiments provide data on impact speed vs cost of repairs and maximum collapse distances.

With respect to cost of repairs, the averages of three estimates received for the X-57 and X-62 striking cars were $710 and $670, respectively, and for the X-57 and X-62 struck cars, $830 and $970, respectively. The slightly greater intrusion for X-62 was reflected in significantly higher repair estimates.

Car Collision Forces

Accelerometer patterns are characterized by their rates of onset, peak accelerations and duration of acceleration at any given level. The relative severity of collisions for corresponding accident types may be established by comparing the peak accelerations attained by intact or noncollapsed portions of the motorist's compartment. Referring to Experiment 57, the striking car, traveling 30 mph at impact, reached a peak acceleration of 10G and this corresponded exactly with the peak acceleration obtained by the 30-mph striking car in Experiment 62. (Acceleration means the striking car decelerates on contacting the side of the struck car but is simultaneously accelerated in the direction the struck car was moving at impact. Triaxial transducers provide the resultant acceleration which reached, in this instant, a peak value of 10G.) The acceleration-time patterns are not identical but their basic characteristics of rate of onset, peak G, and duration show close correspondence. This condition indicates that the motorists in the striking cars were subjected to practically the same collision environment for these correlate exposures. Comparison of the struck cars' peak acceleration shows close correspondence, 16G for X-57 and 17G for X-62. The collision environments for the two struck cars were therefore, essentially the same. This observation takes on added importance when making comparisons between the performance effectiveness for the different restraint configurations worn for X-57 and X-62, as discussed earlier.

Laminated and Tempered Side-Window Glass

For Experiment 57 the struck car side-window glass was tempered and both left rear and left front windows were shattered with greater than 50 percent of the glass dispersal forced inside the car (Fig. 8). For Experiment 62 under the same collision exposure conditions, laminated side-window glass was installed. Both front and rear side-window glass fractured extensively but remained in place, except for about 10 percent of the glass for the upper forward corner of the left rear window that dislodged and was found inside the rear seat compartment.

The high-speed camera mounted on the hat shelf of the struck car, X-62, showed that this small section of laminated glass broke into several smaller pieces as it was projected into the passenger compartment. These fragments were too few to be conspicuous in the individual motion picture frames (Fig. 9), but are observable when

viewing the actual motion pictures. In contrast, a dense shower of fast-moving glass particles from the left front and left rear side-window glass penetrated the passenger compartment during the correlate collision X-57. The only difference for these two exposures was that tempered side glass was installed for X-57 and laminated glass for X-62.

With respect to the tempered side-window glass failures, it was found that each side-window glass ruptures into more than 50,000 particles, and that most of the particles had a diameter of less than 0.01 in. Not all the particles separated as they dispersed and some heavier pieces, 2 to 3 in. in diameter, were seen accompanying this glass "cloud" as it shot across the car interior at speeds sometimes faster than that of the striking car. However, the average particle size of tempered glass is substantially less than that of laminated glass. Also, partial failures of laminated glass leave glass residuals bonded to the window frame that may be extremely hazardous to motorists contacting them. Head impact with side glass was discussed earlier.

Accidental Door Openings

For the twelve Series II intersection collisions (2), no door openings occurred for either car in the 10- or 20-mph collisions. One accidental door opening occurred for the struck car in the 30-mph collisions, but no doors opened for the striking cars. It was the left front door that opened for the car struck at its left front wheel by a 30-mph car. Four accidental door openings occurred in the 40-mph collisions, all in struck cars. To avoid misinterpretation of these findings, it is important to note that the adult dummies were restrained by safety belts in all but one of the twelve Series II experiments; the exception was one of the 40-mph crashes. This research positively established that door latch failures, with subsequent ejection of motorists are in part the result of the unrestrained motorist's body unavoidably hurled against the car door, in battering ram fashion, to contribute to door latch failure. Referring specifically to correlate Experiment 57, no doors opened, although the impact was directed to both doors on the left side of the struck car. In Experiment 62 the right front door of the struck car was forced open during the initial phase of the impact. At the instant that this right front door popped open, both front seat adult dummies were being forced against the left front door (Fig. 10), away from this opening door. Three conditions acting separately, or in combination, may account for this door opening against the transverse inertia forces of collision acceleration:

1. The front seat was pushed to the right against the right front door as the striking car crushed into its left side.
2. Tension-failure action of the latch, as a result of high car body bending forces during impact, undoubtedly contributed to door latch failure.
3. Possible reduced latch-holding efficiency as a result of the higher impact forces to which this car was subjected during a previous 40-mph collision experiment.

In connection with this last item, door latch failure as a result of prior impact exposures, this factor could not be unconditionally identified because of the other two factors operating and tending also to open the door. However, reduced latch-holding efficiency is the only feature of the three that is different from the conditions operating for X-57 wherein no door opened. Consequently, although facilitated by seat thrust and car body bending forces, the door opening for X-62 is considered to be the result of prior collision abuse. Special attention during repair to make sure door latch operation is restored to its original effectiveness is vitally important to subsequent passenger safety. Without belts, at least the front seat passenger of X-62 would have been ejected and quite likely run over by his own car. This statement is based on the observation that the front seat occupants are subsequently released from being displaced towards the left door and abruptly forced towards the open right door, while the car is side-skidding to a stop.

FINDINGS AND CONCLUSIONS

These findings and conclusions are abstracted from the text for the convenience of the reader; however, the statements apply only within the context of the section of the

paper from which they were abstracted. Any generalization of these findings and conclusions may lead to misinterpretations.

Vehicle Collision Dynamics and Damages

General

1. The intersection collision is among the most complex of motor vehicle collision exposures. The principal variables requiring consideration are speed, angle of impact, eccentricities of impact, the structural properties, and weights of the vehicles involved.

2. For right-angle collisions up to 40 mph, a car's collision performance is essentially unimpaired by damage sustained from previous collisions, providing quality repair work has been performed.

3. The automobiles involved in these correlate experiments were observed to follow approximately the same collision sequence of events, to approximate the same changes in direction and spin-out patterns, as well as to reach about the same positions of rest.

4. The correlate collision experiments provided almost perfect replication of the car resultant acceleration data. This close correlation supports the value of carefully controlled collision experiments.

5. Peak accelerations of 10G were obtained by the striking car in X-57 and in X-62, whereas the corresponding peak accelerations for the struck car were 16G and 17G. These observations take on added importance when making comparisons between the performance effectiveness for the different restraint configurations worn in X-57 and X-62.

6. Post-impact movement of vehicles involved in intersection collisions may be categorized as follows:

   (a) The car spins and then rolls on its wheels an additional distance before coming to rest, or
   (b) The car starts to spin at impact approaching a broadside skid (older models of cars may overturn at this point, as was observed in the Series I intersection collision experiments) as it comes to rest, or
   (c) The car's heading is altered by impact but it continues thereafter, to roll towards its position of rest.

Speeds at impact, position of impact and to a lesser extent the respective types of cars involved are the principal independent variables operating to modify collision dynamics.

7. The dispersal of collision debris covered approximately the same area for these correlate experiments. However, the centroid of the debris area was substantially remote from the point of impact.

Collision Generated Skids and Gouges

8. (a) Deviation skid marks, when correctly interpreted, are useful in identifying vehicle position on the roadway at the time of impact. A deviation skid mark is made only during collision:

      (1) As a result of the tire being abruptly stopped or nearly stopped by intruding structure of the opposing vehicle as the wheel is crushed rearward and frequently sidewise, or as a result of a side impact. When the brakes have been previously locked up, the deviation skid characteristics are most conspicuous, or
      (2) As a result of the distressed tire being overridden by the other colliding vehicle making the deviation skid blackest because this places additional load on that tire.

   (b) Non-braked brush skids are generated by tires on the advancing side of the arc that the center of mass of the car is following. Tires on the trailing side may carry a car load insufficient to generate observable rubber brush marks on the pavement. At times, these tires are entirely off the pavement.
   (c) In addition to car rim flanges, undersides of bumpers or fractured bumper

supports and underbody sill-metal or frames occasionally are forced into the pavement leaving gouge marks.

(d) Correlation of these pavement gouges with abraded metal components found on the wrecked vehicle often provide an objective basis for establishing the position of the car when those pavement gouges were generated.

(e) Pavement gouges may be made by the damaged vehicle at its position of impact, or on its way to its position of rest, or both.

Post-Impact Retardation of Vehicles

9. For these intersection collision experiments, the average coefficients of friction were calculated for the uniform, level, clean and dry asphalt surface on which the collision experiments were conducted by evaluating four-wheel locked skid tests made over the same speed range as used for the collision experiments.

(a) The average coefficient of friction for locked skidding was 0.75.

(b) When the car is in a broadside skid, the effective coefficient of friction may exceed the locked wheel skid coefficient of friction over the same surface. This will depend, however, on the extent of rim-gouging, which may occur even though the tires remain fully inflated, and also on whether the car body-sill contacts the pavement.

(c) Such car-metal-to-road contact will generate sparks that may induce post-collision fire and occasionally pavement scrape marks will be visible following the collision.

(d) This car-to-road contact is often more evident, however, by inspecting the car rim flanges and body-sill areas for pavement abrasions.

(e) Examples of specific value for the average effective coefficient of friction for cars primarily undergoing broadside skidding are $f = 0.7$ for the struck car of X-57, $f = 0.6$ for the struck car of X-58, and $f = 0.9$ for the striking car of X-61. The deviation of these values from the locked-skid coefficient of 0.75 for this surface has been explained in connection with car-metal-to-pavement contact and the other factors previously described as accompanying these intersection collisions.

(f) During spin-out, as the car's heading comes into alignment either with the direction (or the reverse direction) the car is moving, the effective coefficient of friction diminishes substantially—as would be expected. Crippled wheel suspension, collapsed frame structure, or driver braking may singularly or in combination act to prevent this coefficient from approaching zero.

Damage Patterns and Repair Costs

10. For these correlated experiments, and with respect to both the striking and struck cars, the location, extent, and nature of damage for the corresponding cars provided excellent correlation. Mutual intrusion for the striking car's windshield as it crushed towards the non-impacted side of the struct car measured 1.9 ft for X-57 and 2.0 ft for X-62. The collision damage sustained by the cars provides a good indication of the relative speeds of the cars at the instant of impact. However, other factors such as the relative weights of the cars, their impact configuration, and secondary or tertiary collisions must also be considered for speed evaluations.

11. With respect to cost of repairs, the average of three estimates received for the striking cars of X-57 and X-62 were $710 and $670, respectively; the corresponding struck car estimates were $830 and $970, respectively.

Door Latch Failure

12. Three conditions acting separately or in combination, may account for the door opening in X-62 against the transverse inertia forces operating during collision acceleration:

(a) The front seat was observed being pushed to the right against the right front door as the striking car crushed into its left side,
(b) Tension-failure action of the latch, as a result of excessive car-body bending forces during impact,
(c) Possible reduced latch-holding efficiency, as a result of the higher impact forces this car was subjected to during a previous 40-mph collision experiment.

13. Prior collision abuse, unless completely repaired, may lead to reduced door latch holding efficiency. With respect to X-62, although facilitated by seat thrust and car body bending forces, the reason the right front door opened for X-62 and did not open for X-57 was attributed to prior collision abuse. Special attention during repair to restore door latch operation to its original effectiveness is vitally important to subsequent passenger safety. Without belts, at least the front seat passenger of X-62 would have been ejected and quite likely run over by his own car.

Side-Window Glass

14. In these correlate experiments, tempered side-window glass performance was compared with laminated side glass.

(a) Tempered glass fracture extends almost instantaneously throughout the entire sheet and is generally accompanied by a complete dispersal of glass fragments.
(b) Laminated glass may fracture with the appearance of a single localized crack or it may fracture with a total breakage accompanied with varying amounts of fragment dispersal.
(c) The resistance that tempered glass exerts against a striking object terminates at fracture. Edge prestressing of tempered glass may rupture the glass prior to head impact or may lower the threshold for rupture by head impact.
(d) For laminated glass, impact resistance continues to function following fracture until the plastic interlayer is ruptured.

15. The following are three causes for side-window breakage during intersection collisions:

(a) Abrupt lateral acceleration of the window frame and glass into the motorist's head,
(b) Comparable action into the motorist's shoulder by the window sill, sufficient to prestress and break the window glass,
(c) Encroachment by the striking car into the struck car side below its window level, or direct contact with its window.

16. The impact of the driver's head shattered out the left front tempered window of the struck car during X-57; the corresponding laminated glass was fractured during X-62 but remained in place.

(a) The tempered glass accounted for 53G peak acceleration, whereas the laminated glass accounted for an 82G peak acceleration. Edge stressing during the initial phases of impact reached a value sufficient to crack the tempered glass and the glass ruptured out completely from its mount. A similar crack or series of cracks developing in the laminated glass did not appreciably diminish its resistance to head impact because the cohesive properties of the plastic interlayer continue to function following initial cracking.
(b) The UCLA-ITTE laboratory studies excluded edge stress concentrations that were identified with full-scale collision studies. Accordingly, the laboratory impact velocity corresponding to the full-scale exposures that produced a peak simulated head acceleration of 83G for laminated glass

produced a corresponding peak acceleration of 130G for tempered glass of the same thickness.

(c) The poor correlation between simulated head impacts of 53G for the full-scale crash, and 130G for laboratory study, provides additional data indicating the sensitivity of tempered glass to coincidental edge stressing during collision.

(d) The close correlation between the simulated head impact peak acceleration of 82G obtained by full-scale crash tests and the simulated head impact of 83G obtained by laboratory tests demonstrates the relative insensitivity of laminated glass to coincidental edge stressing during impact.

17. The following concern side-window glass breakage for these correlate experiments:

(a) The struck car side-window glass was tempered for Experiment 57 and both left rear and left front windows were shattered with greater than 50 percent of the glass dispersal forced inside of the car,

(b) In Experiment 62 under the same experiment conditions, laminated side-window glass was installed. Both front and rear side-window glass fractured extensively but remained in place, except for about 10 percent of the glass for the upper forward corner of the left rear window that dislodged and was found inside the rear seat compartment.

18. With respect to the tempered side-window glass failures, it was found that each side-window glass ruptures into more than 50,000 particles and that most of the particles had a diameter of less than 0.01 in. Not all of the particles separated as they dispersed and some heavier pieces, 2 to 3 in. in diameter, were seen accompanying this glass "cloud" as it shot across the car interior at speeds sometimes faster than that of the striking car. However, the average particle size of tempered glass is substantially less than that of laminated glass. Also, partial failures of laminated glass leave glass fragments bonded to the window frame that may be extremely hazardous to motorists contacting them.

Simulated Motorist Exposures

Adults

19. The kinematics and impacted forces of the anthropometric dummies for corresponding seat positions of these correlate experiments followed a consistent pattern except when influenced by varying types of motorist restraints or by differences in the car interior surfaces encountered.

20. For intersection-type collisions, the lap belt peak-load values may be expected to increase in a rather uniform manner for corresponding increases in impact velocity. Having a tensiometer at each end of the lap belt tends to compensate for the effects of lateral body loading components. This occurs because the tensiometer towards which the body is thrown may show a reduced tension, whereas the other unit, for this same body displacement, would show a correspondingly increased value.

21. Driver interaction with the car's interior provided valid comparative data for these correlate experiments inasmuch as the car's collision performance was found to be substantially the same despite a prior divergent history of collision.

22. Passenger shoulder strap tensiometer readings are valid only with respect to their specification of the tensile force acting at the doorpost anchorage. They do not indicate the actual force magnitude applied to the motorist, although they do provide a useful indication of the relative severity of collisions. The reasons for this limitation were set forth in the text.

23. When the motorist is seated next to the impacted side, his seat belt tensiometer values should not be regarded as realistic data for the following reasons:

(a) The motorist is pinned against the side of the car because of the abrupt acceleration the car receives from the striking car; minor variations in the snugness of his belt are likely to lead to substantial differences in readings obtained under otherwise comparable conditions,

(b) The initial lateral shift of the driver's hips towards the striking car will be restricted by the intrusion of the striking car and this form of restraint is not registered by the tensiometer,
(c) If intrusion is sufficient, the driver may be displaced in the direction the striking car is advancing, thereby developing tensiometer readings that reflect body displacement forced by the intruding car, rather than true body inertial forces,
(d) High-speed motion picture camera coverage showed one dummy shifting during impact to load the other dummy and their respective restraints would reflect an underload for the shifting dummy and an overload for the struck dummy.

24. The slip-link feature for the shoulder cross-strap and lap belt combination allowed hip inertial forces to be transferred, in part, to increase the restraint applied to the chest. As a consequence of this slip-link feature, in the majority of the UCLA intersection collisions directed toward the shoulder cross-strap belt side affording reduced protection, the dummy appeared to be, nevertheless, rather well restrained.

25. The right front seat occupant's sideward movement for the struck car of the two 30-mph correlate experiments was approximately the same for the dummy wearing a shoulder cross-strap and lap belt combination as for the dummy with only the lap belt. Some allowance should be made, however, for the reduced degree of spinal articulation common to anthropometric dummies as compared with their human counterparts.

26. In Experiment 62, the right front seat passenger of the struck car would subsequently have been ejected had he not been wearing a lap belt. Additional protection is provided during forced door openings when the motorist is wearing a shoulder strap and lap belt combination because his head and chest are restrained from flailing outside the protective cabin enclosure where direct impact with another vehicle or a fixed object may occur.

27. When the shoulder cross-strap is anchored to the center doorpost, substantially above shoulder height, severe neck lacerations can result from this strap functioning to restrain upper torso ejection. Accordingly, the upper anchorage point for this strap should not be above average shoulder height; this fact points out the importance of separately designed restraints for children.

Children Motorists

28. Simulated three-year-old and six-month-old children provided preliminary evaluation of several protective restraint configurations:

(a) Simulated children riding in the struck car were exposed to greater potential injury than when riding in the striking car.
(b) The rear seat passenger compartment provides a less hostile environment during these collisions than does the front seat area, primarily because of the adverse forces that the front seat adult may inadvertently apply to the child during collision. Additionally, the more lethal nature of driving controls and the instrument panel as contrasted with the upholstered rear seat compartment points up the other reason why the rear seat is safest for children.
(c) A child standing behind the front seat in the struck car during an intersection collision is subjected to probable extreme abuse. Under identical collision exposure conditions, except with the child dummy sitting in the center of the seat on a cushion and restrained by an adult-type lap belt, the child avoided direct contact by collapsing structures and collision forces were applied to the child through the restraint in a non-injurious manner.
(d) When the three-year-old child dummy stood behind the front seatback on the right side for the striking car, the exposure was substantially less than the comparable position for the struck car because the striking car was abruptly jerked to its left tending to pin the child against the right side of the car in a not too abusive manner. Had the struck car been traveling in the opposite direction, the child would have been thrown violently to her

left paralleling the front seatback. Inasmuch as the motorist does not choose the type of intersection collision he becomes involved in, it is not recommended that children be allowed to stand behind the front seatback.

Infant Motorists

29. For the infant up to six months old, a bassinet was observed to provide effective protection, particularly when its long axis paralleled the long axis of the car and when it was positioned behind the center of the front seatback. The tie-down straps provided with most bassinets, when properly attached, greatly increase infant protection during collision. Additional protection is afforded by the use of a covering such as a net to prevent the infant from being thrown out of the protective confines of the bassinet. Older children occupying the rear seat area should wear restraints not only for their own protection but also to prevent their being thrown against the infant's bassinet during impact.

30. Small children from about six months and older may receive adequate protection from well-designed restraining harnesses. The protective harness for small children should include the following features:

(a) A harness configuration that applies forces approximately equally to the shoulder and pelvic girdles.
(b) A slip-loop feature that permits the small child to stand, sit, or lie down on the seat while continuously restrained.
(c) An anchorage that prevents the seatback from shifting forward during impact. This anchorage can at the same time be used to limit the motion of the small child, but must be arranged to prevent the seat inertial forces from being applied to the child.
(d) Attachment of child restraints to the car seat should be made only where the car seat is anchored by special devices to the floor pan.
(e) Restraints that apply forces to the viscera or adjacent areas of the body midway between the pelvic and shoulder girdles are dangerous and unworthy of consideration.

Belt Elongation

31. For these intersection collision exposures no belt elongation or permanent set occurred. This was because the forces applied to the safety restraints did not approach the loop strength limits prescribed for these belts. These protective restraints met the strength requirements prescribed by SAE. Properly restrained, the 30-mph intersection collision is survivable, except possibly for motorists sitting next to the impacted side of the struck car.

Data Reduction

32. Reduction of large volumes of impact-type data has been successfully accomplished by computer techniques. The process of extracting the square root of the sum of the squares and several tens of thousands of triaxial data points, of applying the various channel-scaling factors and of regraphing to a common scale is a laborious task quite appropriate for the digital computer. The program that has provided satisfactory data reduction uses a sequence of overlapping parabolic curves for computer presentation of the accelerometer curve. This procedure enabled the computer to follow faithfully the sharp peaks occurring at irregularly spaced intervals that are characteristic of acceleration patterns generated during collision.

REFERENCES

1. Severy, D. M., Mathewson, J. H., and Siegel, A. W., "Automobile Head-On Collisions, Series II." SAE Trans., 67: 238-262 (1959).
2. Severy, D. M., Mathewson, J. H., and Siegel, A. W., "Automobile Side-Impact Collisions, Series II." Paper, Soc. of Automotive Engineers National Automobile Week Session, Detroit, Mich. (1962).

3. Severy, D. M., and Snowden, W. H., "A Review of the State of Knowledge and Research Concerning Laminated and Tempered Safety Glass in Motor Vehicles." Special Report, Institute of Transportation and Traffic Engineering, Univ. of Calif., Berkeley and Los Angeles (Nov. 1, 1962).
4. Radt, H. S., and Milliken, W. F., "Motions of Skidding Automobiles." Society of Automotive Engineers Preprint 205A (June 1960).

Development of Crash Research Techniques At the General Motors Proving Ground

K. A. STONEX, Assistant Engineer-in-Charge, Technical Liaison Section, General Motors Engineering Staff, Warren, Mich., and
P. C. SKEELS, Engineer-in-Charge, Engineering Services, General Motors Proving Ground, Milford, Mich.

•VEHICLE DESIGNERS in General Motors have been interested in crash research for more than thirty years. A few tests were conducted in the early 1930's to evaluate the integrity of the body structure at the time of the adoption of the all-steel turret top and to get some information on collision-type tests under controlled conditions that could be correlated with highway accident damage.

Figure 1 shows an early roll-over test conducted by driving the car onto a spiral ramp located at the top of a hill. This test was conducted in 1933 (1). Figure 2 shows a barrier impact test conducted in 1934. In this test, the driver aimed the car at the barrier at a speed low enough so he could get out of it just before the impact. Figure 3 shows a level roll-over test which was conducted by driving the car into a skid on a level sod field.

These tests were made before the development of high-speed cameras or precise, high-response accelerometers; the results were in terms of visual observation made at the time and the damage to the vehicle. Because most tests of this nature look alike to the unaided eye and the gross damage on repeated tests is quite similar, it did not seem to be necessary to conduct them on successive yearly models.

After World War II there began a growing intensification of engineering effort in body design, and changes were evaluated much more carefully than had seemed necessary in the development of prewar designs.

The 1933-type spiral ramp test was deficient in that there was almost no forward speed; in most roll-overs in highway accidents there is an appreciable forward velocity component, and much of the damage may be done as the roof or corners of the top strike the ground at high velocity of slide over the usually rough roadside at nearly the speed of the car before the accident occurred. It became necessary to gain

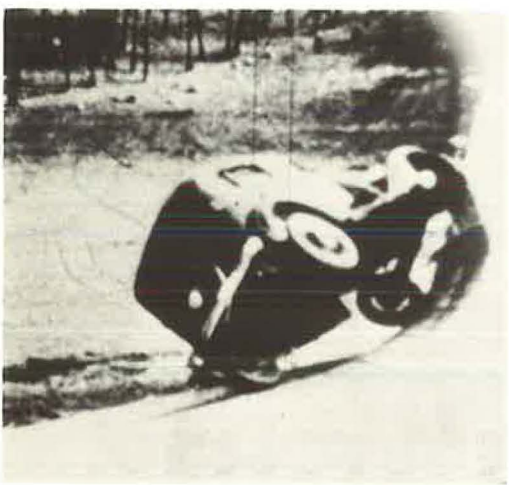

Figure 1. Spiral ramp roll-over test, 1933.

Figure 2. Early barrier impact test, 1934.

Paper sponsored by Committee on Highway Safety Research.

Figure 3. Ground level roll-over test on 1935 turret top body.

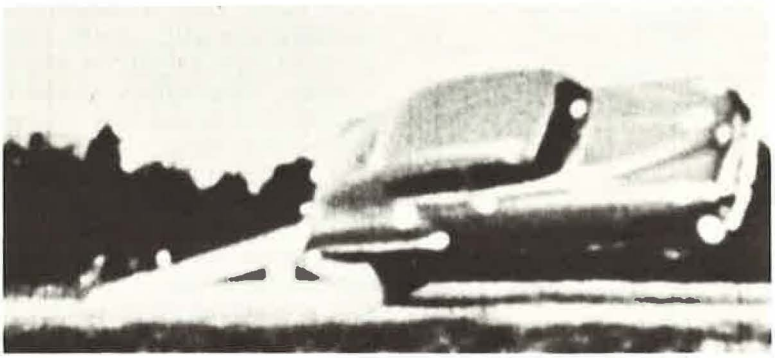

Figure 4. Ramp roll-over of 1948 car.

Figure 5. Ramp roll-over test on 1956 car.

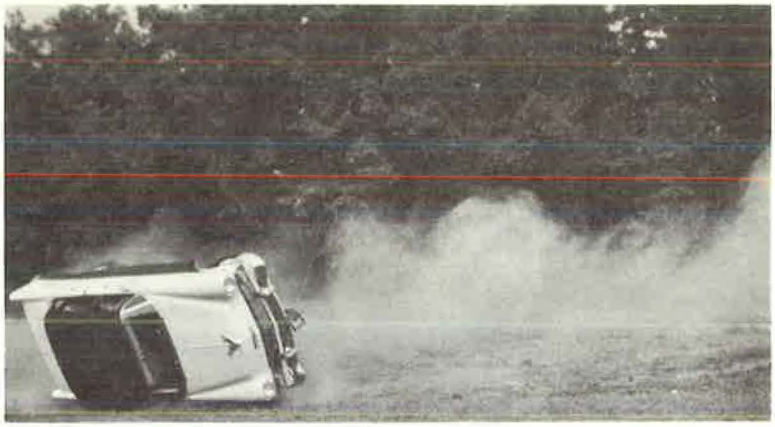

Figure 6. Ground level roll-over on side slope.

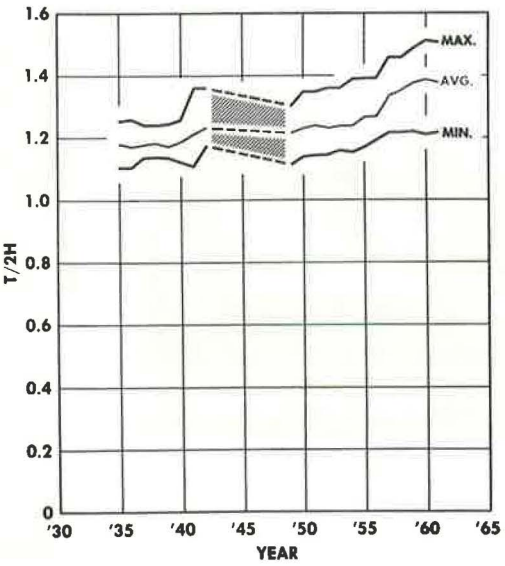

Figure 7. Trend of stability factor from 1935 to 1962.

some experience with a roll-over technique in which the forward velocity was preserved.

Figure 4 shows a roll-over test of a pilot model 1948 car conducted by towing an offset car with a quick-release mechanism so that one pair of wheels could climb a ramp. This technique was relatively effective, and it was used frequently for eight or ten years.

Figure 5 shows a 1956 car. This ramp roll-over test is effective in evaluating the effect of forward velocities during roll-over accidents; however, it is somewhat unrealistic in the sense that the car is lifted 4 or 5 ft off the ground, which is quite unusual in highway accidents. The test results were not as reproducible as desired, and it came to be recognized generally that there was need for a technique that would reproduce the conditions more representative of a typical ground-level roll-over.

Figure 6 shows a ground-level roll-over; the roll-over is accomplished by towing the car up to speed by means of a quickly detachable towing mechanism, then quickly turning the front wheels to the full left-turn position by means of a remotely controlled steering device. On a suitably steep side slope with proper ground conditions, cars can be rolled over with considerable success and reasonably good reproducibility.

The objective of roll-over testing is to establish the sturdiness of the roof and body pillars, to evaluate door lock designs, and in a preliminary fashion, at least, to learn something about the injury-producing potential of interior components. The development of a ground-level roll-over test technique is difficult because the progressive lowering of the over-all height has caused a significant reduction in the height of center of gravity and a corresponding increase in stability.

Figure 7 shows the trend of the stability factor since 1935 of the best, the average, and the poorest car in the fleet at the Proving Ground. This stability factor is the ratio

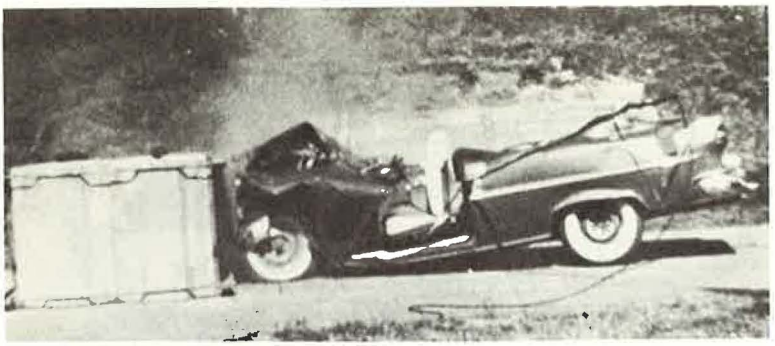

Figure 8. Barrier impact test.

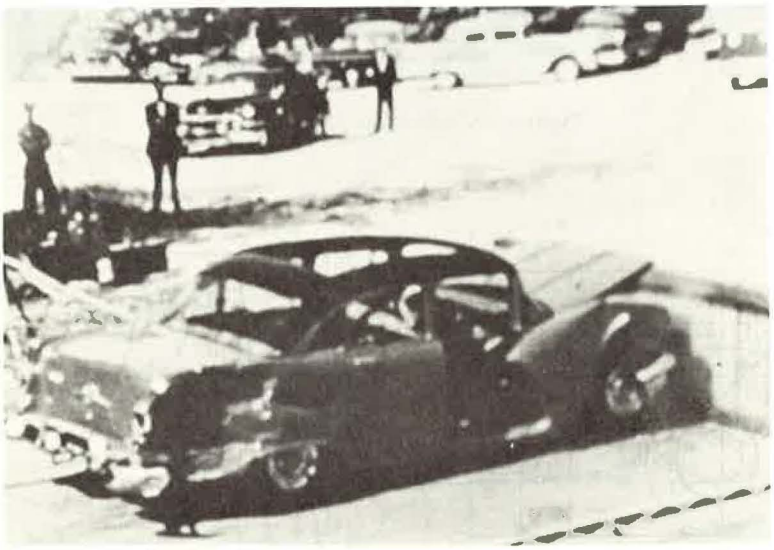

Figure 9. Barrier impact test.

of one-half the tread to the center of gravity height, and it changes most rapidly with the change in center of gravity height (2).

Because the head-on crash or direct impact with a solid obstacle is such an important consideration in highway safety, it is necessary to have a factual background to determine what happens, to gain an understanding of the potential for injury reduction through design, and to arrive at the scale relationships between severity and speed at impact.

Figures 8, 9, and 10 show the results of barrier impact tests. These were run by letting a remotely controlled car coast down a steep grade and collide with a massive concrete barrier. In these tests the impact speeds were approximately 30 mph, and the deceleration rates on the undeformed part of a car frame of the order of 30g. The total and catastrophic nature of these tests leads the investigator to believe that the threshold of serious and probably fatal injury is far below normal highway speeds; it leads to the conclusion that it is impossible to provide secure protection during impacts

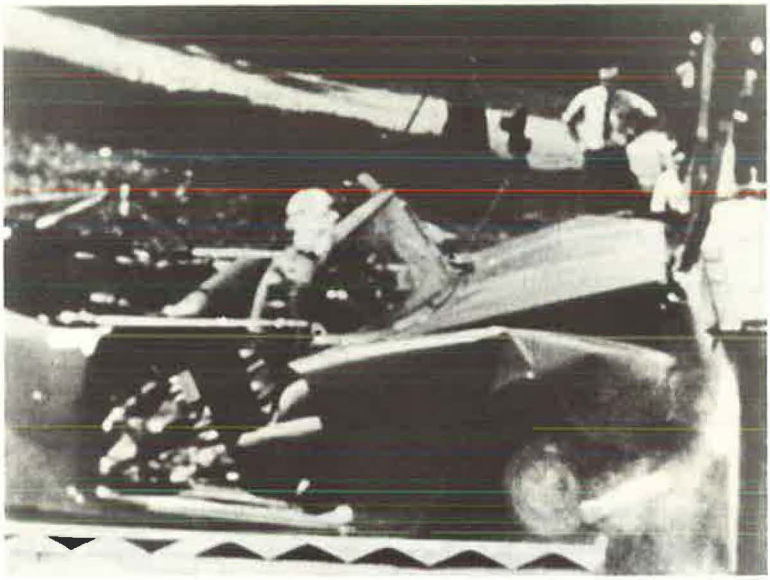

Figure 10. Barrier impact test.

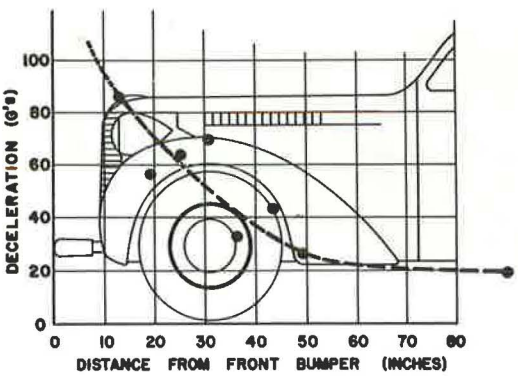

Figure 11. Deceleration during impact with fixed object as function of distance back of front bumper.

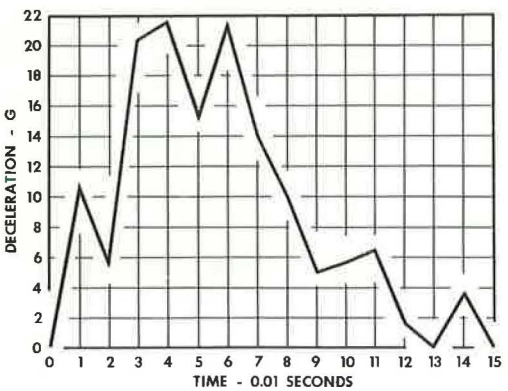

Figure 12. Typical deceleration-time curve, barrier impact test.

of this nature by any amount of design modification, or by the use of any restraining devices that the average customer would be willing to use.

There is extensive literature on tests of this nature, including car head-on and side impact accidents contributed by Mathewson and Severy and others (1, 3). Of considerable interest is a typical result from their work (Fig. 11). This shows the deceleration during impact with a fixed object as a function of the distance back of the point of impact. The deceleration falls from a value of well over 100g at the point of impact to a nearly stabilized value of 20g at points more than 60 in. back of the point of impact. This reduction in deceleration of more than 80g illustrates the energy-absorbing capability of the front-end chassis and sheet metal; this is a most effective device, and it is probably much more satisfactory than any practical hydraulic shock absorber installation would be.

Figure 13. Remotely controlled tree impact at 35 mph.

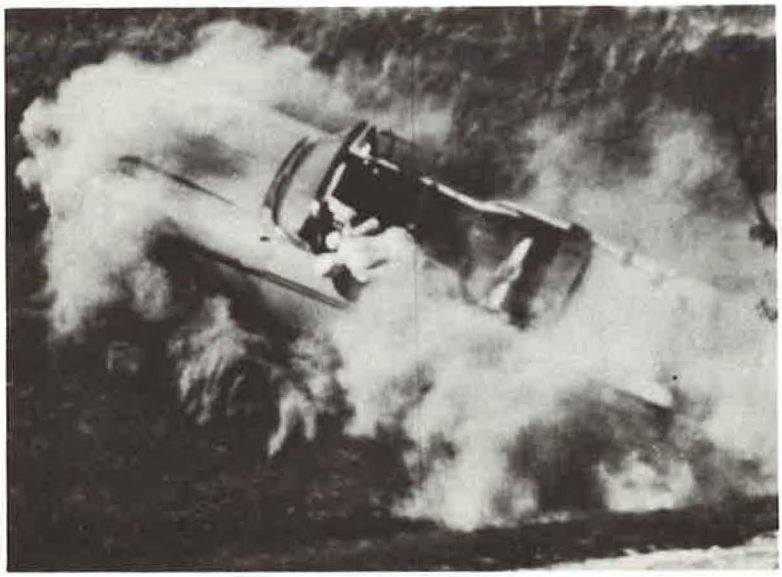

Figure 14. Impact test, ditch with 2:1 back slope.

This absorption characteristic is shown in another way in terms of a deceleration-time curve as in Figure 12. This shows a rather slow rate of rise of deceleration. In fact, nearly one-third of the time of the impact has passed before the deceleration reaches the peak. This is a characteristic of the direct impact tests that is found many times.

Figure 13 shows another type of impact characteristic of the single-car, non-collision accident. This car was driven by remote control at 35 mph against a tree of medium size. The severity of the impact at such a low speed is demonstrated graphically, and the energy-absorbing deformation of the front-end chassis and sheet metal is again demonstrated.

Figure 15. Proving Ground crash test against 2:1 bank.

Figure 16. Car passing through ditch, bumper strikes ground.

There are other types of roadside crashes of extreme severity of operation where some background is required to evaluate the potential of design improvement.

Figures 14 and 15 are two views of the same test where a remotely controlled car was driven off the road at 35 mph into a 2:1 back slope (4). It is evident that the injury threshold in these conditions can be raised materially by the use of simple restraining devices such as seat belts. On the other hand, much more interesting is the fundamental treatment of these situations, which is to eliminate the hazardous characteristics of the roadside. This has been discussed at an earlier meeting of the Highway Research Board (2) but Figures 16 and 17 follow the last two as a simple transition from a very dangerous roadside (Figs. 14 and 15) through one of moderate severity (Fig. 16) to one so gentle that the car can be driven through it easily at 60 mph (Fig. 17). Present Proving Ground standards are to design for a computed severity of no more than 0.5g at design speed and to remove obstacles out to 100 ft on all roads where operating speed is expected to be equal to rural highway speeds.

Figure 17. 60-mph test, driving through flat-bottom ditch.

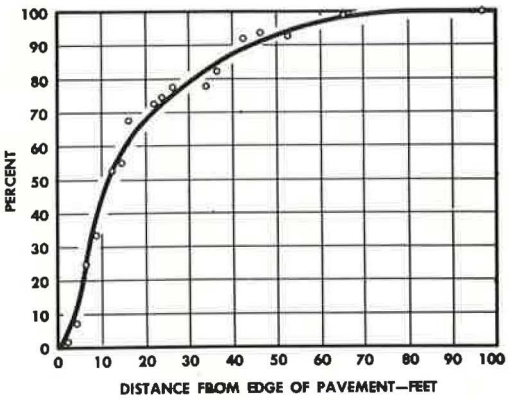

Figure 18. Percentile distribution of 56 Proving Ground "accidents" as function of distance from edge of road.

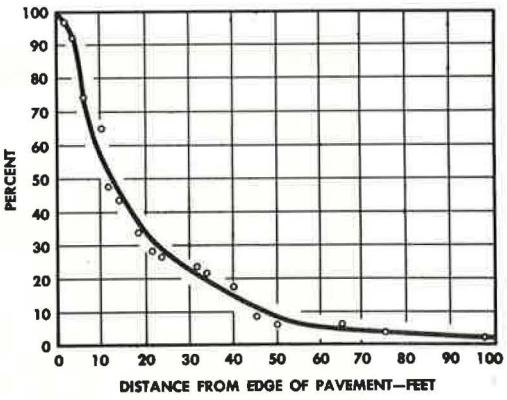

Figure 19. "Hazard" curve, Proving Ground "accidents."

Consideration of the elimination of roadside obstacles invites the question of what is an effective and practical width of the traversable area. Because the Proving Ground roadsides have been modernized, there have been 56 cases where the car left the road; in none of these cases was an obstacle struck and none resulted in injury to the driver; Figure 18 is a percentile distribution of the distances from the edge of the pavement to the point of maximum deviation; in most cases the vehicle was stopped, but in several the driver merely turned back onto the road and continued on his way. Figure 19 shows the same data reversed in the form of a "hazard" curve. The maximum distance or deviation exceeded 50 ft in only 10 percent of the cases and 25 ft in only 25 percent of the cases. There is little general relationship with speed; however, the most extreme points are associated with rural highway speed levels. Taken at face value, these data suggest that provision of traversable roadsides 50 ft wide would eliminate 90 percent of the non-collision serious accidents.

Figure 20 is a hazard curve showing the distribution as a function of distance of impacted obstacles in 82 fatal accidents reported in the Cornell Automotive Crash Injury Research study (5).

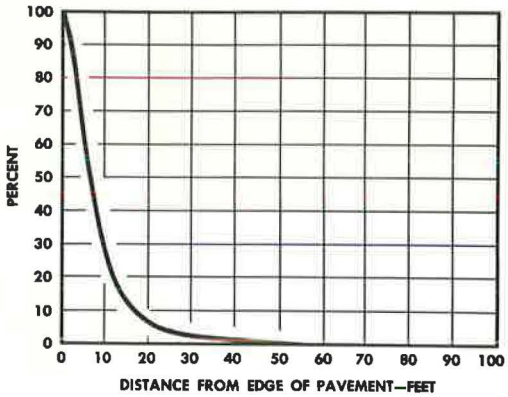

Figure 20. Distribution of impacted roadside obstacles vs distance from edge of pavement (from 82 "accidents" in Cornell study).

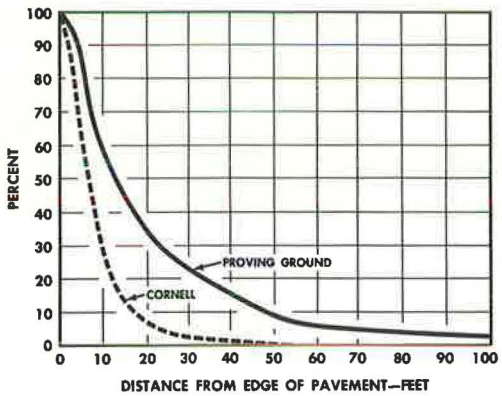

Figure 21. Comparison of Proving Ground and Cornell "hazard" curves.

Figure 22. 35-mph guardrail test showing remote control.

Figure 21 is a comparison of these two hazard curves. This shows that the cars in the Cornell group struck obstacles, with injurious and fatal results, at distances considerably less than the maximum deviations of the Proving Ground drivers.

The Proving Ground hazard curve should be considered as a first approximation to the deviations drivers will make on a traversable roadside, and it may be regarded as a first approximate guide to the determination of an effective and practical width of traversable area.

Another type of highway crash which occurs too frequently is the collision with a guardrail. This situation also required some background evaluation. Although it is easily possible to raise the threshold of injury in certain types of guardrail collisions by the use of packaging devices such as seat belts and crash helmets, other types are

Figure 23. 35-mph guardrail test remote control.

Figure 24. 65-mph guardrail test.

closely similar to collision with a tree, and no effective vehicle design treatment exists. It was found that here, too, there was tremendous room for improvement in guardrail design and installation and that inexpensive modifications would eliminate the most serious guardrail deficiencies. This work has also been discussed, but the highlights are relevant to this paper (6, 7).

Figure 22 shows a remote-control technique in making a test of guardrail installation at 35 mph.

Figure 23, run at 35 mph and at a 33^{0} angle of impact, shows a failure which is typical of the standard installations. The bolt in the last post pulled through the guardrail, allowing it to lose tension and fail completely.

Figure 24 was taken during a test at 65 mph on a design which had shown satisfactory results at 35 mph. Here too, the end pulled loose and the guardrail failed, resulting in a very serious accident.

Figure 25. Successful 65-mph guardrail test.

Figure 26. Standard guardrail end impact.

Figure 25 shows a successful test at 65 mph; this installation redirected the car with only a slight reduction in speed.

Figure 26 shows the result of a direct impact against the end of the guardrail. In some cases, if the collision occurs at one side or the other of the engine block, the car is impaled on the guardrail. In accidents of this type at normal highway speeds, it seems impossible to provide secure protection for the occupants by any means within the control of the vehicle designer. However, Figure 27 shows a satisfactory solution to the problem. Here the end of the guardrail is buried in the back slope and anchored in the concrete block, thus preserving tension from the very beginning of the guardrail and eliminating the hazardous end.

In automotive engineering development work, the interests are generally in one component at a time or, at the most, in a very few components, and the total destruction during barrier impact tests at speeds even as low as 30 mph is generally out of keeping with the objectives of such a development test. It would be extravagant of both time and material to attempt the evaluation of several seat belt anchorages by barrier impact tests.

Figure 27. Guardrail buried in back slope and anchored in concrete block.

Figure 28. Proving Ground snubber test technique.

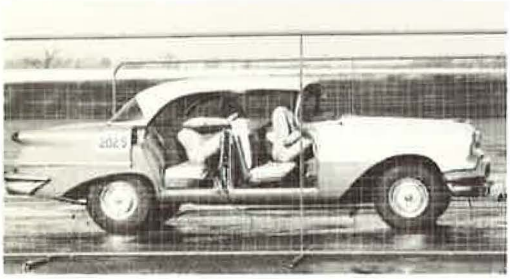

Figure 29. Snubber test conducted at 5g.

Figure 30. Snubber test conducted at 10g.

Figure 28 shows a practical tool for such development work. This is a heavy-duty hydraulic snubber developed in 1955. Relatively precise control is provided from 3g to 35g by regulating the air pressure behind the relief valve and by choosing the test speeds carefully. The engine and transmission are removed from the test vehicle to reduce the total energy. A heavy cable is attached to the car at the center of gravity

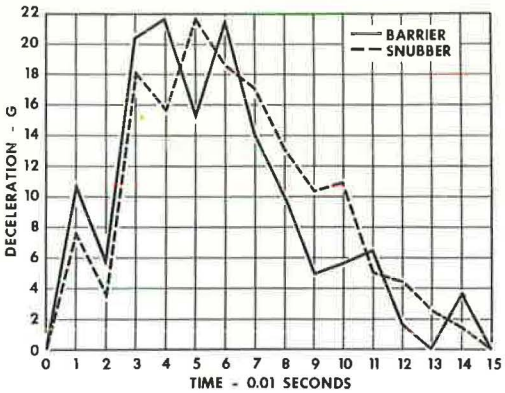

Figure 31. Barrier and snubber comparison.

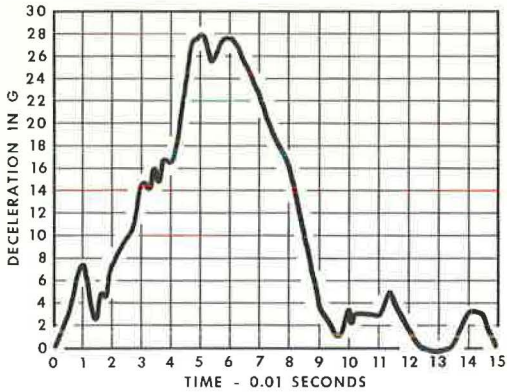

Figure 32. Car-to-car deceleration (Severy data).

Figure 33. Snubber test using current platform.

height and threaded through a yoke at the back of the snubber. A steel slug on the end of the cable bottoms on the yoke as the car is towed at test speed, and the car is stopped at a predetermined rate.

Figure 29 shows a typical test where the car is stopped at 5g, and Figure 30 shows a comparable test at 10g. With this device it is very easy to make repeated tests, or a series of tests, at intervals of only a few minutes and without damage to the test vehicle chassis. This device gives a deceleration-time curve very closely similar to that measured during barrier impact tests (Fig. 31). For comparison, a typical deceleration-time curve from Severy's work is shown (Fig. 32).

For a great deal of component testing, such as seat belt anchorages and seat anchorage, only the floor of the car body needs to be involved. Figure 33 shows a simplification of the snubber technique where a test bed and a platform are substituted for the test car; this makes it possible to make comparative tests of a number of design proposals in quick succession.

There are simplifications of other component test programs. One such example is shown in Figure 34. Here a series of steering wheel designs can be screened in the

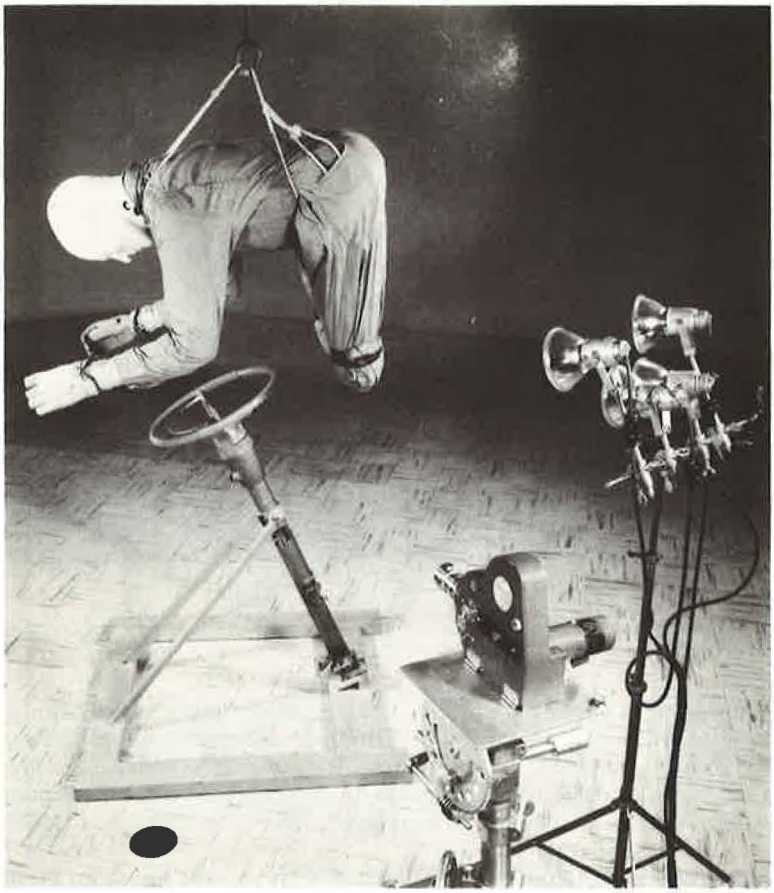

Figure 34. Steering wheel drop test.

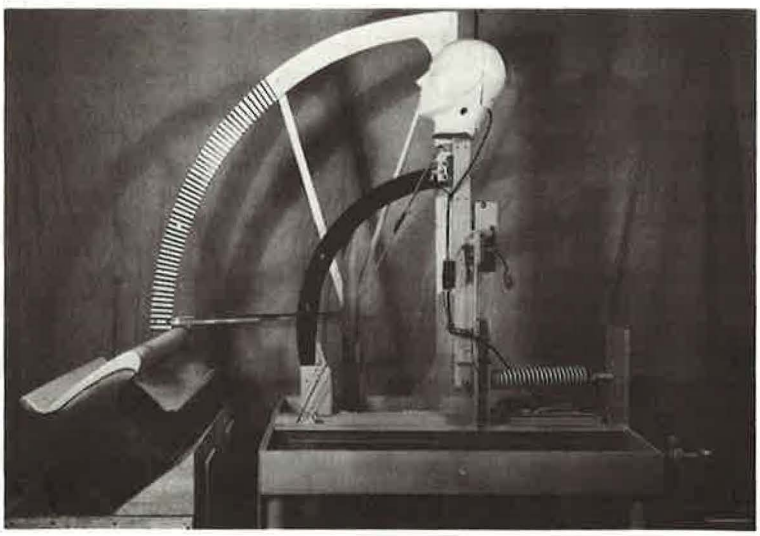

Figure 35. Head knocker test.

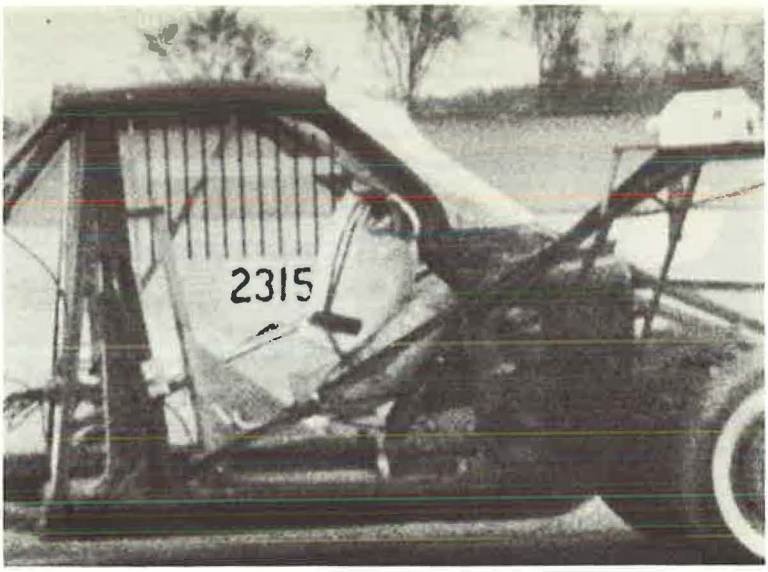

Figure 36. Windshield test.

laboratory by dropping a dummy on them. For more definitive evaluation, the best designs can be tested further when mounted in a car and subjected to the snubber test.

Figure 35 shows a relatively simple laboratory apparatus which may be used to evaluate various types of instrument panel pads or seat-back construction or other components which might be struck by the driver's or passenger's head during an accident.

For evaluation of windshield design, windshield frame and seat can be mounted on the snubber platform (Fig. 36).

The snubber technique has the inherent disadvantages of conducting tests with high transients outdoors. During cold winter weather, sunlight is lacking or weak; sunlight is essential because high-speed photography is the most valuable, single measuring device for this technique. Control is limited by the short stroke available, changes in viscosity of the hydraulic oil with temperature, and the difficulty of reaching exact towing speeds in the short available towing distance.

The volume of development testing in this general area made it essential to devise a facility that would be more conveniently located indoors so that programs could be carried on independent of weather and lighting conditions. The installation of an impact machine (shown in layout in Fig. 37) has just been finished. This is a scaled-up version of an accelerator available commercially that was developed originally for shock testing military components. This is a high-capacity, air-powered accelerating device which can be controlled very precisely within a range up to 50g; test components up to the size and weight of a complete automobile can be mounted on the bed in any orientation. Fixed lighting and camera installations are available for the most effective use.

The following are the general capabilities of the facility:

1. Lighting of 10,000 foot-candles which will permit photography up to 3,000 frames per second.
2. Air pressure up to 3,000 psi to supply operating power.
3. Operating force up to 200,000 lb.
4. Performance capacity exceeding 50g at 1,500 lb load or 20g at 5,000 lb load.
5. Stroke adjustable up to 5 ft.
6. Pulse duration 6 to 75 msec.
7. Pulse wave form variable by choice of metering pin.

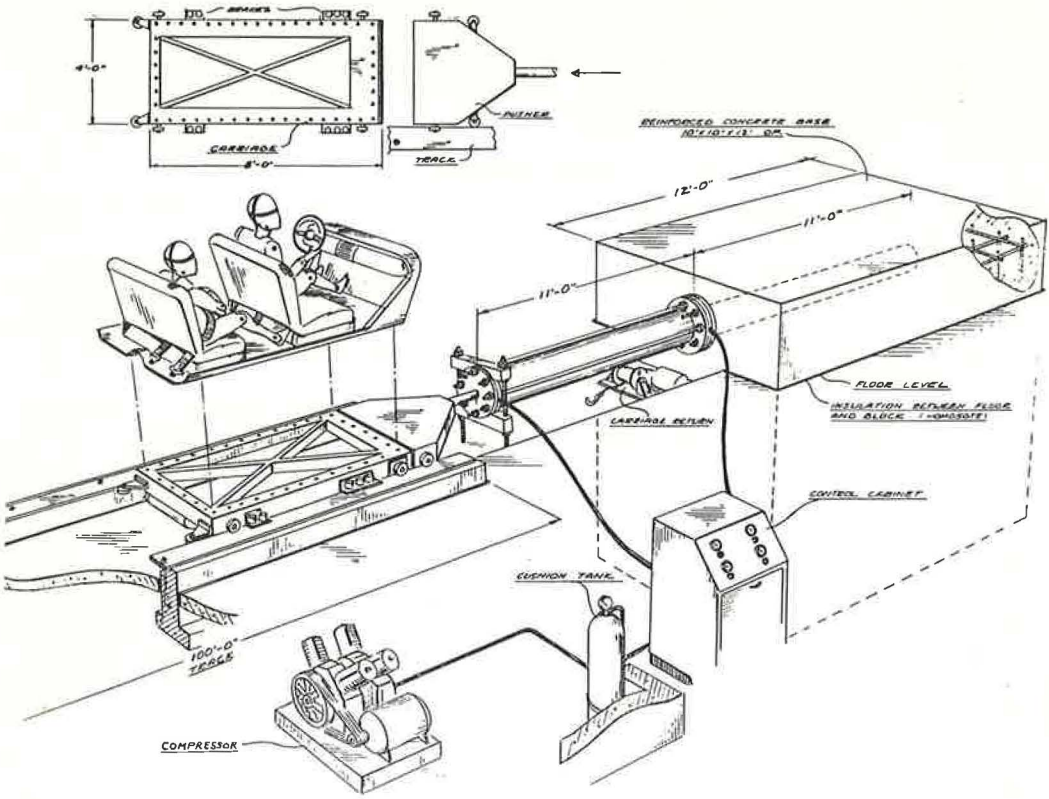

Figure 37. Impact machine layout.

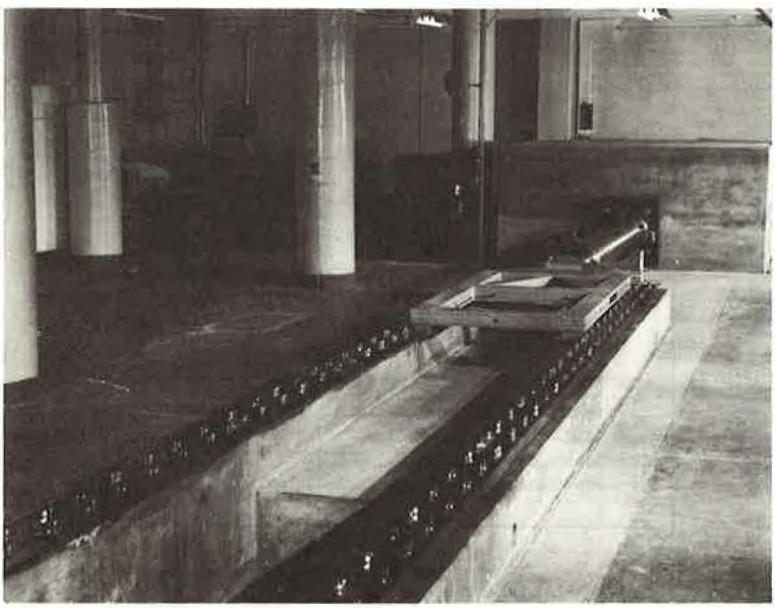

Figure 38. Impact machine.

Figure 38 shows the device. Unfortunately, there has not been time to accumulate data through the use of this facility. Typical test results will be discussed in a later paper, and a more complete description of operating principles and controls will be reserved until then. It will probably surpass any previous techniques in precision of control and the efficient use of test time.

REFERENCES

1. Stonex, K. A., "Vehicle Aspects of the Highway Safety Problem." Traffic Safety Res. Rev., 6:15-24 (June 1962).
2. Stonex, K. A., "Roadside Design for Safety." Proc., HRB, 39:120-156 (1960).
3. Mathewson, J. H., Severy, D. M., and Siegel, A. W., "Head-On Collisions, Series III." Society of Automotive Engineers Paper 211D (Aug. 16-19, 1960).
4. Lundstrom, L. C., "Safety Aspects of Vehicle-Road Relationships." Society of Automotive Engineers Paper 66B (June 8-13, 1958).
5. Stonex, K. A., "Vehicle Aspects of the Single-Car Accident Problem." Paper, 2nd Regional Conf. on "Single-Car" Accidents, Flint, Mich. (Oct. 18, 1962).
6. Cichowski, W. G., Skeels, P. C., and Hawkins, W. R., "Appraisal of Guardrail Installations by Car Impact and Laboratory Tests." Proc., HRB, 40:137-149 (1961).
7. Lundstrom, L. C., and Skeels, P. C., "Full-Scale Appraisals of Guardrail Installations by Car Impact Tests." Proc., HRB, 38:353-355 (1959).

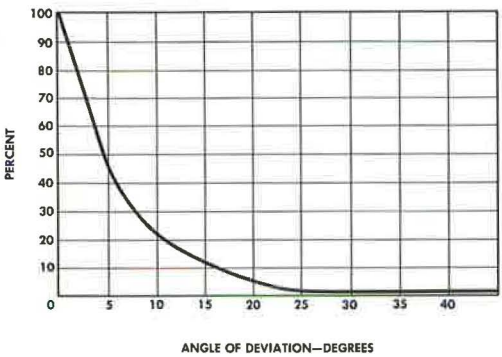

Figure 39. Percentile distribution of angle of vehicle encroachments.

Appendix

Since the preparation of this paper, data have been received from John Hutchinson, of the University of Illinois, from his study of median encroachment. The data include 91 cases observed primarily on Route 66, which is a divided highway with a 40-ft median.

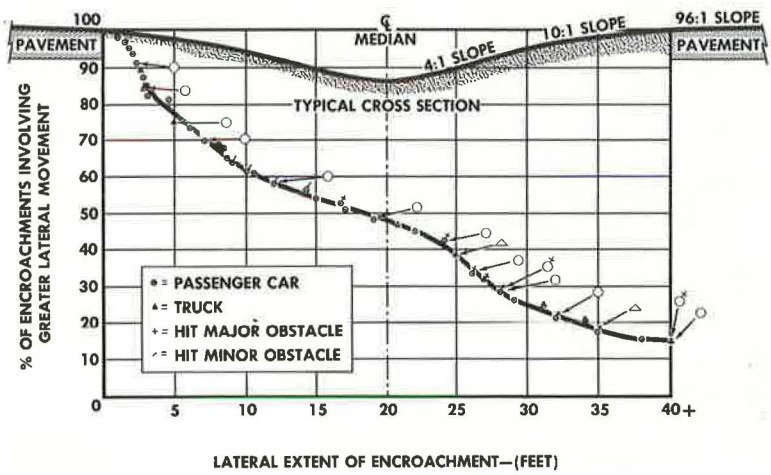

Figure 40. Distribution of median encroachments (Hutchinson).

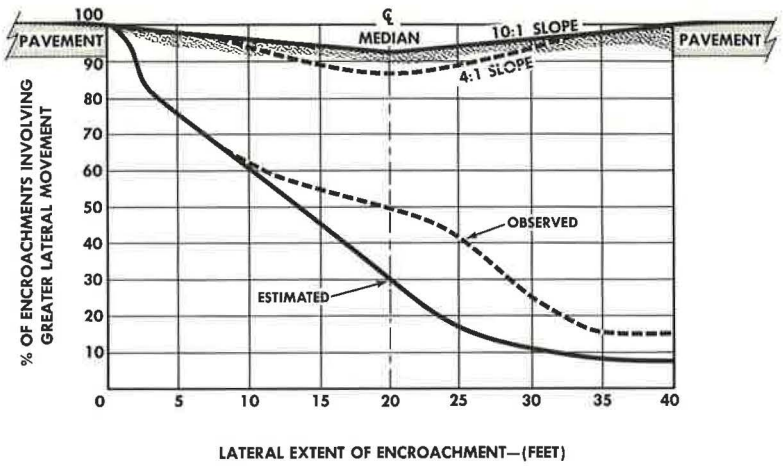

Figure 41. Distribution of median encroachments (Hutchinson).

Angles of departure, the lateral distance of encroachment and the length of travel in the median, among other things, were observed.

Figure 39 is a percentile distribution of the angle of departure. The 80th percentile is at approximately 10^0 and the 90th percentile at approximately 17^0; in other words, more than 80 percent of the vehicles left the pavement at an angle of less than 10^0.

Figure 40 is the distribution of lateral encroachment into the median. The passenger car data are designated by circles, truck data by triangles, multiple points by circles and arrows, and collisions with major obstacles by small crosses. The 80th percentile is at approximately 33 ft and the 90th percentile is more than 40 ft; that is, 80 percent of the vehicles entered the median at distances less than 33 ft but more than 10 percent of them crossed the median onto the opposing traffic lane.

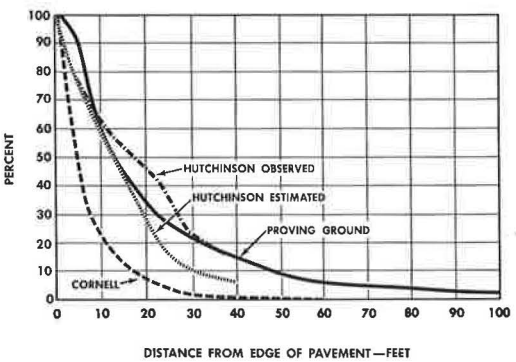

Figure 42. Comparison of Proving Ground, Hutchinson, and Cornell "hazard" curves.

Hutchinson believes that the collision with obstacles in the median has influenced the encroachment distribution somewhat; in Figure 41, his estimated curve of what encroachment might have been without obstacles is shown in comparison with the observed data.

Figure 42 is a comparison of the Cornell, Proving Ground, and Hutchinson curves. There is a close agreement between the Proving Ground distribution and the Hutchinson observed data. Both are influenced by factors of possible significance. There were almost no restrictions on the freedom of movement of the Proving Ground drivers and they may have made wider excursions than were required to stop safely, or regain control. No doubt, drivers from the Hutchinson sample were unimpeded in many locations even though several collisions with obstacles were noted. The behavior of a driver leaving the pavement and going into the median may be different from that of a driver leaving the road on the right shoulder.

These fragmentary data, however, suggest that an obstacle-free roadside of 33 ft would provide safety for at least 80 percent of the drivers leaving the road on either side, and that safety would be assured for more than 90 percent of them on a roadside free of obstacles on both sides for 50 ft.

Prediction of Recorded Accidents and Violations Using Non-Driving Predictors

EDWARD LEVONIAN, HARRY W. CASE, and RAYMOND GREGORY, University of California, Los Angeles

• TRAFFIC ACCIDENTS and violations are studied in relation to many variables, such as personality, attitudinal, sensory-motor, and physiological variables. Many studies involve several of these variables, and in such studies a common approach is to analyze each of these variables in turn in relation to accidents or violations.

In many such studies each analysis is made for the sample as a whole, whereas in other studies each analysis is made for a subsample homogeneous with respect to the other variables. When the entire sample is employed, and when each analysis involves a simple correlation or variance ratio, then the result is not controlled for other variables. When a homogeneous subsample is employed, the result, although controlled for the other variables, is less reliable.

Multivariate analysis not only provides for statistical control but also retains that reliability associated with the entire sample. An important consequence is the likelihood that the prediction of accidents and violations will be enhanced when several predictors are used. An even more important consequence of multivariate analysis is the clarity with which results can be interpreted; this last consequence accrues from the fact that multivariate results can be presented in an integrated fashion, rather than piecemeal.

Prediction is one criterion of knowledge. Unless one can predict accidents, in some sense, above the chance level, one cannot meaningfully claim to understand the processes involved in accidents.

The present study is an attempt to predict recorded traffic accidents and violations using objective multivariate techniques. The predictor variables were limited to those for which data could be collected before licensing.

The design of the study was simple. The subjects were divided randomly into two groups: a predictor group and a predicted group. Data from the predictor group were used to compute an objective criterion for predicting whether each subject in the predicted group had, or did not have, an accident during the preceding three years. Such a prediction was made for each subject in the predicted group, and this prediction was tested against the subject's accident record. An identical procedure was followed for violations.

METHOD

Subjects

The sample consisted of 720 truck drivers working for companies with headquarters in California. The companies were of two types: commercial carriers and those with fleets. The 720 drivers involved in this study included all persons examined at the Driver Testing Center, a facility of California Trucking Associations, Inc., during a 6-week period in the spring of 1960 and for whom measures were available on all the variables listed in the next section. Most subjects had come to the Center under the periodic testing program of their employing companies; the remaining subjects were applicants for driver positions. The test procedure was the same for both types of subjects. All data were collected under the prevailing standardized conditions, and the subjects were not aware that a study was in progress.

Paper sponsored by Committee on Highway Safety Research.

Independent Variables

The study involved 27 independent variables. These variables are capitalized in this report whenever they are defined by the descriptions and operations given in this section. The variables are divided into six categories; the 22 variables subsumed under the first five categories were specified before analysis began, whereas the five variables under the last category were determined from initial analyses involving the predicted group.

Personal. —The four variables in this category were Marital Status (score of 0 for single, 1 for married), Age (in years at the time of testing), Weight (in pounds), and Height (in feet, with inches expressed in decimal equivalents).

Cognitive. —The three variables in this category were Knowledge of Regulations (20-item open-book test of the Interstate Commerce Commission regulations, no time limit, and with subject's score representing the number of items answered correctly), Form Identification Speed (L. L. Thurstone's Identical Forms Test, Research Form 1F47, distributed by Science Research Associates, involving 60 items in which subject is required to match a semi-abstract pattern against five alternatives, and with subject's score representing the number of items completed in $4\frac{1}{2}$ min), Form Identification Accuracy (same test, with subject's score representing the number answered correctly in $4\frac{1}{2}$ min).

Visual. —The 11 variables in this category were Vertical Imbalance (as measured according to the Keystone Telebinocular Driver Vision Series, with a score of 0 for below normal, 1 for normal), Lateral Imbalance (same), Right Visual Acuity (Keystone Telebinocular Driver Vision Series scoring), Left Visual Acuity (same), Right Side Vision (subject focuses both eyes on a fixed object straight ahead while a white object is moved from a point initially behind subject along a perimeter in the plane of subject's eyes, with subject's score representing the angular location, with respect to the line straight ahead, of the moving object at the instant the subject reports detection of the object), Left Side Vision (same, but white object moves in from left side), Depth Perception (Keystone Telebinocular Driver Vision Series, with a score of 0 for below normal, 1 for normal), Distance Judgment (subject controls movement of a black block against a white background and attempts to bring block parallel with a similar block fixed at 20 ft, with subject's score representing the alignment error in millimeters), Night Vision (Porto-Glare device which involves five letters, O D Q G C, similar in size to 20/40 letters on Snellen eye chart and a 10-step light source behind each letter, with subject's score representing the minimum intensity or step, starting from the lowest, at which subject first reports the letter correctly when viewed at a distance of 10 ft in a semi-darkened room), Glare Recovery (same device presents glaring lights for about 5 sec while subject looks slightly down and away from lights, with subject's score representing the time in seconds between the termination of the lights and the subject's correct reporting of a display letter), and Glasses During Test (score of 0 for no glasses, 1 for glasses).

Motor. —The two variables in this category were Foot Reflex Time (left foot rests initially on the brake pedal of a simulated driver compartment, with subject's score representing the time in seconds between the presentation of a flash of red light and the depression of the pedal), and Foot Braking Time (right foot rests initially on the accelerator pedal, with subject's score representing the time in seconds between the presentation of a flash of red light and the depression of the brake pedal).

Medical.— The two variables in this category were Diastolic Blood Pressure (measured by a physician using the conventional procedure involving a sphygmomanometer), and Systolic Blood Pressure (same).

Personality. —The five variables in this category were determined in the course of this study, and were based on responses to a questionnaire prepared by the Institute of Transportation and Traffic Engineering. This 25-item questionnaire presented the respondent with driving situations involving personal interaction. From past experience it was found that other items of the same format were as readily answered by non-drivers as by drivers (1). It was assumed that responses to these driving items were indicative of personality, and that these responses could be obtained before licensing. The subject's scores on these five variables are discussed later.

TABLE 1

RECORDED ACCIDENTS AND VIOLATIONS OF PREDICTOR GROUP IN RELATION TO PREDICTOR VARIABLES

Variable	Mean	Standard Deviation	Recorded Accidents				Recorded Violations			
			Order of Emergence	Corr. with Rec. Acc.	Proportion of Variance	Proportion of Variance	Order of Emergence	Corr. with Rec. Viol.	Proportion of Variance	Proportion of Variance
Personal:										
Marital Status	0.886	0.318	16	-0.0463	0.0016		9	-0.0793	0.0046	
Age	36.514	9.281	7	-0.0482	0.0032	0.0035	1	-0.1991	0.0336	0.0344
Weight	176.461	25.343	27	0.0111	0.0000		8	0.0520	0.0042	
Height	5.858	0.201	4	0.0966	0.0060	0.0066	4	0.0901	0.0035	0.0077
Cognitive:										
Knowledge of Regulations	17.286	2.067	22	-0.0285	0.0004		2	-0.1408	0.0171	0.0177
Form Identification Speed	41.794	10.153	19	0.0530	-0.0041		3	-0.0409	0.0066	0.0038
Form Identification Accuracy	39.328	10.253	11	0.0637	0.0079		19	-0.0237	-0.0015	
Visual:										
Vertical Imbalance	0.986	0.117	13	-0.0298	0.0014		22	0.0390	0.0005	
Lateral Imbalance	0.844	0.363	5	0.0799	0.0062	0.0064	16	-0.0416	0.0014	
Right Visual Acuity	19.369	6.722	26	-0.0160	0.0000		13	0.0178	0.0009	
Left Visual Acuity	19.706	7.921	17	0.0139	0.0004		14	-0.0279	0.0015	
Right Side Vision	89.567	2.423	21	0.0071	0.0001		5	0.0954	0.0112	0.0073
Left Side Vision	91.044	1.850	25	-0.0203	0.0001		7	-0.0152	0.0014	
Depth Perception	0.958	0.200	14	0.0250	0.0015		15	0.0271	0.0014	
Distance Judgment	2.764	1.617	12	-0.0175	0.0010		18	0.0176	0.0006	
Night Vision	5.258	0.481	9	0.0791	0.0056		25	-0.0297	0.0003	
Glare Recovery	2.404	0.418	10	0.0386	0.0024		27	-0.0028	0.0000	
Glasses During Test	0.161	0.368	3	0.0912	0.0076	0.0077	26	-0.0395	0.0001	
Motor:										
Foot Reflex Time	0.215	0.019	2	-0.0485	0.0059	0.0055	10	-0.0174	0.0007	
Foot Braking Time	0.411	0.030	1	0.1028	0.0135	0.0150	17	-0.0057	0.0002	
Medical:										
Diastolic Blood Pressure	80.294	6.903	23	-0.0294	-0.0004		12	-0.1031	0.0044	
Systolic Blood Pressure	124.594	12.406	15	-0.0592	0.0024		6	-0.1043	0.0066	0.0061
Personality:										
Factor 1	2.847	1.746	6	-0.0730	0.0058	0.0058	24	-0.0058	0.0001	
Factor 2	4.156	1.500	24	0.0375	0.0002		21	0.0270	0.0005	
Factor 3	3.569	0.874	8	0.0710	0.0046	0.0049	11	0.0280	0.0017	
Factor 4	1.906	1.383	18	0.0007	0.0000		20	0.0366	0.0006	
Factor 5	3.372	0.988	20	-0.0126	0.0002		23	-0.0335	0.0004	
					0.0735	0.0554			0.1026	0.0770

The first two columns of Table 1 give the means and standard deviations of these 27 independent variables. The means of the five dichotomously scored variables (Marital Status, Vertical Imbalance, Lateral Imbalance, Depth Perception, and Glasses During Test) indicate the proportion of the subject's receiving a score of 1.

Dependent Variables

Recorded Accidents constituted the first dependent variable, with the subject's score representing the number of accidents involving (a) injury or (b) property damage in excess of $100 which were reported to the California Department of Motor Vehicles for the three-year period preceding the time data were collected on the 27 independent variables.

Recorded Violations constituted the second dependent variable, with the subject's score representing the number of violations reported to the DMV during the same three-year period. A distinction is made here between conviction and violation. A conviction is associated with a citing instance, whereas a violation is associated with each section of the California Vehicle Code which was cited for that instance. If a subject was stopped once but cited for speeding and failure to signal, he would receive one conviction but two violations.

PROCEDURE AND RESULTS

The procedure involved six steps: (a) division of the sample into two equal-size groups, (b) analysis of the questionnaire based on the data of the predicted group, (c) generation of two multiple regression equations based on the data of the predictor group, (d) use of the second equation to compute an accident score for each subject in the predicted group, (e) prediction for each subject in the predicted group of whether he had a recorded accident during the past three years, and (f) comparison of this prediction against the subject's accident record. Steps 3 through 6 were repeated for violations.

Step 1: Sample Division

Step 1 involved the division of the 720 subjects into two groups of 360 each. The

division was performed by ordering the subjects from 1 to 720, then placing all the even-numbered subjects in the predictor group, and all the odd-numbered subjects in the predicted group.

The subjects were ordered according to their California chauffeur license number. No account was taken of a driver (non-chauffeur) license that the subject might have had, because both chauffeur and driver license numbers would have been identical, and, in fact, only one type of license has been issued by California since 1958. The subjects tended to be ordered by age, because California has issued permanent license numbers since 1944, and many subjects would have had their license number assigned when they first became of eligible age.

Step 2: Questionnaire Analysis

Step 2 involved the analysis of the 25-item questionnaire based on the responses of the predicted group. At the beginning of the study the number of questionnaire variables was not known. Because these questionnaire variables were to be included as independent variables in the prediction equation, it was necessary to specify these questionnaire variables before further analyses could be undertaken.

The analysis of the questionnaire resulted in the grouping of items according to statistical considerations: each group consisted of items which tended to correlate with each other, and the groups tended to be independent. The procedure involved a series of factor analyses. Each factor analysis started with Pearson correlations and involved the insertion of the square of the multiple correlation (of each item on the remaining items) in the principal diagonal of the correlation matrix. The limit on the number of factors was equal to the number of eigenvalues which were greater than zero (2). However, only those factors were rotated which had at least one loading of 0.20 or greater. These orthogonal factors were rotated by the Kaiser Varimax method (3), an analytic procedure that maximizes for the table as a whole the variance in the factor loadings. The variance in the loadings for each factor is computed, then summed over factors, and it is this sum which is maximized. Rotational iterations were continued until the difference between four successive sums failed to exceed 10^{-7}.

At the end of each factor analysis, an item was eliminated if it (a) had a communality less than 0.10, or (b) failed to have a loading greater than 0.20 in a factor that had at least one other loading greater than 0.20, or (c) had loadings greater than 0.20 in at least two factors. The three criteria, respectively, were intended to eliminate items that (a) shared little in common with the remaining items, (b) were associated only with

TABLE 2

QUESTIONNAIRE ANALYSIS: FINAL ROTATED FACTOR MATRIX

Item	Factor					
	1	2	3	4	5	h^2
3	-0.39	0.12	-0.09	0.08	0.07	0.18
5	0.46	0.06	-0.03	0.09	0.04	0.23
25	0.50	0.15	-0.09	-0.03	-0.03	0.28
11	0.00	-0.35	-0.09	0.06	-0.04	0.13
21	-0.02	0.28	0.06	-0.16	0.16	0.13
24	0.08	0.31	-0.08	0.03	-0.05	0.11
1	-0.01	0.04	-0.38	0.02	-0.01	0.14
10	0.02	-0.08	-0.35	0.05	-0.08	0.14
7	-0.05	0.01	0.00	0.32	-0.03	0.11
20	-0.06	0.14	0.10	-0.33	0.02	0.14
9	-0.19	0.01	-0.03	0.17	-0.26	0.14
19	0.08	-0.03	-0.06	0.00	-0.35	0.14

TABLE 3

QUESTIONNAIRE ANALYSIS: ITEMS IN FINAL FACTOR MATRIX

Factor 1	
3.	Do you think if you ever got in a serious accident it would more likely be your fault or the other person's fault? (my fault = 0, uncertain = 1, other person = 2)
5.	Do you feel that you are able to park a little better than, or about as well as most drivers? (as well as = 0, uncertain = 1, better than = 2)
25.	Would you say your driving is better than average or average? (average = 0, uncertain = 1, better than average = 2)
Factor 2	
11.	An old car is stalled ahead on the highway. The driver is waving, but you are not sure what he wants. Do you usually drive by, or do you stop to see what he wants? (drive by = 0, uncertain = 1, stop = 2)
21.	When you reach an intersection at the same time as a car approaching from the side street, do you usually wait for it to cross first, or do you try to cross first? (cross first = 0, uncertain = 1, wait for it = 2)
24.	Suppose while you're waiting at a signal, the car ahead of you rolls back and hits your bumper. Would you get out to see if your car was damaged? (no = 0, uncertain = 1, yes = 2)
Factor 3	
1.	Would you double park to let a passenger out even though it meant that the driver behind you would have to wait? (yes = 0, uncertain = 1, no = 2)
10.	Do you feel that you can exceed most speed limits without endangering yourself or others? (yes = 0, uncertain = 1, no = 2)
Factor 4	
7.	Suppose you are prepared to enter a parking space and another driver grabs the space. Do you sometimes tell him off? (no = 0, uncertain = 1, yes = 2)
20.	Suppose you have stopped in the street waiting for a driver to pull out of a parking space so that you can enter. A car behind you honks to get by. Do you move on and try to find another space, or do you stay where you are? (move on = 0, uncertain = 1, stay put = 2)
Factor 5	
9.	Suppose you are stopped in bumper-to-bumper traffic and the car ahead of you moves forward, but before you have a chance to move up yourself, the driver on your left cuts in front of you. Do you occasionally honk at him? (yes = 0, uncertain = 1, no = 2)
19.	Suppose you are waiting in the front row of a stop signal. After a long time you begin to feel that the signals must be stuck, but see that the other drivers are not moving. Would you cross the intersection against the signal? (yes = 0, uncertain = 1, no = 2)

item-specific factors, and (c) tended to have their variance contributed by more than one factor. Only one item was eliminated after each factor analysis, and analyses were continued until no item could be eliminated according to the three criteria.

It was necessary to perform 14 factor analyses before the remaining items passed all three criteria. At this time only five factors and 12 items remained. This final factor matrix is given in Table 2, with the factors and items rearranged for clarity. Table 3 presents the 12 items grouped by factor.

Having determined that five questionnaire variables would be included in the study, it was necessary to compute a score on each variable for each subject. A subject's score for a variable was determined by his responses to the items grouped under the associated factor. Each item had three choices, which were orignially assigned the values 0, 1, and 2, with the 1 representing the uncertain choice. This assignment was arbitrary, but some numerical assignment was necessary in order to perform the factor analyses. However, after the factor analyses were finished, the numerical assignment was reversed for each item whose major factor loading was negative (Table 2). These final numerical assignments are given in Table 3 in parentheses after each item. A subject's score was based on these final values. Scores ranged from 0-6 for the first two questionnaire variables, and 0-4 for the last three. A higher score indicates more of that characteristic which is measured by the variable.

Now, with five questionnaire variables established, it was possible to add them to the 22 other independent variables and to proceed with the generation of the multiple regression equations.

Step 3: Regression Analyses

Step 3 involved the generation of two multiple regression equations, each with Recorded Accidents as the dependent variable and based on the data of the predictor group.

The first multiple regression equation involved all 27 independent variables, and the results are given in Table 1.

The four columns under "Recorded Accidents" indicate (a) the order in which each independent variable emerged, (b) its correlation with Recorded Accidents, (c) its contribution to the variance in Recorded Accidents for the first multiple regression analysis, and (d) its contribution in the second multiple regression analysis.

The Order of Emergence column was determined step-wise, one independent variable at a time (4). At the first step that independent variable was selected among the 27 that accounted for the greatest proportion of variance in Recorded Accidents. At the second step that independent variable was selected among the remaining 26 that accounted for the greatest proportion of variance in Recorded Accidents not already accounted for by the variable selected in the first step. This procedure was repeated for 27 steps, and the numbers in the third column of Table 1 indicate the step at which the independent variable made its appearance.

The second multiple regression equation involved a subset of the 27 independent variables chosen on the basis of their contribution to the variance in the dependent variable: Recorded Accidents. The independent variables were added step-wise, in the order shown in the third column of Table 1, starting with Foot Braking Time. The 2nd, 3rd, ... kth independent variable was added successively as long as it increased the significance level of the F ratio of the contributed variance to the error variance. This criterion resulted in the inclusion of eight independent variables. The data from the predictor group on these eight variables were used to compute the second multiple regression equation, and it was this second equation which was used to compute an accident score for each subject in the predicted group.

The same procedure was followed for Recorded Violations as the dependent variable, and the results are given in the last four columns of Table 1. Using the criterion just given, the first six independent variables, according to their order of emergence, were included in the second multiple regression equation.

Step 4: Accident Score

Step 4 involved the computation of an accident score for each subject in the predicted

group. A given subject's accident score was computed by multiplying his score on one of the eight independent variables by the regression coefficient for that variable, summing eight such products, and adding the constant. An identical procedure was followed for computing the subject's violation score, but in this case, of course, there were only six products to sum.

Step 5: Accident Prediction

Step 5 involved the prediction of whether a subject in the predicted group had a recorded accident during the previous three years. This prediction was based on whether his accident score, computed in Step 4, exceeded a critical accident score.

The critical accident score was computed from the predictor group data as follows: (a) an accident score was computed for each subject in the predictor group according to the procedure outlined in Step 4; (b) the predictor group was dichotomized on Recorded Accidents as close to the median as possible, resulting in a dichotomy point between no accidents and one or more accidents; (c) the accident scores of these dichotomized groups were used to compute a critical accident score by use of an equation derived by Guilford and Michael (5, 6).

The critical accident score turned out to be 0.758. Thus, a prediction of no accident was made for each subject in the predicted group whose accident score was less than 0.758, and a prediction of at least one accident was made for each subject whose accident score was greater than 0.758.

An identical procedure was followed for violations. The dichotomy point fell between 3 and 4 Recorded Violations over the previous three years. Thus, subjects in the predictor group with 0-3 violations fell below the dichotomy point, whereas those with 4 or more were assigned to the upper category. The critical violation score was 4.926.

Step 6: Accident Prediction Validation

Step 6 involved a test of significance of the relation between Recorded Accidents and predicted accidents of the predicted group. A fourfold table was formed with Recorded Accidents (none vs one or more) on one axis and predicted accidents (none vs one or more) on the other axis. Because the distribution was so extreme, the probability of such a distribution (and all other distributions more extreme) was computed directly (7), rather than determined indirectly through a Yates-corrected χ^2. The exact probability was 0.0298.

An identical procedure was followed for violations, but in this case a χ^2 could be computed legitimately. The prediction of violations was in the right direction, but the χ^2 of 1.31 was not statistically significant. The details of the accident and violation predictions are shown in Figure 1.

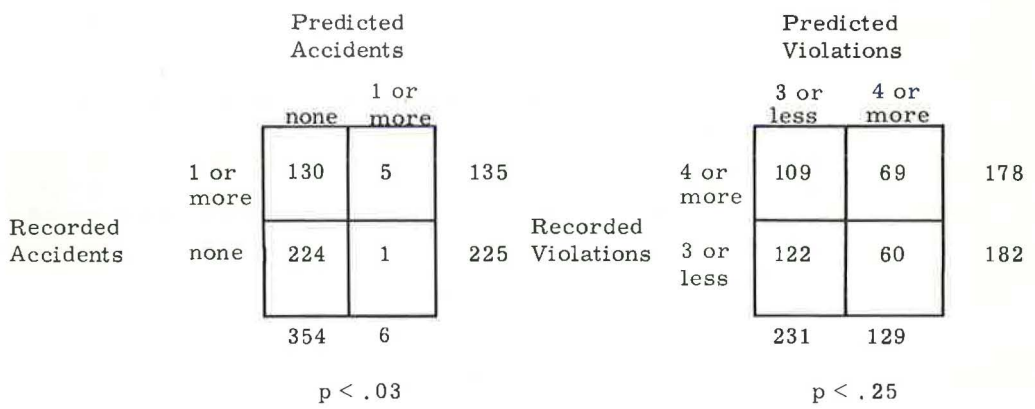

Figure 1. Recorded accidents (and violations) in relation to predicted accidents (and violations) for the predicted group.

ANALYSIS

Before presenting the interpretation of the substantive results, a brief discussion is presented concerning (a) the validity of the statistical procedure employed, and (b) the conditions of this study which made prediction more difficult.

Statistical Procedure

Two aspects of the procedure are likely to be of interest. First, product-moment correlations and multiple regression analyses were employed despite the fact that many of the variables were not normally distributed. Under this condition, the results of multiple regression analyses cannot be, and were not, tested for significance. The values given in Table 1 should be taken only as approximations of the values that would have resulted from normally distributed variables. Despite the procedural liberties taken with the analysis of the data of the predictor group, the probability of the relation between recorded and predicted accidents (and analogously for violations) for the predicted group is valid for the conditions under which it was determined--the probability was computed under the nonparametric conditions that prevailed.

Second, the predicted group was used for the analysis of the questionnaire, and the resulting five variables were used in the prediction equation, which was then applied to each subject in the predicted group. In general, a sample that is used preliminarily in such a way as to influence scores computed subsequently cannot, thereafter, be used in a statistical test involving these scores. In this study, however, the predicted group determined only the number of variables in the questionnaire, not the weights (coefficients in the prediction equation) to be attached to these variables. The alternative of using the predictor group to determine both the number of variables as well as their weights would most certainly have created a bias. Such a bias would occur because the factor analyses lead to an independence of the variables, an independence optimized with respect to the predictor group data. This independence in turn would result in a positive bias in the weights attached to these variables by the multiple regression analysis.

Factors Influencing Prediction

The results indicate that it is possible to predict at a statistically significant level whether each of 360 truck drivers had or did not have at least one recorded accident during a three-year period. This result emerged despite the composition of the sample and despite the predictor variables employed.

First, the sample was undoubtedly restricted in the range of Recorded Accidents, leading to a more difficult prediction of accidents. This restriction is the result of the common employment practice of not retaining employees who are involved in too many accidents. All subjects were employed by companies that had the freedom to fire those drivers whose performance proved inadequate. Truck accidents tend to involve considerable financial loss to the employer, though accident data do not reveal the extent of this loss, accident culpability, or the number of accidents that may have been incurred while the employee was off-duty and driving his own car. Another factor that tended to limit the range in the two dependent variables is the California negligent operator program. When recorded accidents and convictions reach a critical value, State authorities, after considering accident culpability and driving exposure, may restrict the driving privilege for a period of time.

Second, the predictor variables used were those on which data could be collected before licensing. It is relatively easy to predict accidents above the chance level if driving variables (previous exposure rate, accident rate, violation rate, etc.) are used for prediction. If the objective is prediction only, then these driving variables should be employed, but if the objective is to gain some appreciation of pre-driving variables associated with subsequent accidents, then the use of driving variables is likely to compound further an already resistant problem.

Of course, in the present study the data were not collected before licensing. Such a refinement in research design will become more desirable as the delineation of varia-

bles becomes more clarified as the result of studies using a cruder design, such as the one employed in the present study. The following discussion assumes that the relations obtained in the present study are only a crude approximation to the relations that would have been obtained if the data on the predictor variables had been collected before licensing, or at least before the three-year period to which the Recorded Accidents and Violations apply. But it is also assumed that even these crude approximations are likely to give direction to subsequent studies.

Variables Contributing to Recorded Accidents

The prediction of Recorded Accidents demonstrated in this study justifies a discussion of the independent variables involved in the prediction. This discussion is based only on the results from the predictor group, as given in Table 1, unless otherwise specified.

Before discussing independent variables individually, two generalizations are made. A comparison of columns 5 and 6 indicates that Foot Braking Time makes essentially the same contribution in the second regression analysis as it did in the first, and this constancy holds also for the other seven variables in column 6. This implies that the 19 variables that do not appear in column 6 did not act in the first analysis as suppressor variables with respect to the 8 that do appear.

Another generalization can be made on the basis of the totals of columns 5 and 6, as shown at the bottom of Table 1. Each total represents (a) R^2, the square of the multiple correlation of Recorded Accidents with the independent variables, and (b) the proportion of variance in Recorded Accidents accounted for by the independent variables. The eight variables account for much of the variance accounted for by all 27 variables. However, in each analysis, the independent variables account for only a small proportion of the total variance in Recorded Accidents.

The independent variables are discussed according to the six categories given in Table 1, beginning with the personal variables. Age correlated with Recorded Accidents in the expected direction—younger men tended to have more accidents--but age was not a dramatic predictor of accidents. This divergence from what might be expected probably lies in part on the employment selection process already discussed, and in part on the statistical control of other variables used in this study. The relation of age to recorded accidents is not clear, though the relation appears to be rather complex. Because more efficient functioning of the body tends to be associated with younger drivers, one might expect younger drivers to have fewer accidents. As everyone knows, quite the opposite is true. Obviously there are other factors associated with youth which tend to counteract the more efficient functioning of the body. Until the contribution of age to the variance in accidents can be completely eliminated, any claim to the understanding of the factors in the age-accident relationship should be considered conjectural.

The cognitive variables contributed essentially nothing to the variance in Recorded Accidents. The contribution of Form Identification Accuracy in the 27-variable analysis is due primarily to the suppressor effect of Form Identification Speed, with which it is highly correlated ($r = 0.96$). If Form Identification Accuracy or Form Identification Speed, but not the other, had been included in the second regression equation, its entry in column 6 would have been less than that which appears in column 5.

Of the visual variables, Lateral Imbalance and Glasses During Test contributed moderately to the variance in Recorded Accidents, as did Night Vision, although the latter was not one of the eight predictor variables. The positive correlation of Lateral Imbalance with Recorded Accidents indicates that subjects with normal lateral imbalance tend to be involved in more accidents. Also, the positive correlation of Glasses During Test with Recorded Accidents indicates that subjects who wore glasses during the visual tests (and presumably while driving) tend to be involved in more accidents.

Both motor variables were retained as predictor variables. Foot Braking Time emerged first on predictive order because it was the independent variable with the highest correlation with Recorded Accidents.

Neither of the two medical variables contributed to the variance in the dependent variable.

The last five variables have been designated as personality variables, though admittedly there is no critical evidence to uphold this interpretation. But even if the questionnaire factors do represent personality variables, the sparseness of the items makes difficult the identification of these personality variables. Personality Factors 1 and 3 made small contributions to the variance in Recorded Accidents. A high score on the three items of Factor 1 (Table 3) seems to imply self-confidence, and the negative correlation in Table 1 indicates that drivers with accidents tend to have less self-confidence. Factor 3 may be a social desirability factor—a tendency to respond so as to appear in favorable light. In any case, drivers with accidents tend to have higher scores on this factor.

To ascertain the accident results given in Table 1, a similar table was prepared, but with the results based on the combined data of the predictor and predicted groups. The five questionnaire variables were not included in the analysis, because these variables were defined originally on the basis of the predicted group. The results from the remaining 22 independent variables were similar to those already given. In a rough sense, accidents are more likely to be associated with the younger driver with glasses who is slower in braking.

Variables Contributing to Recorded Violations

It is recalled that the prediction of Recorded Violations was in the right direction but was not statistically significant. The failure to achieve a higher prediction was due in large part to the shrinkage that resulted from dichotomizing (so as to retain the same procedure for violations as was used for accidents) Recorded Violations, a variable that is essentially continuous with substantial frequencies in violation categories 0, 1, ... 10 for both the predictor and predicted groups. Evidence of this shrinkage is given by the product-moment correlation between Recorded Violations and violation scores (also continuous) for the predicted group. This correlation of 0.14 was significant at the 0.01 level, indicating that the basis for the computation of violations scores has validity. This result suggests that Recorded Violations could have been predicted at a sufficiently high level as to warrant a discussion of the variables that entered into the prediction equations. Again, this discussion is based only on the results from the predictor group as given in Table 1, unless otherwise noted.

First, Table 1 reveals that three of the six prediction variables show different contributions to the variance in Recorded Violations for the two multiple regression analyses (the 27-variable and the 6-variable analyses). There are two cases of a decrease in the 6-variable analysis, and one case of an increase. These three cases are discussed separately.

In considering Right Side Vision, which accounts for less variance in the 6-variable analysis, the enhanced contribution in the 27-variable analysis is probably due to the suppressor action of Left Side Vision. This action tends to inflate the apparent contribution of Right Side Vision.

Form Identification Speed also accounts for less variance in the 6-variable analysis. Again, the explanation probably lies in the suppressor action contributed by Form Identification Accuracy in the 27-variable analysis. Such a decrease was already anticipated in the preceding discussion on accidents. Despite this reduction, the selection of variables to be included in the prediction equation should be based on predictive order, rather than on the proportion of variance revealed in the 27-variable analysis. Had this latter criterion been used, Height would not have been included in the prediction equation, and its eventual contribution would have been lost.

For Height, the increase in contribution for the 6-variable analysis is probably due to the common variance between Weight and Height. The sum of the variance contributed by Weight and Height in the 27-variable analysis appears to be contributed by Height alone in the 6-variable analysis.

These cases highlight an interesting question: if two variables in the 27-variable analysis share a common variance, and if only one of these variables is retained in the 6-variable analysis, why does one retained variable show a decrease, whereas another retained variable show an increase? The answer lies in the extent to which the variance

shared by the independent variables is also common to the variance that each independent variable shares with the dependent. Often the correlations among the independent variables and the dependent variable allow one to predict the effect of eliminating one of the independent variables.

Consider first the correlations between Right Side Vision and Left Side Vision ($r = 0.47$), between Right Side Vision and Recorded Violations ($r = 0.10$), and between Left Side Vision and Recorded Violations ($r = 0.02$). Although Left Side Vision has an essentially zero correlation with the dependent variable, it has a substantial correlation with a variable (Right Side Vision) which is correlated with the dependent variables. Under these conditions, Left Side Vision is likely to suppress that variance which is shared by Right Side Vision and Left Side Vision but which is not shared by Right Side Vision and Recorded Violations. Left Side Vision becomes a suppression variable, increasing the contribution of Right Side Vision. If Left Side Vision were to be removed, the contribution of Right Side Vision would be decreased, as in fact occurs in the 6-variable analysis. Thus, an independent variable that correlates near-zero with the dependent variable may still aid in predicting the dependent variable.

In considering next the correlations between Weight and Height ($r = 0.53$), between Weight and Recorded Violations ($r = 0.35$), and between Height and Recorded Violations ($r = 0.09$), the correlation between the independent variables is essentially the same as in the previous case, but unlike the first, the two correlations of the independent variables with the dependent are rather similar in magnitude. Under these conditions, the elements that Weight shares with Recorded Violations are also likely to exist in the Height variable. If so, when Weight and Height are included in the same analysis, they are likely to split the total variance they share with Recorded Violations. If one of the independent variables is removed, the retained variable will contribute most of the variance previously contributed by the two. Thus, when Weight is eliminated in the 6-variable analysis, Height accounts for as much of the variance in Recorded Violations as was previously accounted for by Weight and Height combined. Thus, for prediction purpose two independent variables are not necessarily better than one.

Form Identification Speed emerged third on predictive order, despite the fact that its correlation with Recorded Violations was exceeded by seven other variables which emerged later. This occurred because only Form Identification Speed contributed variance to Recorded Violations not already contributed by Age, which had already emerged. This is substantiated by the fact that only Form Identification Speed correlated significantly with Age in a direction opposite to what would be expected on the basis of the correlations between Recorded Violations and the independent variables being considered. Again, this points out the limitations of considering only the correlation with the dependent variable as the criterion for the selection of predictor variables.

The relative contribution of the independent variables to the variance in Recorded Violations is discussed according to the six categories shown in Table 1. The personal variables yield fully one-half the accounted variance in Recorded Violations. Age, the most important contributor, is correlated with Recorded Violations in the same direction as that noted in many other studies—younger drivers incur more violations. The second personal variable to be included in the violation prediction equation, Height, is correlated positively with Recorded Violations, but it is not clear why taller truck drivers should incur more violations.

Of the cognitive variables, Knowledge of Regulations is the only one that contributes appreciably to the variance in Recorded Violations. The direction is one that would be expected on a logical basis—the person with a lower Knowledge of Regulations score is likely to have more violations.

The only visual variable included in the final prediction equation was Right Side Vision, with a higher score being associated with more violations. Neither motor variable is included in the final prediction equation.

The medical variables are correlated negatively with Recorded Violations. This is as one would expect from his knowledge that blood pressure is correlated positively with age, which in turn is correlated negatively with violations. But it is surprising that Systolic Blood Pressure emerged as high as it did on predictive order. One might have expected that since Age, which emerged first, is correlated positively with Systolic

Blood Pressure (and to a lesser extent with Diastolic Blood Pressure), any variance that Systolic Blood Pressure shares with Recorded Violations would have been pre-empted by Age. Apparently Age alone does not account for the relation between Systolic Blood Pressure and Recorded Violations.

Finally, none of the personality variables was included in the violation prediction equation.

To ascertain the violation results given in Table 1, a similar table was prepared, but with the results based on the combined data of the predictor and predicted groups. As previously mentioned under the discussion on accidents, the five personality variables were not included in the analysis. The results from the remaining 22 independent variables were similar to those given previously for the predictor group alone. In a rough sense, violations are more likely to be associated with the younger, taller (or heavier) driver whose knowledge of regulations is low, whose right side vision (and possibly night vision) is better than average, and whose systolic blood pressure is lower than average.

SUMMARY

An attempt was made to predict whether each of 360 truck drivers had at least one accident recorded during the past three years with California's Department of Motor Vehicles. The prediction was based on 27 non-driving variables on which data could have been collected before licensing. The same prediction procedure was also used in an attempt to predict recorded violations for the same time period.

The prediction of recorded accidents, although not high in any absolute sense, was statistically significant. Thus, a justification existed for a discussion of the variables that contributed to that prediction. In a rough sense, accidents are more likely to be associated with the younger driver with glasses who is slow in braking.

The prediction of recorded violations was in the right direction, but it failed to reach a statistically significant level. Analysis seemed to indicate that this failure was due to the use of the same procedure for recorded accidents; had a procedure been used that would utilize the essentially continuous characteristic of recorded violations, the prediction of recorded violations would also have been significant. Thus, it was felt justified to discuss also the variables that contributed to that prediction. In a rough sense, violations are more likely to be associated with the younger, taller (or heavier) driver whose knowledge of driving regulations is low, whose side vision (and possibly night vision) is better than average, and whose systolic blood pressure is lower than average.

ACKNOWLEDGMENT

The authors are pleased to acknowledge the cooperation of Wade Sherrard, Managing Director of the California Trucking Associations Inc., and of Robert Hansen, Manager of the Associations' Driver Testing Center. All computations were performed at UCLA's Computing Facility.

REFERENCES

1. Levonian, E., and Case, H. W., "Behavioral and Demographic Correlates of Re-Sponses to a Driving Questionnaire." HRB Proc., 40:582-592 (1961).
2. "BIMD Computer Programs Manual." BIMD 17, Div. of Biostatistics, Dept. of Preventive Med. and Public Health, School of Med., UCLA (1961).
3. Kaiser, H. F., "The Varimax Criterion for Analytic Rotation in Factor Analysis." Psychometrika, 23:187-200 (1958).
4. "BIMD Computer Programs Manual." BIMD 29, Div. of Biostatistics, Dept. of Preventive Med. and Public Health, School of Med., UCLA (1961).
5. Guilford, J. P., and Michael, W. B., "The Prediction of Categories from Measurements." Sheridan Supply Co., Bevery Hills, Calif. (1949).
6. Guilford, J. P., "Fundamental Statistics in Psychology and Education." McGraw-Hill (1956).
7. Kendall, M. G., "The Advanced Theory of Statistics." 3rd ed., Vol. 1, Griffin, London (1951).

Dynamic Tests of Automobile Passenger Restraining Devices

IRVING MICHELSON, Consumers Union of U. S., Mt. Vernon, N. Y.;
BERTIL ALDMAN, Official Swedish Council on Road Safety Research, Stockholm;
BORIS TOURIN, Consumers Union of U. S., Mt. Vernon, N. Y.; and
JEREMY MITCHELL, Consumers' Association, London, England

•THE APPLICATION of dynamic test methods to automobile safety belts is not a new idea. Indeed, the type of seat belt in use in American cars today was developed through information from dynamic tests of restraining devices for aviation by Stapp (1), and for automobiles by Mathewson and Severy (Table 6, 2). The latter performed their studies with controlled collisions of actual automobiles, with the vehicles, the passengers (usually dummies), and the seat belts instrumented to determine the magnitudes and durations of the forces produced in actual accidents. Similar controlled collision studies using automobiles have been done by research engineers of automobile companies (3). In addition to these research activities, laboratory dynamic tests have been used for several years for certifying seat belts for public sale in California by the California Highway Patrol (4) and in Sweden by the National Institute for Materials Testing. Another laboratory dynamic test device has been used for some years in auto safety research at the University of Minnesota (5).

In spite of these examples of the use of dynamic methods in laboratory tests of automobile seat belts during recent years, there has been a general reluctance in the seat belt field to accept dynamic testing. During 1962, however, an increased interest developed, both here and abroad. The British Standards Institution, the Inland Transport Committee of the U. N. Economic Commission for Europe, and automobile and seat belt manufacturers in the United States and Great Britain have been considering adopting such a method. Indeed, several of these organizations have built dynamic test equipment during the past year. Very recently, the Society of Automotive Engineers and the Federal Supply Service (G. S. A.) have become interested. Nevertheless, dynamic testing is still not an accepted method in official or semi-official standards (6, 7) in the United States, except in California.

The objections raised against dynamic testing are mainly three: (a) that dynamic testing offers no advantage over static testing; (b) that even were it to offer advantages, it cannot be controlled well enough to constitute a standard test; and (c) that dynamic tests are much more expensive than static ones. Although the economic problem is not a subject for discussion at this forum, dynamic testing is sufficiently important to warrant an intensive effort to develop an economically feasible method, and there are indications that the problem can be solved satisfactorily. In any case, only the first two objections are discussed here.

The basic reason for even considering dynamic testing is that, in actual use, seat belts are subjected to dynamic loading conditions; that is, very large loads are applied in very short time intervals to elastic structures that respond to short-interval loading in a different way than they respond to slower loading (8). The mathematical physics of phenomena of this general type is described elsewhere (9, 10, 11). These treatises leave no doubt that qualitative and quantitative differences in effects exist between a transient and a relatively slow application of force to an elastic system; consequently, a dynamic test method should provide a closer simulation of actual use conditions than

Paper sponsored by Committee on Highway Safety Research.

a static test. The question is really whether a particular laboratory dynamic test simulates the dynamic force and time conditions of severe car collisions more closely than the static tests now in general use.

Fortunately, controlled automobile collision studies have provided some data on the magnitudes and durations of forces generated in automobile collisions. These data can be used to judge whether a laboratory dynamic test, such as the Swedish one, gives a close simulation of actual collision conditions. Table 1 gives some of the dummy deceleration and lap belt loading data from controlled car crashes at the Ford Motor Company (3) and at the Institute for Transportation and Traffic Engineering (12). The data represent severe collisions into fixed barriers and head-on collisions.

The Swedish dynamic test (described in detail in the Appendix) attempts to simulate severe crash conditions. It has been criticized as possibly being too severe because of the short stopping distance of its cart—a lead cone at the front of the cart causes it to stop in about 3 in. from an impact speed of 25 mph when it strikes the fixed barrier. The impact speed and the short stopping distance of the cart have been known, but because no other data have been available, it has been possible to speculate that dummy decelerations and belt loadings were very much higher, and durations very much shorter, than those typical of actual severe car collisions. For these reasons the Swedish test method was considered likely to be yielding a poor simulation of car collision conditions. Instrumented tests with the Swedish method have now been made and are reported herein, so that comparisons with controlled car collisions are now possible.

Before proceeding to make these comparisons, it must be noted that the two sets of controlled car collision data in Table 1 are themselves not strictly comparable. The UCLA data included both belt loads and dummy decelerations, but the seat belts used in their tests were 3 in. wide instead of the conventional 2 in. On the other hand, the Ford tests used belts of conventional width, but furnished only belt load data; no dummy decelerations were reported. Comparison of the UCLA and Ford belt load data indicate that the UCLA tests at 21-mph impact speed produced roughly the same forces as the 27- to 29-mph Ford tests.

Table 2 gives the results of instrumented runs made with the Swedish test rig during the summer of 1962; these runs were made with conventional lap belts. Comparison of Tables 1 and 2 shows that the dummy decelerations and the belt loadings generated in the 21-mph Swedish test, and the durations of these, were of the same order of mag-

TABLE 1

FORCES GENERATED IN CONTROLLED CAR CRASHES USING LAP BELTS

Type of Collision	Ref. No.	Impact Speed (mph)	Dummy Decelerations		Belt Loadings	
			Peak (g)	Duration[a] (millisec)	Peak (lb)	Duration[a] (millisec)
Two-car, head-on	11	21	44	55	7,000	60
		21	40	60	5,000	60
		21	30	90	-	-
		21	34	60	4,500	65
		27	48	90	7,500	45
		27	38	80	5,000	80
		47	55	95	9,000	130
		52	72	90	9,000	135
		52	73	95	15,000	150
Car, fixed barrier	3	27	-	-	5,700	75
		29	-	-	5,800	65

[a]Durations of deceleration are for 5g and over; durations of loading are for 1,000 lb and over, because of indefiniteness of endpoints in many cases.

nitude as those observed in the UCLA and Ford controlled car collisions at 21- to 29-mph impact speeds; in fact, the ranges of the Swedish test data overlap the ranges found in the controlled car collisions in all factors involved.

These comparisons, and the graphs of the instrument data shown in the Appendix demonstrate that, contrary to the earlier speculations, the Swedish cart's short stopping distance (and its consequently very high deceleration) do not control the deceleration of the dummy nor the load on the belt. The major part of the stopping of the dummy occurs after the cart is completely stopped (8). The major factors that control the dummy deceleration and the belt load are the impact velocity, weight of the dummy, and the elongation characteristics of the seat belt itself. It is therefore not surprising that the Swedish test method generates forces of the same magnitudes and durations as those of actual collisions.

TABLE 2

FORCES GENERATED IN SWEDISH DYNAMIC TESTS USING LAP BELTS AND RIGID DUMMY

Impact Speed (mph)	Dummy Deceleration		Belt Loading	
	Peak (g)	Duration[a] (millisec)	Peak (lb)	Duration[a] (millisec)
21	32	60	5,400	52
21	25	47	5,400	50
21	35	50	6,600	50
21	27	63	5,700	63
15	22	45	3,800	42
15	23	43	4,000	49
15	30	40	5,200	42
15	-	-	5,300	50
15	20	45	4,400	58
15	29	43	5,400	44

[a]Durations of deceleration are for 5g and over; durations of loading are for 1,000 lb and over, because of indefiniteness of endpoints in many cases.

On the other hand, the static test methods prescribed in the official Federal Government specification (6) and in the SAE standard (7), which is official in some States, impose loadings on the belt relatively slowly, so that the peak loading is reached in a time period of the order of 2 min, several thousand times as long as the loading durations observed in car collisions. Thus, it is clear that the Swedish test method produces a very much better simulation of actual belt loadings than the static method.

The reproducibility of the impact speed has been studied by the Swedish laboratory, using microswitches along the track. The variations have been found to be within ± 0.3 mph at 25 mph, so that the variation in kinetic energy does not exceed ± 2.5 percent. This demonstrates good control of the cart speed. At the three speeds studied (15, 21, and 25 mph), the stopping time remained fairly constant at about 18 millisec, but the peak decelerations increased considerably at the higher impact speeds (Table 3). (A detailed study of the deceleration characteristics of the cart will be published shortly by Aldman; the cart decelerations shown in Table 3 and in the graphs in the Appendix are average values and typical patterns included only to illustrate the order of magnitude and the time relationship between the decelerations of the cart and the dummy.)

In the testing of seat belts, it is the reproducibility of the dummy decelerations and the belt loadings which is of primary concern. Table 4 gives a summary of the dummy decelerations and belt loadings for various test conditions: impact speeds of 15 and 21 mph using lap belts and a rigid dummy, and impact speeds of 21 and 25 mph using harnesses and a jointed dummy. In addition to the average peak values, the ranges of the dummy decelerations and the belt loadings in each case are also presented. There is considerable overlapping of ranges among the various test conditions. However, when differences among the belts themselves are taken into account, a good deal of this overlapping is eliminated, and, moreover, some of the effects of differences in design of the belts are learned.

TABLE 3

SWEDISH TEST CART

Impact Speed (mph)	Stopping Time (ms)	Deceleration[a] (peak g)
15	19	54
21	17	86
25	17	150

[a]Durations of deceleration are for 5g and over; durations of loading are for 1,000 lb and over, because of indefiniteness of endpoints in many cases.

The term "harness" is used in this report to designate any seat belt that restrains the upper torso, whether it has a

TABLE 4

AVERAGE FORCES AND DURATIONS IN SWEDISH TEST

Device	Type of Dummy	Position of Accelerometer	Impact Speed (mph)	No. of Runs	Dummy Decelerations (peak g)		Belt Loads (peak lb)		Avg. Duration[a] (millisec)	
					Avg.	Range	Avg.	Range	Decel.	Loads
Lap belts	Rigid	Lower body	15	6	25	20- 30	4,700	3,900- 5,400	43	48
			21	9	30	25- 35	6,100	4,700- 7,500	55	54
Harness	Jointed	Chest	21	8	62	35- 82	6,000	4,000- 8,100	50	60
			25	7	88	40-112	7,800	6,300-11,000	51	58

[a]Durations of deceleration are for 5g and over; durations of loading are for 1,000 lb and over, because of indefiniteness of endpoints in many cases.

lap strap as well. It therefore includes diagonal chest straps, combinations of lap straps and diagonal chest strap, and combinations of lap strap and double shoulder straps.

The jointed dummy used by the Swedish laboratory for testing harnesses was found unsuitable for testing lap straps; the rigid dummy was made for the purpose of testing lap straps alone. The accelerometer was located on the lap of the rigid dummy and in the chest of the jointed dummy.

WEBBING ELONGATIONS

Table 5 gives the averages and ranges of dummy decelerations and belt loadings for various test conditions, but this time broken down into separate groups on the basis of known differences in webbing elongation. The "high elongation" webbings were those ranging from 21 to 29 percent elongation under a 2,500-lb load (using the SAE test method) and the "low elongation" webbings were in the 14 to 15 percent range. Most of the overlapping has been eliminated for any given set of test conditions by this grouping on the basis of webbing elongation, and the apparent reproducibility of the results is improved considerably.

Ranges within groups have not been entirely eliminated, however, because as was stated earlier, the characteristics of the belts themselves influence the deceleration of the dummy and the loads on the belt, and the belts within each group were not completely alike: variations of webbing elongation existed within each group (small variations are known to exist even among different pieces of webbing from a single roll), and, among the harnesses, the geometric configurations of the harnesses themselves varied; e.g., some had the chest strap anchored to the doorpost, others to the floor. The 25-mph runs are not separated into elongation groups because only high elongation webbings were used in these runs. The comparisons are not complete because of still another factor—the three low-elongation lap belts tested at 21 mph broke when they reached the peaks noted. Had they not broken, the 21-mph peaks may have been higher, and overlapping may have been completely absent as it was in the 15-mph tests in which no breakage occurred.

In spite of the qualifications just described, the separations between the high and

TABLE 5

EFFECTS OF WEBBING ELONGATION

Device	Type of Dummy	Impact Speed (mph)	Dummy Deceleration (peak g)				Belt Load (peak lb)				Avg. Duration[a] (millisec)			
			High Elong.		Low Elong.		High Elong.		Low Elong.		Decel.		Loads	
			Avg.	Range	Avg.	Range	Avg.	Range	Avg.	Range	High	Low	High	Low
Lap belt	Rigid	15	22	20-23	29	29-30	4,100	3,900-4,400	5,300	5,200-5,400	45	42	50	45
		21	30	25-35	Broke at 30-35		5,800	5,400-6,600	Broke at 6,200-7,500		55	Broke	54	Broke
Harness	Jointed	21	55	40-70	78	72-82	5,500	4,000-7,300	6,800	5,600-8,100	50	53	65	58

[a]Durations of deceleration are for 5g and over; durations of loading are for 1,000 lb and over, because of indefiniteness of endpoints in many cases.

low elongation groups were sufficiently consistent to demonstrate that differences in webbing elongation produce substantial differences in effects. In accidents of equal severity (that is, equal impact velocity and equal vehicle stopping distance), the low elongation webbing produced deceleration peaks and belt load peaks about one-third higher than the high elongation webbing. Because of this difference, it was observed that lap belts whose low elongation webbings were stronger in static tests (7,200 lb as against 6,800 lb) did not survive the dynamic tests at 21 mph, whereas the lower-strength high elongation belts did survive.

The implication of these observations is very significant in weighing the respective merits of the static and dynamic tests. In static testing there is an assumption that belts withstanding equal static loadings are equally meritorious and can therefore survive equally severe crash conditions. But the tests show that in collisions in which all other conditions are equal, a difference in webbing elongation produces different loads on the belts. With respect to this phenomenon, the dynamic test is certainly superior in that it permits the elongation characteristics of the belt to influence the load on the belt, whereas the static tests ignore this factor completely.

Incidentally (inasmuch as it does not bear on the matter of test methods), these tests show that low elongation webbings place more load on the body being restrained than do high elongation webbings; a 33 percent decrease in elongation (e.g., from 21 to 14 percent elongation) produced an increase of roughly 33 percent in load, with virtually no change in the duration of the loading. This is a point that should be considered in designing seat belts from the medical point of view.

LOCATIONS OF THIRD ANCHOR

Test results on harnesses, grouped in this case by location of the chest strap anchor (either shoulder-high on doorpost, or on the car floor behind the seat) are given in Table 6. These data indicate that the location of the third anchor does affect the dummy deceleration and its rate of onset, the belt load, and the durations of the forces. Perhaps the most significant of these differences is that the floor-anchored chest straps produce the highest peak decelerations of the upper torso and yet require more time to stop the dummy than do those anchored to the doorpost shoulder high. The significance of these apparently contradictory effects of anchor location is revealed by a different kind of study (high-speed photography) described later. Only one point should be emphasized here—that a study of this type is possible with a dynamic test using a jointed full-size dummy, but a static test would reveal nothing along these lines.

All of the observed effects of different webbing elongations, and some of those of different anchor locations, could have been derived from theoretical considerations, or, at least, they are reasonable and self-consistent in hindsight. For example, lower elongation webbing could be expected to decrease the stopping distance of the dummy,

TABLE 6

EFFECTS OF LOCATION OF CHEST STRAP ANCHOR OF HARNESSES

Impact Speed (mph)	Dummy Decel. (peak g)		Belt Load (peak lb)		Avg. Duration[a] (millisec)			
					Deceleration		Loads	
	Doorpost Anchor	Floor Anchor	Doorpost Anchor	Floor Anchor	Door	Floor	Door	Floor
21	59	64	7,000	5,400	32	61	48	67
25	72	100	8,800	7,000	37	61	48	66

[a]Durations of deceleration are for 5g and over; durations of loading are for 1,000 lb and over, because of indefiniteness of endpoints in many cases.

TABLE 7

BASIC TEST DATA

Run No.	Impact Speed (mph)	Dummy[a]	Belt Type[b]	Elong. (%)	Third Anchor	Dummy Decel.		Belt Loading					
								Peak (lb at anchors)				Duration[c] (millisec)	
						Peak (g)	Duration[c] (millisec)	Left	Right	Third	Total	Total	Notes[d]
3	25	J	LD	21	Door	85	25	2,500	4,400	2,000	8,900	37	
4			LD	21	Door	92	27	4,000	4,500	2,500	14,000	53	
5			LD	21	Floor	105	63	1,800	3,300	2,400	7,500	75	
6			LD	21	Floor	108	70	1,700	3,500	2,400	7,600	72	
7			L2S	21	Floor	112	60	2,400	2,400	1,500	6,300	58	
8			LD	-	Door	40	60	1,800	2,600	2,200	6,600	53	1, 3
9			LD	-	Floor	75	51	2,700	1,400	2,300	6,400	58	1, 3
14	21	J	LD	21	Door	70	26	1,900	3,100	2,300	7,300	53	
15			LD	14	Door	72	24	2,100	3,800	2,200	8,100	40	
16			LD	21	Floor	42	57	1,800	2,200	1,200	5,200	75	
17			LD	14	Floor	82	55	2,200	2,900	1,500	6,600	72	
18			L2S	21	Floor	55	66	1,500	1,600	900	4,000	68	
19			L2S	14	Floor	78	80	2,000	2,100	1,500	5,600	61	
20			LD	-	Door	35	46	1,500	2,200	1,900	5,600	50	1, 3
21			LD	-	Floor	65	48	2,000	2,100	1,200	5,300	58	1
51	21	R	L	21		32	60	2,600	2,800	-	5,400	52	3
52			L	21		25	47	2,800	2,600	-	5,400	50	3
53			L	21		35	50	3,300	3,300	-	6,600	50	
54			L	14		30	-	3,500	3,700	-	7,200	-	2
55			L	14		35	-	3,750	3,750	-	7,500	-	2
56			L	29		27	63	2,850	2,850	-	5,700	63	1, 3
57			L	23		35	-	3,100	3,100	-	6,200	-	1, 2
58			L	23		25	-	2,700	2,000	-	4,700	-	1, 2
59			L	15		30	-	2,700	3,500	-	6,200	-	1, 2
60	15	R	L	21		22	45	1,900	2,000	-	3,900	42	
61			L	21		23	43	2,000	2,000	-	4,000	49	
62			L	14		30	40	2,500	2,700	-	5,200	42	
63			L	14		-	-	2,400	2,900	-	5,300	50	
64			L	29		20	45	2,200	2,200	-	4,400	58	1
65			L	15		29	43	2,700	2,700	-	5,400	44	1

[a] J = jointed full-size dummy, without arms, with soft abdomen, 154 lb, accelerometer in chest; R = rigid dummy, torso and thighs only, seated position, 150 lb, accelerometer in lower back.

[b] L = lap strap only; D = diagonal chest strap only; LD = combination belt, lap and diagonal chest straps; L2S = combination belt, lap and two shoulder straps.

[c] For decelerations of 5g and over, for total belt loads of 1,000 lb and over, and for individual anchor loads of 500 lb and over.

[d] 1 = belt included buckle; all others continuous webbing from anchor to anchor to minimize chance of slippage; 2 = webbing broke at or near peak load; 3 = slippage in one anchor.

which would increase its deceleration rate, resulting in turn in an increased peak load on the belt. Nevertheless, the ability of the Swedish test method to demonstrate these reasonable effects with a high degree of consistency is another factor that increases confidence in the method.

Table 7 gives the pertinent test data obtained in 30 runs. Several typical graphs of instrument data are in the Appendix, which also contains descriptions of the Swedish dynamic test equipment and the instruments used in this study.

One final point deserves mention—with the Swedish test method, peak belt loads up to 11,000 lb and peak dummy decelerations up to 112g were observed with the use of floor-anchored combination lap and chest strap belts. That these values are not atypical of severe automobile crashes is indicated by the controlled car crash data given in Table 1, in which peaks as high as 15,000 lb and 73g were observed with lap belts alone. The question of whether such forces are tolerable by the human body is beyond the scope of this report, but the data indicate the ways in which the designs of harnesses may be changed to avoid excessively high peaks.

Valuable as the test data presented herein may be, they also indicate that considerably more exploration of the performance of seat belts by dynamic methods would be profitable, particularly in the evaluation of current models and in the development of better designs and materials.

RESTRAINT OF UPPER TORSO

The data that have been presented up to this point have had a bearing on problems involving decelerations of the belt wearer and loads on the belts themselves. But such instrumented runs furnish no direct information on how well a particular type of belt limits the body's forward motion; that is, on how well it restrains the wearer. The

problem of restraining the upper torso to minimize head and chest injuries is considered particularly important in automobile accidents.

It is still another advantage of the Swedish dynamic test method that it can be used to observe by means of high-speed photography the degree of restraint of parts of the body by belts of various geometric configurations. A study of this kind was also performed in the summer of 1962 on nine models of harnesses then available in the United States. This study revealed, among other things, that diagonal chest straps alone may permit the wearer to slide out from under the belt or suffer severe internal injuries, and that combination belts with shoulder-high anchors for the chest strap limit the forward motion of the upper torso to about one-half that permitted by floor-anchored chest straps. These tests are described in detail elsewhere (13, 14); however, (a) the larger forward motion permitted by floor-anchored chest straps correlates well with the longer stopping time observed in the instrumented tests, and (b) the floor-anchored chest straps first permit the shoulders to lean forward into the chest strap and then produce a sudden very high peak deceleration when the dummy has leaned forward as much as it will go (compare dummy deceleration curves in Figs. 3 and 4 of the Appendix, for example).

Not all types of dynamic test apparatus are capable of producing information of this type. For example, the California Highway Patrol equipment is unable to observe restraint of the upper torso because it uses as its dummy a body block that is equivalent to the hips alone; it is therefore suitable only for testing lap belts. Modification of this equipment to make it capable of testing harnesses is likely because several harnesses are now on the American market. It is also likely that laboratory apparatus for dynamic testing of seat belts for quality control in manufacturing (or other routine testing) will not need to be capable of demonstrating restraining characteristics if these characteristics have been shown to be satisfactory in the design development stage. But the restraining characteristics of any new design, even if it is only a "slight" modification of an old design, should be tested first for its restraining characteristics in equipment of the kind used in Sweden.

SUMMARY AND CONCLUSIONS

Results of instrumented tests of seat belts by the Swedish dynamic test method have shown that (a) the peaks and durations of the decelerations of the belt wearer, as well as the loads on the belts, are of the same order of magnitude as those observed in controlled car crashes of a severe nature, (b) the characteristics of the belt itself exert a major influence on the deceleration rate of the belt wearer and on the magnitude and duration of the load on the belt, and (c) belts made of webbings found to be equally strong by the standard static test are not necessarily equally resistant to the forces developed in collision conditions of equal severity. These facts taken together indicate a clear superiority of dynamic testing over static testing.

The results have also demonstrated that the laboratory dynamic test is capable of producing information on the performance characteristics of belts of different geometric configurations and of various materials, to aid in evaluation and development of better safety belts. The specific effects of different webbing elongations and of third-anchor locations (for combination lap and chest strap belts) have also been demonstrated. The standard static tests are incapable of furnishing research and development information of this type.

In view of the need to develop seat belts that are effective in restraining the upper torso and are conventient to install and to don, more extensive use of dynamic testing is clearly called for.

ACKNOWLEDGMENTS

The authors wish to acknowledge with thanks the financial assistance of Consumers Union of U. S., Inc., Mount Vernon, N. Y., and Consumers' Association, Ltd., of London.

REFERENCES

1. Stapp, J. P., "Human Exposures to Linear Deceleration." Air Force Technical Report 5915, Pt. 2, (Dec. 1951); "Effects of Mechanical Force on Living Tissues." Jour. Aviat. Med. (Aug. 1955).
2. Severy, D. M., Mathewson, J. H., and Siegel, A. W., "Automobile Side-Impact Collisions, Series II." Society of Automotive Engineers Publication SP-232 (1962).
3. Fredericks, R. H., and Connor, R. W., "Crash Studies of Modern Cars with Unitized Structure." Society of Automotive Engineers, National West Coast Meeting (Aug. 1960).
4. Finch, D. M., and Palmer, J. D., "Dynamic Testing of Seat Belts." Society of Automotive Engineers Preprint (June 1956), and unpublished supplement.
5. Ryan, J. J., and BeVier, W. E., "Safety Devices for Ground Vehicles." Automotive Safety Research Project, Univ. of Minnesota (Sept. 1, 1960).
6. "Belt; Seat, Passenger Type, Automotive." Federal Supply Service, General Services Administration, Fed. Spec. JJ-B-185a (Jan. 19, 1960).
7. "Motor Vehicle Seat Belt Assemblies." Society of Automotive Engineers Standard J4 (1962).
8. Aldman, B., "Biodynamic Studies on Impact Protection." Acta Physiol. Scand., vol. 56, suppl. 192 (1962).
9. Frankland, J. M., "Effects of Impact on Simple Elastic Structures." Taylor Model Basin, U. S. Navy, Report 481 (April 1942).
10. Muller, J. T., "Transients in Mechanical Systems." Bell System Tech. Jour., 27:657-683 (Oct. 1948).
11. Muller, J. T., "Optimum Properties of a Packaging Material." Society of Automotive Engineers, Los Angeles Aeronautic Meeting (Oct. 1954).
12. Severy, D. M., Mathewson, J. H., and Siegel, A. W., "Automobile Head-On Collisions—Series II." SAE Trans., vol. 67 (1959).
13. Tourin, B., Aldman, B., Michelson, I., and Mitchell, J., "Restraining Characteristics of Harnesses." 6th Stapp Car Crash and Field Demonstration Conference (Nov. 1962).
14. Consumer Reports (Oct. 1962).

Appendix

Apparatus

The apparatus used in these tests is located in Stockholm, Sweden, at the Statens Provningsanstalt (National Institute for Materials Testing). An over-all view is shown in Figure 1 (details are shown in Fig. 14).

The cart, constructed of steel beams, is 7.5 ft lóng and 2.3 ft wide, with the wheels mounted outside the frame. The wheel base is 4.6 ft, and the lateral distance between wheel centers is 2.8 ft. The cart weight is approximately 660 lb, including the bucket seat which is rigidly fixed on the frame, with its front edge about 6 in. behind the front wheel axles.

The cart is accelerated by a 2,200-lb falling weight connected to the cart by a cable; the pulley system has a mechanical advantage of 2, and the net acceleration imparted to the cart is 0.9g. When the acceleration is applied for a distance of 23 ft, a speed of 25 mph is achieved; lower speeds are obtained by appropriately shortening the run. The falling distance of the weight is so adjusted that the cart reaches the desired speed 5 ft before impact, and runs free to impact.

To cushion the impact, a lead cone (90 mm long, with 40- and 50-mm diameters at the ends) is fastened to the front of the cart. The cart frame has suitable cross-members behind the seat to accommodate any kind of floor anchor, and a braced vertical post to accommodate shoulder-high anchors.

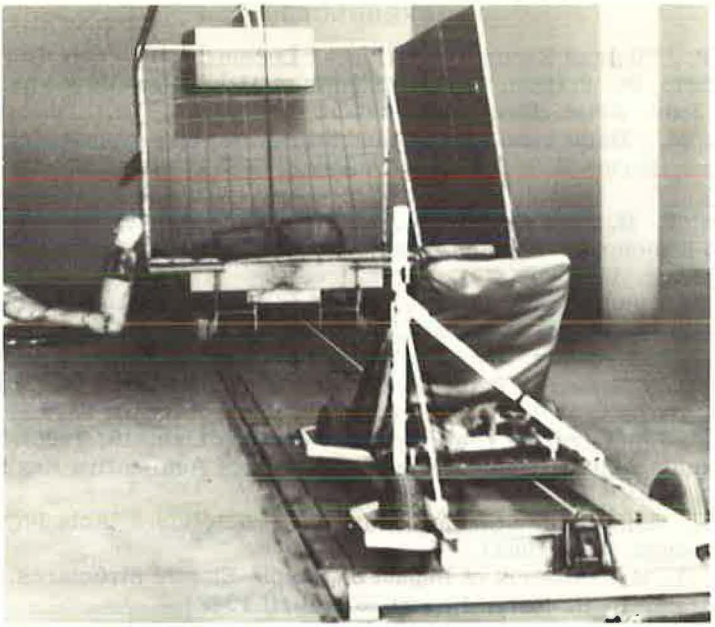

Figure 1. Swedish dynamic test equipment, looking down the track toward the barrier—falling weight is at top center, behind fixed barrier; cart held at starting point by quick-release mechanism fixed in floor; jointed dummy shown at left.

Dummies

The dummy used for harness tests is jointed; that is, its head, chest, pelvic section, and parts of the leg are made of wood, and between the wood parts are heavy sponge rubber blocks (between the hips and the chest, and parts of the legs). Steel plates are also used in some sections. The various parts are kept together by chains and springs running through the center of the parts. Thus the neck, the midsection, the thighs, and the legs are capable of being flexed. The various parts weigh as follows: head, 10.6 lb; breast, 36.3 lb; abdominal section, 17 lb; pelvic section, 51.7 lb; legs (including thighs) 38.5 lb. Total weight is 154 lb. The length of the dummy is approximately 5 ft 8 in.

The dummy used for lap belt tests is rigid, constructed of wood and steel channel. It consists only of that part of a body between the neck and the knees; it has no head, arms, or legs. It is in a sitting position, and its hip section, where the lap belt rests on it, is shaped like the body block used in the SAE, GSA, and California tests. As on these body blocks, the lap is covered with a layer of sponge rubber. The weight of this dummy is 150 lb. Figure 2 shows this dummy seated on the cart's bucket seat and some details of the cart itself.

Instrumentation

The instruments used were an accelerometer, and three load cells mounted directly on specially constructed ladder brackets through which the webbings were threaded for attachment to the anchors. Two dual beam oscilloscopes, with Polariod cameras, were used to record the instrument data.

Acceleromenter:	Statham Model KPF 402; range $\pm$ 200 g; output linear up to 750 cps. Used in conjunction with low pass filters; 370 cps with the rigid dummy, 530 cps with the jointed dummy.
Load cells:	Bonded strain gages, Philips 9812; range 4, 400 lb.
Oscilloscopes:	Tektronix Type 502, dual beam; range 0-100 kc.

Plots of the instrument data obtained in 11 typical runs are shown in Figures 3 through 13. The cart deceleration curves shown are not determined in this study, but are typical curves obtained in a separate study by Dr. Aldman; these typical curves were inserted here only to show the order of magnitude of the cart deceleration and the time-relationship between the deceleration of the cart and the dummy.

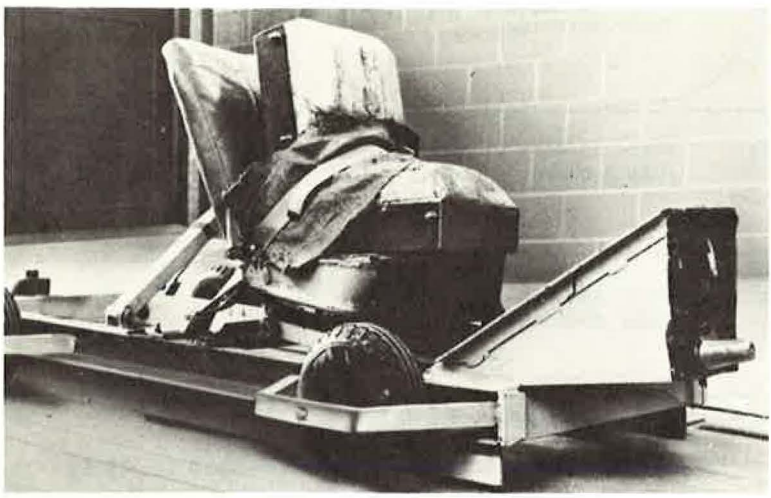

Figure 2. Swedish dynamic test cart, with lead cone fixed on front end—rigid dummy shown in bucket seat, held by lap belt.

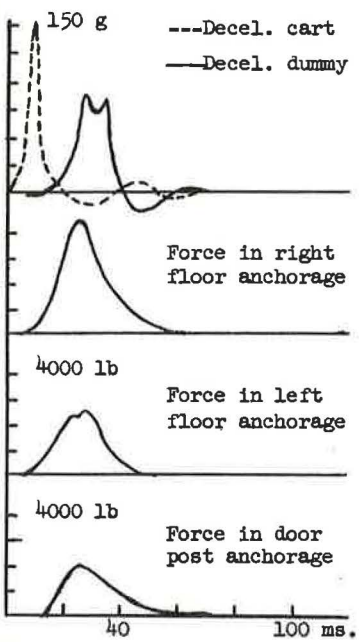

Figure 3. Test 3: 25 mph, jointed dummy; combination lap and chest strap, third anchor on doorpost; 21 percent elongation webbing.

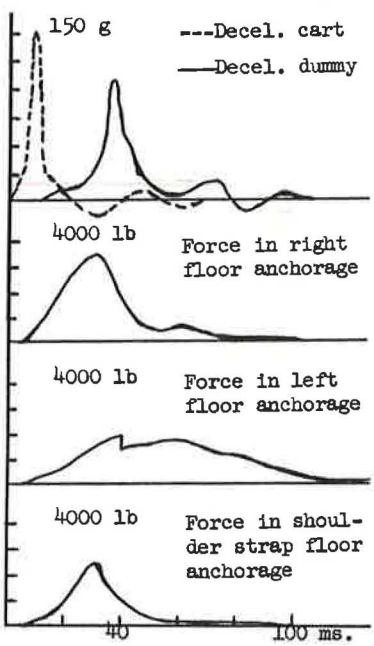

Figure 4. Test 5: 25 mph, jointed dummy; combination lap and chest strap, third anchor on floor; 21 percent elongation webbing.

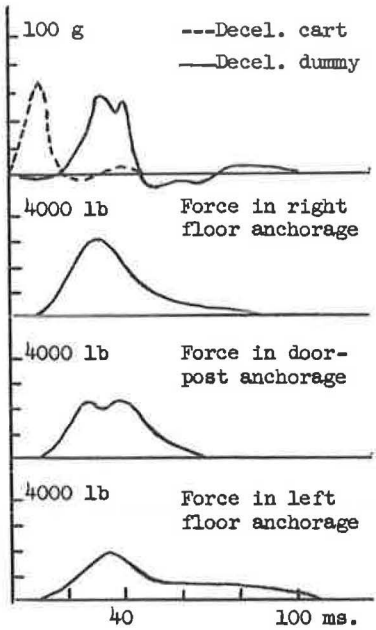

Figure 5. Test 14: 21 mph, jointed dummy; combination lap and chest strap, third anchor on doorpost; 21 percent elongation webbing.

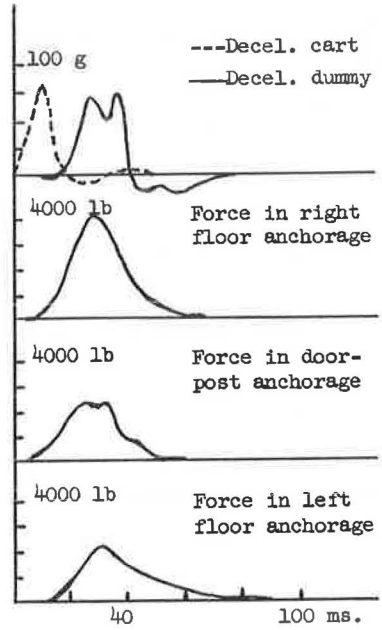

Figure 6. Test 15: 21 mph, jointed dummy; combination lap and chest strap, third anchor on doorpost; 14 percent elongation webbing.

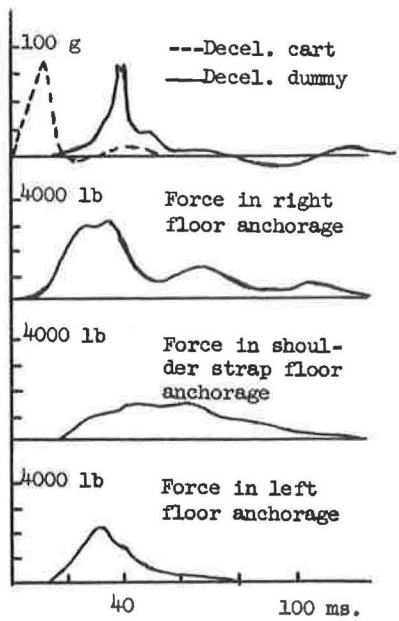

Figure 7. Test 17: 21 mph, jointed dummy; combination lap and chest strap, third anchor on floor; 14 percent elongation webbing.

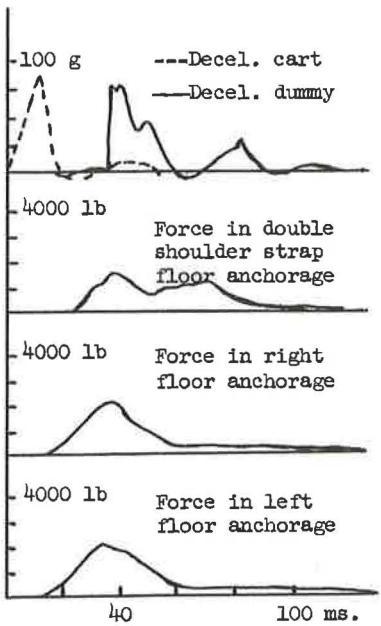

Figure 8. Test 19: 21 mph, jointed dummy; combination lap and double chest strap, third anchor on floor; 14 percent elongation webbing.

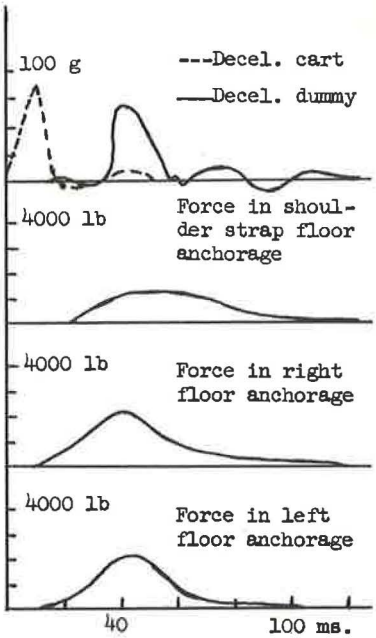

Figure 9. Test 21: 21 mph, jointed dummy; combination lap and chest strap, third anchor on floor; elongation not determined.

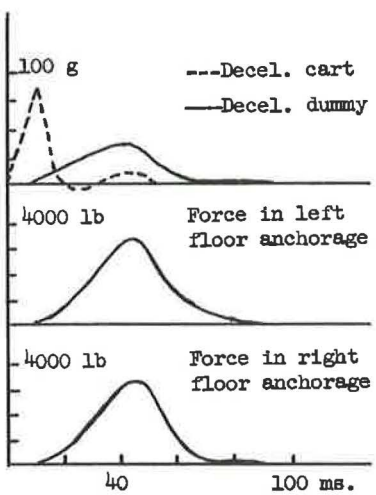

Figure 10. Test 53: 21 mph, rigid dummy; lap strap only, 21 percent elongation webbing.

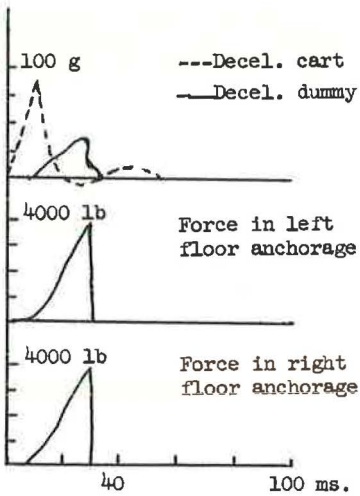

Figure 11. Test 55: 21 mph, rigid dummy; lap strap only, 14 percent elongation webbing.

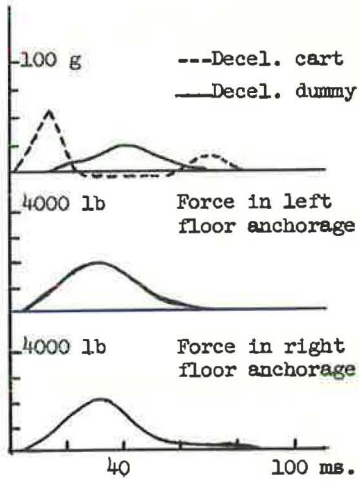

Figure 12. Test 60: 15 mph, rigid dummy; lap strap only, 21 percent elongation webbing.

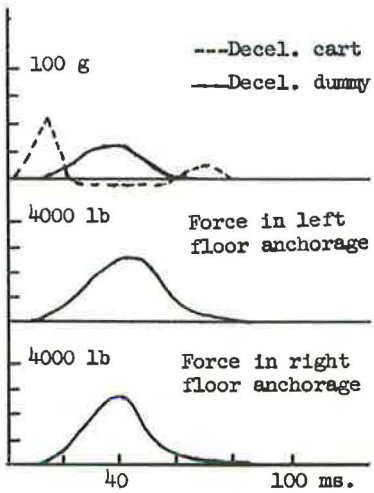

Figure 13. Test 62: 15 mph, rigid dummy; lap strap only, 14 percent elongation webbing.

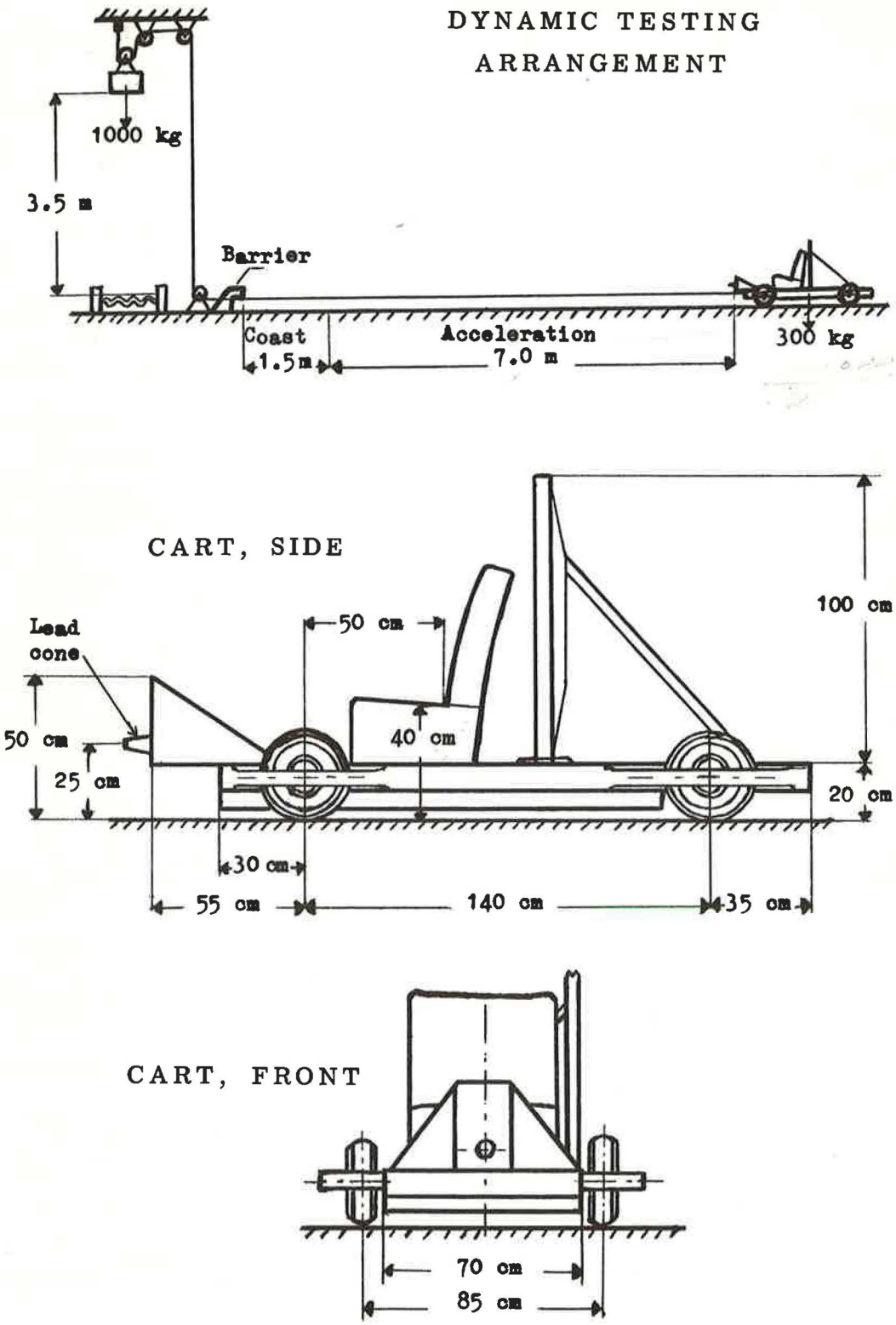

Figure 14. Details of test apparatus.

Effect of Seat Harness on Movement of Car Occupant in a Head-On Collision

G. GRIME, Senior Principal Scientific Officer, Traffic and Safety, Road Research Laboratory, Harmondsworth, Middlesex, England

•IN SPITE OF all that can be done to prevent road accidents, by improvements to vehicles and to roads and by training drivers and other road users to use the road more carefully, a certain number—probably a large number—of accidents will continue to take place. The problem of providing protection for car occupants in accidents, therefore remains an important one.

The nature of the problem is becoming clear as facts are collected concerning the circumstances of car accidents and the most serious types of injuries to the car occupants. In fatal accidents, more than 60 percent of the injuries are to the head and neck, and almost all other fatal injuries are to the trunk (1). Detailed investigations by the Road Research Laboratory, United Kingdom, into about 500 accidents that occurred near the Laboratory showed that about two-thirds of these accidents involved frontal collisions (i.e., within ± 45° of straight-ahead), about 12 percent were to the sides of cars, and about 7 percent were rear-end collisions. Thus, the most important problem is how to protect the heads and bodies of occupants in head-on collisions. This, therefore, indicates the primary purpose of a seat harness.

The forces and decelerations to which a person held in a seat harness is exposed in a head-on impact have long been a matter for discussion and, although some experimental values have been obtained, chiefly in America, there have been no established figures. It is possible, however, to calculate maximum values for these decelerations and forces if certain simplifying assumptions are made, and this is done in the present paper. A brief account of a similar analysis of the motion of a body held by a safety harness has also been given in a paper by Ryan and BeVier (2).

It is generally agreed that in European cars, which have only a limited space in front of the passenger, it is desirable to wear a harness that restrains the upper as well as the lower part of the body; that is, either a diagonal belt, a diagonal and lap belt, or a full harness having two shoulder straps (Fig. 1). The movement of the body of a person supported by one of these harnesses and exposed to the deceleration arising from a head-on impact is obviously likely to follow a complicated pattern; the lower trunk and the upper trunk may move forward at slightly different speeds, depending on the construction and fixing of the harness; the head will bend forward; the arms will rise to shoulder level, and the legs will tend to rise to hip level, but will probably be checked by the pressure of the feet against the floor or by the knees coming into contact with the dashboard.

In the present paper, no attempt is made to calculate the movements of the parts of the body in detail, but because three-quarters of the weight of the body is in those parts which are closely held by the seat harness (the trunk, thighs, and head), it seemed likely that a simplified representation of the human body could be used in calculations to determine the main features of the movement of a car occupant held by a seat harness. It has therefore been assumed that the passenger can be represented by a single mass, negligible compared with that of the car, that he exerts no muscular effort to prevent forward movement relative to the car, and that there is no pivoting about the legs or feet against, for example, the package shelf; the body is assumed to be rigid, not elastic or yielding, and the assumption is made that there is no damping due to friction with the seat or the harness. The mass representing the passenger is restrained

Paper sponsored by Committee on Highway Safety Research.

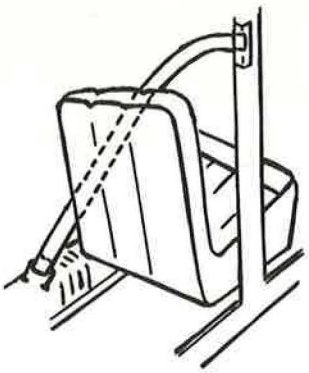

Diagonal belt fitted to door pillar.

Combined lap belt and single diagonal shoulder strap. (Alternatively, shoulder strap may be brought over back of seat and anchored to floor instead of door pillar.)

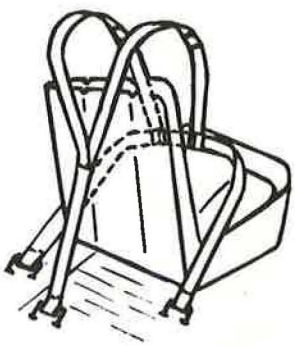

Lap belt and double shoulder straps. (Alternatively, shoulder straps may be anchored directly to floor at their front ends.)

Figure 1. Types of safety harness.

by a linear spring; that is, one in which the restraining force is proportional to the distance moved. This is approximately true for the materials of which seat harnesses are made.

This model is, of course, much simplified, but its behavior may be expected to correspond in many important details with what happens in practice.

STIFFNESS OF HARNESS

Stiffness is the force (in pounds) needed to stretch the harness 1 ft in a horizontal direction. The only harnesses for which the stiffnesses are readily calculable are those consisting of single loops, such as the single diagonal loop and the lap strap. It is assumed for purposes of calculation that the webbing, at its anchorages, lies at 45^{0} to a plane at right angles to the length of the car.

The next simplest arrangement—the lap belt combined with a single shoulder strap fixed to the door pillar—can be regarded, with rather less accuracy, as consisting of two loops, and its stiffness is, therefore, twice that of the single diagonal or lap strap.

In all other commonly used harnesses, whether full harness or combined lap and diagonal straps, the shoulder straps are anchored to the floor behind the seat and it is

difficult to calculate the contribution to the stiffness made by the shoulder loops. However, because these loops are each about 4 ft 6 in. long and are set at an angle to the floor which may be as great as 90°, their contribution to the stiffness is probably less than that of a single loop anchored to the door pillar. It will therefore be assumed that the diagonal belt is the arrangement of lowest stiffness and the lap belt with diagonal shoulder loop attached to the doorpost that of highest stiffness.

The materials usually used in the construction of harnesses give about 20 percent elongation for a 2,250-lb load. The stiffness of a diagonal belt of this material, 5 ft long, is calculated to be about 4,500 lb per ft. With a lap strap added, it is approximately twice this figure; that is, 9,000 lb per ft. Stiffer materials are also used for harnesses, the stiffest giving a calculated value of about 53,000 lb per ft for a combined lap strap and diagonal belt.

The stiffness alone is not sufficient to determine the behavior of a body held in a seat harness. The important factor is the stiffness in relation to the weight of the body (or more strictly its mass). The mass usually taken is 200 lb. This is an overestimation for the average vehicle occupant, but allows for the possibility that the harness may have to retain the seat in place as well as the person sitting on it. The lower limit for mass has been set at 112 lb, corresponding to a small woman on a well-anchored seat.

DECELERATION OF VEHICLE

The deceleration patterns of vehicles in head-on collisions have been recorded in many experiments, chiefly in the United States. A set of six records of head-on collisions at speeds from 21 to 52 mph obtained by Severy, Mathewson, and Siegel (3) is shown in Figure 2. Figure 3 shows records obtained at the Road Research Laboratory when light cars were run into street lighting columns at speeds of about 20 mph (4).

No two of these records are exactly alike, but if short duration fluctuations are neglected and an average curve is drawn, the most important parts of the resulting curves are usually single humps lasting for 0.05 to 0.20 sec. If the curves are smoothed out in this way, to simplify calculations, the resulting movement of the vehicle is changed very little. Two types of decelerations of the vehicle have therefore been assumed (Fig. 4). The first represents uniform deceleration; that is, a square-topped wave, with an instantaneous rise to a constant value. This is an approximation of cases like (e) and (f) for car 1 in Figure 2 where the deceleration rises to its maximum in a very short time. The second type has the form of one-half of a sine wave and resembles the smoothed records of many other examples in Figure 2.

In head-on collisions at a particular speed, other conditions being similar, the duration of impact may be expected to be less for small cars than for large ones, and the maximum decelerations may be correspondingly higher. Experiments to determine the magnitude of these differences are being carried out at the Road Research Laboratory.

BEHAVIOR OF ELASTIC HARNESSES

Figure 5 shows a schematic diagram of the car, passenger, and seat harness (the symbols are defined in the Appendix). It is required to determine the movement of the mass, representing the passenger, when the point of attachment of the spring (the harness) is decelerated from an initial velocity V by the application of decelerations of two assumed forms to the vehicle to which the spring is attached. Problems of this type are described in textbooks of physics and applied mathematics and only an outline is given here.

Constant Deceleration

If the vehicle is decelerated with a constant deceleration A, then the movement of the seat anchorage,

$$x - x_0 = Vt - \frac{At^2}{2} \qquad (1)$$

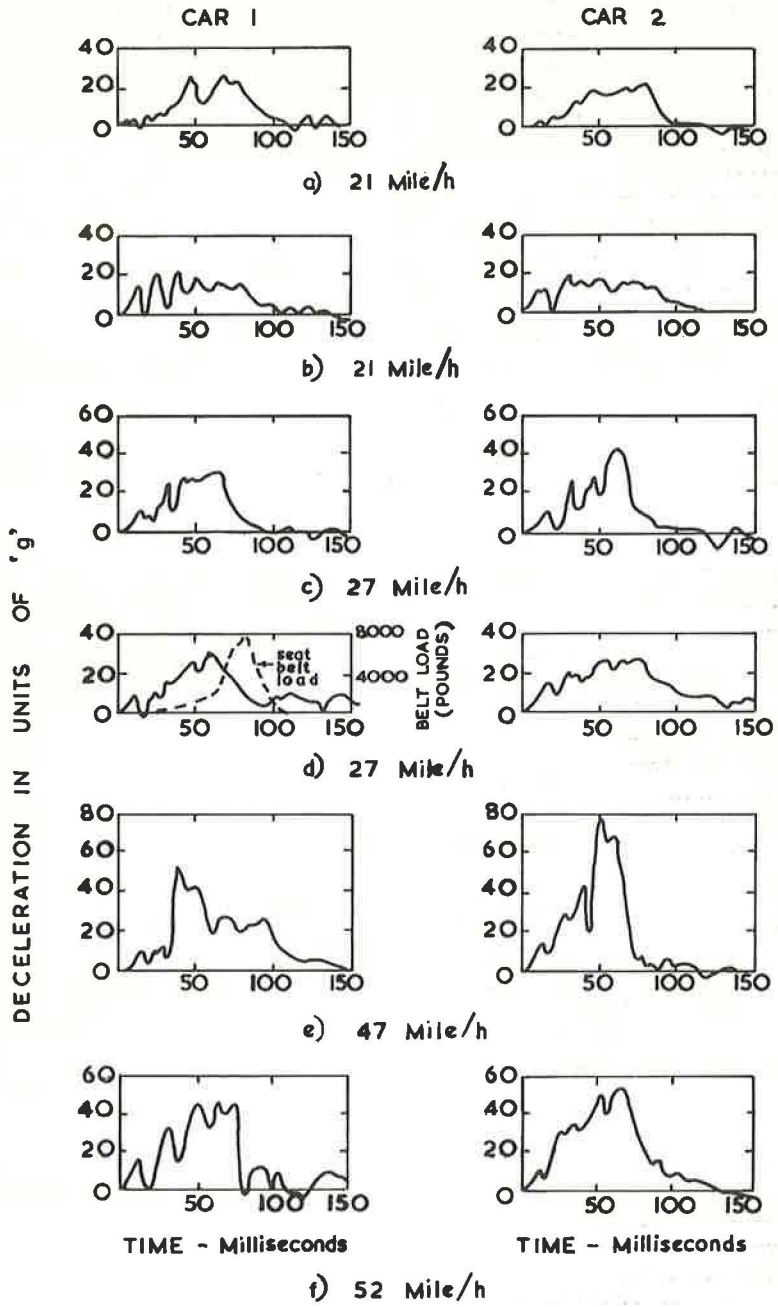

Figure 2. Decelerations of pairs of American cars of approximately equal weights in head-on impacts from various speeds.

The movement of the passenger restrained by the harness is given by

$$m \frac{d^2y}{dt^2} + k [(y - y_0) - (x - x_0)] = 0 \qquad (2)$$

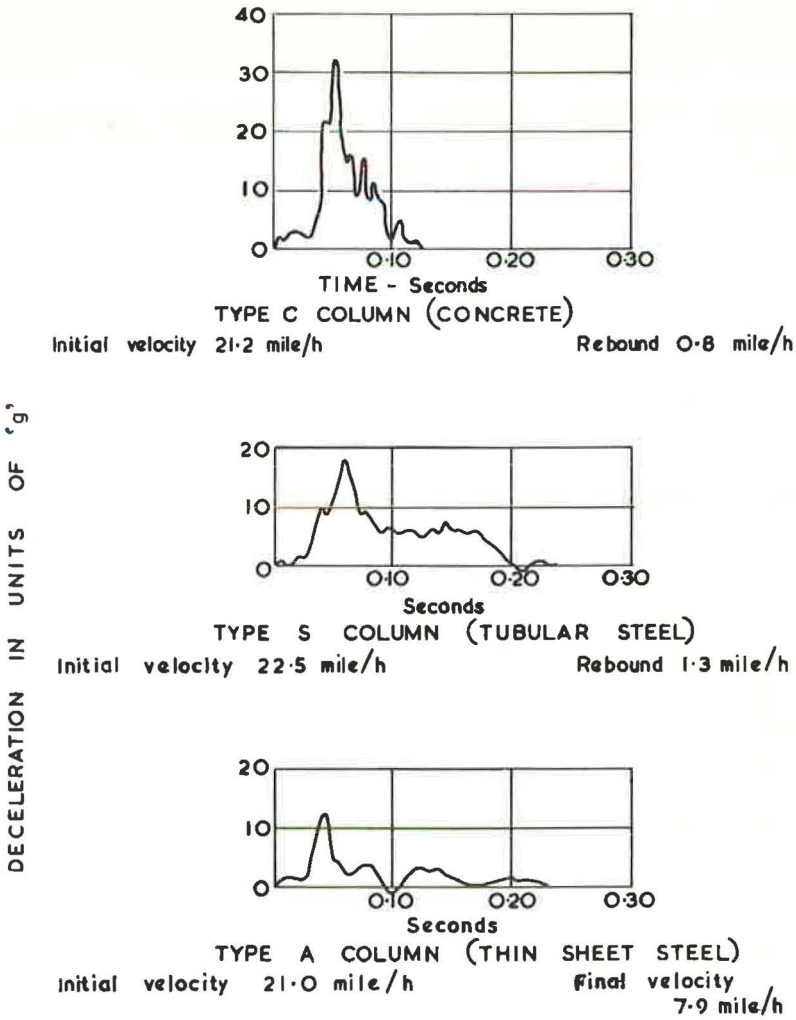

Figure 3. Decelerations of light cars in head-on collisions at about 20 mph with three types of lighting columns.

It is shown in the Appendix that a solution of this equation, in terms of the movement $(y - y_0)$ of the passenger is

$$y - y_0 = Vt - \frac{At^2}{2} + \frac{A}{p^2}(1 - \cos pt) \qquad (3)$$

in which $p^2 = k/m$.

The stretch S of the harness is the difference between the movement of the passenger and that of the vehicle:

$$S = (y - y_0) - (x - x_0)$$

$$= \frac{A}{p^2}(1 - \cos pt) \qquad (4)$$

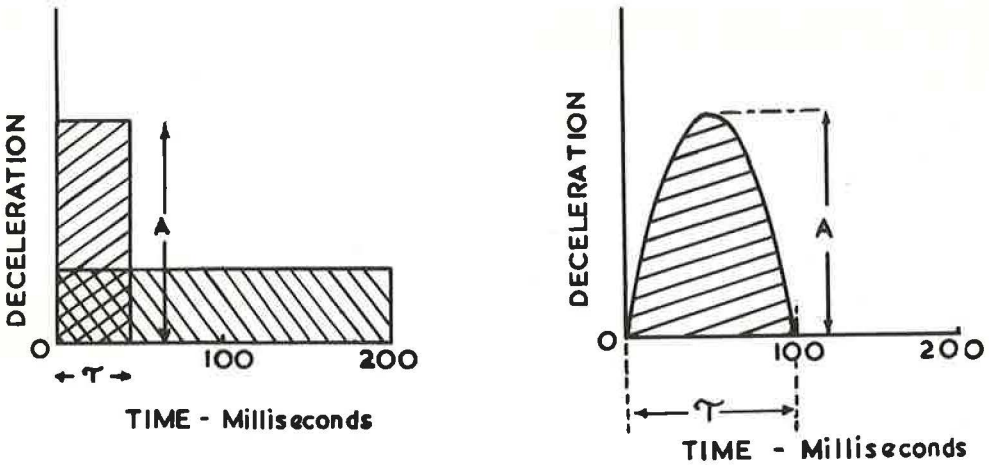

Figure 4. Assumed forms for decelerations of car: left, instantaneous rise, constant maximum; right, half-sine wave, -A sin ωt.

It is more instructive to rearrange this as

$$\frac{p^2 S}{A} = (1 - \cos pt) \tag{5}$$

because p^2S is the deceleration of the passenger, so that p^2S/A is the ratio of the deceleration of the passenger to that of the vehicle.

A constant deceleration applied instantaneously and maintained would result in an oscillation of the passenger on the harness, which behaves like a spring. The maximum deceleration of the passenger can then be as much as twice that corresponding to the steady deceleration of the vehicle; similarly, the maximum stretch of the harness is also twice that caused by a static force corresponding to the steady deceleration of the vehicle.

In practice, however, the deceleration of the vehicle is of short duration; for head-on impacts, as has been stated earlier, durations of between 0.05 and 0.20 sec are likely. With the values of the period of oscillation of the passenger on the harness likely to be met in practice, therefore there may not be time for the peak of the first oscillation to be reached before the vehicle comes to a stop; the maximum deceleration of the passenger is then less than twice that of the vehicle; its exact value depends on the ratio of two times, the duration τ of the deceleration, and the period of oscillation $2\pi/p$ of the passenger on the harness. It is shown in the Appendix that the maximum stretch of the harness is then

$$S = \frac{A}{p^2} \sqrt{2 (1 - \cos p\tau)} \tag{6}$$

Then,

$$\frac{p^2 S}{A} \max = \sqrt{2 (1 - \cos p\tau)} \tag{7}$$

Figure 6 shows how the "magnification" factor p^2S/A varies with this ratio. This figure also shows values of the deceleration times in seconds. These refer to a value of $2\pi/p = 0.23$ sec, for the most extensible harness and a 200-lb passenger. For de-

celerations of this square shape, therefore, the magnification of the deceleration of the car is less for the shorter durations in the practical range.

Although the magnification factor for decelerations increases with the duration of the deceleration (as in Fig. 6), if stops from a given speed are considered, the actual decelerations of the passenger decrease as the duration of the deceleration increases. This is because the maximum value of the deceleration in this case decreases as the duration increases, and this decrease more than compensates for the increased magnification. Figure 7 shows this effect for a 30-mph stop; for other speeds, the maximum stretch of the harness, and therefore the maximum deceleration of the passenger, changes in proportion to the speed.

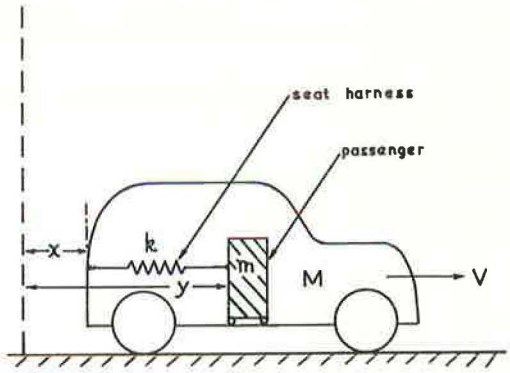

Figure 5. Representation of car, passenger, and seat harness.

Sine Wave Deceleration

The assumption that the deceleration time curve for the car has the form of a sine wave, lasting for one-half a period only, is usually a better approximation than that of

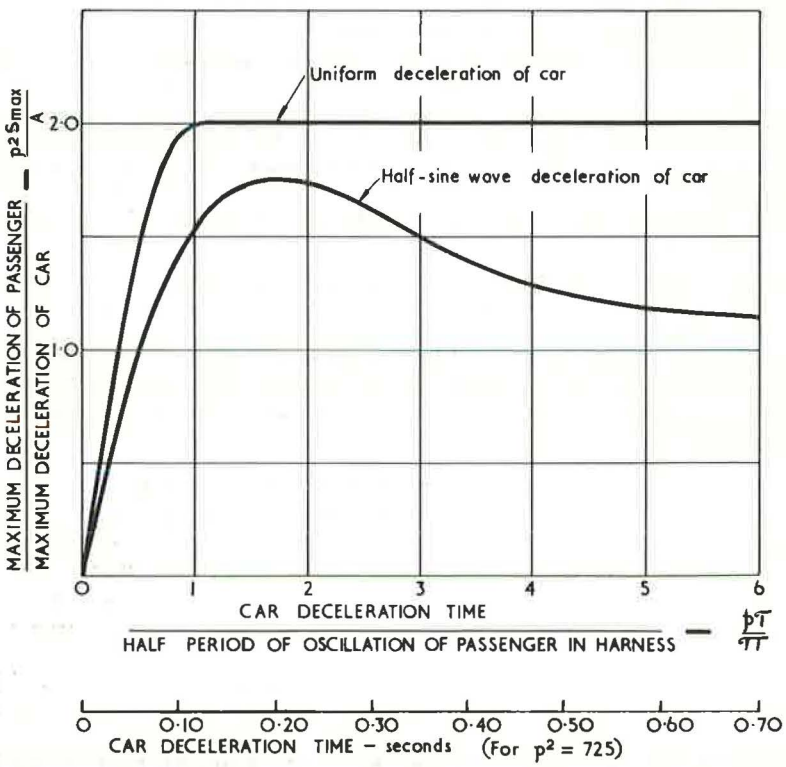

Figure 6. Maximum deceleration of passenger compared with that of car for various values of ratio of car deceleration time to half-period of oscillation of passenger in harness.

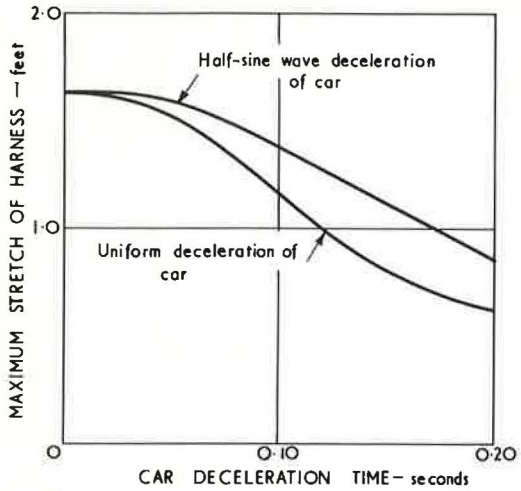

Figure 7. Maximum stretch of elastic harness ($p^2 = 725$) for stops of various durations from 30 mph.

a constant deceleration, instantaneously applied.

If the sine wave deceleration is assumed, $d^2x/dt^2 = -A \sin \omega t$, for $0 \le t \le \frac{\tau}{\omega}$ and $d^2x/dt^2 = 0$, for all other times under consideration, then the movement of the seat anchorage is given by

$$x - x_0 = \left(V - \frac{A}{\omega}\right) t + \frac{A}{\omega^2} \sin \omega t \qquad (8)$$

The movement of the passenger, restrained by the harness, is therefore

$$y - y_0 = \left(V - \frac{A}{\omega}\right) t - \frac{A}{p^2 - \omega^2} \left(\frac{\omega}{p} \sin pt - \frac{p^2}{\omega^2} \sin \omega t\right) \qquad (9)$$

in which as before, $p^2 = k/m$.

The stretch of the harness (Eq. 3) is in this instance

$$S = -\frac{A}{p^2 - \omega^2} \left(\frac{\omega}{p} \sin pt - \sin \omega t\right) \qquad (10)$$

and the magnification factor is

$$\frac{p^2 S}{A} = -\frac{p^2}{p^2 - \omega^2} \left(\frac{\omega}{p} \sin pt - \sin \omega t\right) \qquad (11)$$

These expressions are valid only for $0 \le t \le \pi/\omega$. After the deceleration has ceased (that is, after the car has stopped), the passenger may still continue to move forward, and the stretch of the harness and the resulting deceleration of the passenger may still continue to increase. In such cases, the maximum stretch of the harness is

$$\frac{p^2 S}{A} \text{ max } = \frac{p\omega}{p^2 - \omega^2} \sqrt{2 (1 + \cos p\tau)} \qquad (12)$$

As with the constant deceleration, the magnitude of the deceleration suffered by the passenger depends on the relation between the duration of the deceleration $\tau = \pi/\omega$ and the period of the oscillation of the passenger on the harness, $2\pi/p$. Figure 8 shows the way in which the stretch of the harness varies with time for various values of $p\tau/\pi$.

The time lag between the maximum deceleration of the car and the maximum stretch of the harness should be noted. Such time lags are always observed in experimental crashes where seat belts are used (Fig. 2). Figure 6 shows the variation of the magnification factor for the sine wave deceleration with duration of deceleration. Compared with the square wave result, also shown in Figure 6, the curve rises more slowly to a maximum of less than 2 and then falls off gradually to a value tending toward unity.

Again, as with the square wave deceleration, if the maximum stretch of the harness for a stop from a particular speed is plotted against time taken to stop, the stops that take longer to achieve produce lower decelerations for the passenger. This is shown by the top curve in Figure 7; for other speeds, the maximum stretch of the harness changes in proportion to the speed. The assumption of a sine wave deceleration instead of a square wave one makes a little difference to the maximum stretch of the harness for decelerations of short duration, and no more than 25 percent difference

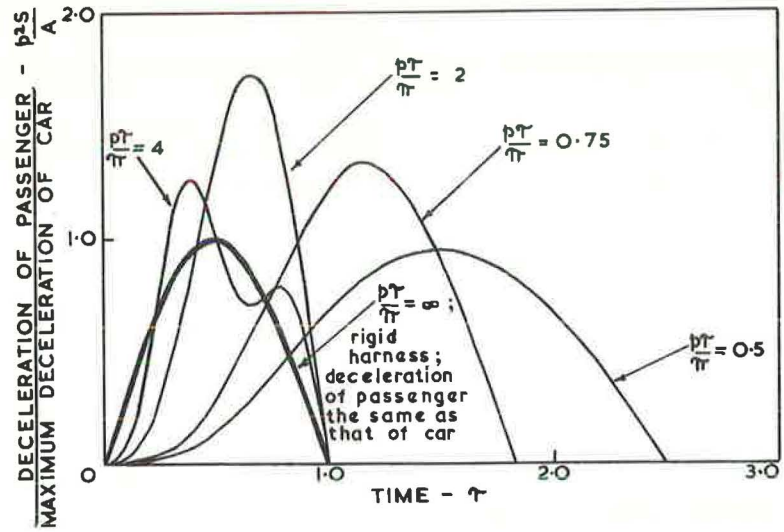

Figure 8. Deceleration of passenger held by elastic restraint compared with that of car at various times, showing different values of ratio of car deceleration time to half-period of oscillation of passenger ($p\tau/\pi$), assuming half-sine wave form for deceleration of car.

for the longest duration; thus, the sine wave approximation is probably adequate for calculations on seat harnesses. It follows too that the fine structure of the deceleration time curve is likely to be of secondary importance to a person held in by a seat harness; it may also be shown that the rate of rise of deceleration of the passenger is affected far more by the elastic properties of the harness than by the rate of increase in the deceleration of the car.

There is much experimental evidence to substantiate the conclusion that the deceleration of a passenger held in an elastic seat belt may sometimes exceed that of the vehicle when the vehicle deceleration is represented by an equivalent half-sine wave. Severy et al. (3) illustrate this phenomenon by a graph of the results from six experimentally produced head-on impacts in which the peak deceleration of dummy passengers, measured at the hips, varied from about 0.75 to 1.9 times that of the vehicle. They also draw attention to the time lag between the maximum deceleration of the vehicle and that of the passenger.

To make calculations from Severy's results is difficult, however, because the conditions differ from those assumed here; the seat belts used in his tests permitted rotation of the upper body, and the test results indicate that the energy of this rotation was by no means negligible compared with that necessary to stretch the belt.

The analysis also leads to the conclusion that a more extensible harness is not in all cases better than a less extensible one, in terms of the deceleration experienced by the passenger in the harness. Harnesses that extend very little are represented by the right-hand side (large values of $p\tau/\pi$) of Figure 6. The deceleration of the passenger than tends to become the same as that of the vehicle.

On the left-hand side of Figure 6 (small values of $p\tau/\pi$) the curve starts at zero and rises steeply to a maximum. It appears probable that practical values of $p\tau/\pi$ lie between 0.5 and 2.0. If this is the case, the maximum deceleration of the passenger may, in some cases, be higher than would be the case with an inextensible harness.

Table 1 shows this conclusion by reference to harnesses having three different values of p^2, covering the practical range of values; $p^2 = 725$, the most extensible, has a stiffness of 4,500 lb per ft combined with a mass of 200 lb; $p^2 = 1,800$, of medium stiffness, has a stiffness of 9,000 lb per ft combined with a mass of 160 lb; $p^2 = 15,000$, a very rigid harness, has a stiffness of 53,000 lb per ft and a mass of 112 lb. The table gives

TABLE 1

MAXIMUM DECELERATIONS OF PASSENGERS HELD IN SEAT HARNESSES OF DIFFERENT ELASTIC CHARACTERISTICS IN HEAD-ON IMPACTS FROM 30 MPH

Duration of Impact (sec)	Maximum Deceleration (g) for Harness of		
	Low Stiffness ($p^2 = 725$)	Medium Stiffness ($p^2 = 1,800$)	Very High Stiffness ($p^2 = 15,000$)
0.025	36	55	133
0.05	35	53	74
0.10	32	38	28
0.15	27	25	17
0.20	19	17	12

the calculated maximum decelerations of the passenger for different durations of head-on impact, all from 30 mph; for other initial speeds, the maximum decelerations are directly proportional to speed.

The results indicate that although the harness of lowest stiffness (most "give") yields lowest decelerations for impacts of very short duration, the one with highest stiffness is best for impacts of durations greater than 0.09 sec, such as those shown in Figures 2 and 3.

Figure 9 shows the same figures in graph form; a limiting line for the maximum possible deceleration defined by $p^2S = 1.75A$ has been included, so that it can be seen where the three lines for $p^2 = 725$, 1,800, and 15,000 touch this curve.

Too much weight should not be attached to the exact numerical values in the table and figure, however, as the experimental measurements to give accurate values of p have not yet been made. The other unknown factor is the amount of frictional resistance to the movement of the passenger which may be present for various reasons; for example, because of friction of the harness over the seat and the passenger's body, and of friction of the passenger's clothes on the seat. Departures from perfect elasticity of this kind will probably reduce the magnification factor and make the peak less pronounced; the calculated decelerations are therefore likely to be maximum values, not usually attained in practice.

An approximate idea of the maximum forces that a seat harness has to withstand is also given in Table 1. For a severe impact, with a duration of 0.1 sec, the maximum deceleration for the harness of medium stiffness ($p^2 = 1,800$) may be as high as 38g; the maximum force on the 160-lb man would therefore be about 6,000 lb. This is probably more than the practical value as some part of the weight of the legs is taken by the floor, but even so, it is clear that the forces can be very large and that breakages of harnesses might occur at speeds of about 30 mph.

IMPROVING SEAT HARNESS CHARACTERISTICS

The following are two methods of improving the characteristics of seat harnesses:

1. Alterations to the characteristics of harness material.—It has been suggested, on several occasions, that the material from which safety harnesses are made should have energy-dissipating characteristics; for example, the energy of recoil of the wearer of the harness should be not more than a certain fraction; say, one-half that of his forward motion. This requirement gives rise to a dynamic load extension curve like that in Figure 10 in which AD is one-half of AC and the area DBC is one-half area ABC. The effect of such a characteristic curve is as follows: First, the maximum stretch of the harness is, in general, determined by the curve AB as if it were a perfectly elastic harness with the same load extension curve, because, in the practical

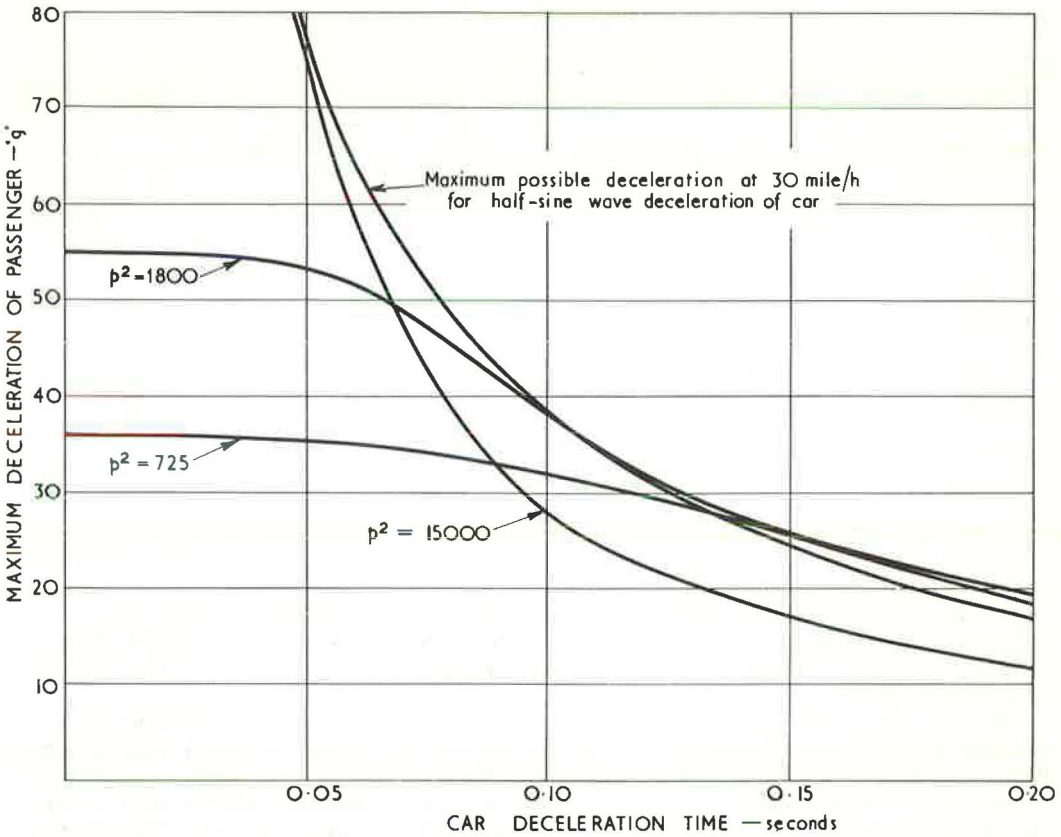

Figure 9. Maximum deceleration of passenger in stops of various durations from 30 mph with elastic harnesses of three different stiffnesses.

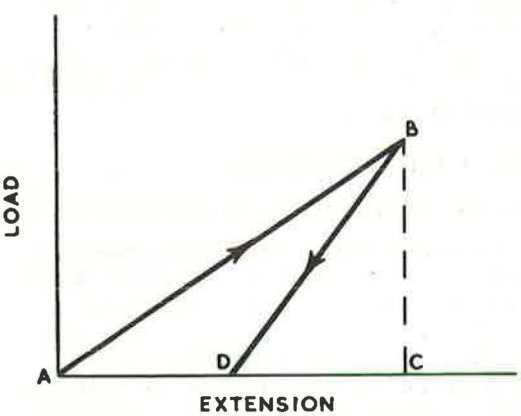

Figure 10. Idealized curve for energy-dissipating harness material.

cases in Figure 8 where $p\tau/\pi$ has values between 0.5 and 2.0, the curves have only a single maximum; for any particular load-extension curve this maximum is the same, whatever the origin of the forces opposing the first extension of the harness.

Second, the return velocity is less than that calculated, assuming perfect elasticity. The new return velocity v'_r is related to v_r for a perfectly elastic harness,

$$v'_r = v_v \sqrt{\frac{\text{area DBC}}{\text{area ABC}}} \qquad (13)$$

The effect of these characteristics is, therefore, to reduce the likelihood of the "slingshot" effect but to have no influence on the maximum deceleration of the passenger in the harness.

2. Harness that yields at a predetermined load. —With a harness that yields at a predetermined load, a very stiff or almost inextensible harness is attached

to the vehicle through a link that yields when a predetermined load is reached; movement then takes place against a constant force.

The total forward movement of the passenger's body in relation to the vehicle when the deceleration time curve has the form of a half-sine wave can be shown to be, for most cases of practical interest,

$$S_{max} = \frac{V}{2}\,\tau\left[\frac{mA}{F}\cdot\frac{1}{\pi}\cdot(1+\cos\omega t_1) - \left(1-\frac{t_1}{\tau}\right) + \frac{F}{mA}\cdot\frac{1}{2\pi}\right] \qquad (14)$$

in which

F = force at which link yields and $A > \frac{F}{m}$;
$\tau = \pi/\omega$ = duration of half-sine wave deceleration; and
t_1 = time, measured from beginning of impact, at which deceleration of vehicle becomes equal to F/m.

Eq. 13 is correct only for conditions in which the forward movement of the passenger's body continues until or after the vehicle stops, but this covers most cases of interest.

Figure 11 shows the behavior of a seat harness having these properties. It shows the maximum extension of a harness with the yield point set at 20g when the duration of impact is 0.10 sec; the extension is less than 1 ft at all speeds up to 49 mph. With two out of three of the elastic harnesses considered in Table 1 and Figure 9, the extension is greater than that of the yielding harness; with all three, the decelerations of the passenger are greater than those with a yielding harness.

Harnesses of the yielding type, therefore, suggest the possibility of harnesses that are effective in head-on impacts at speeds up to nearly 50 mph, without subjecting the passenger's body to excessive forces and without stretching more than 1 ft. This is probably about 15 mph more than existing elastic harnesses will withstand.

To provide for an impact of shorter duration than 0.10 sec, some increase in the yield point and, therefore, in passenger deceleration will have to be tolerated. The dashed curve in Figure 11 is drawn for an impact of duration of 0.05 sec and a harness yielding at 30g. This, again, has the desired characteristics up to speeds of 47 mph.

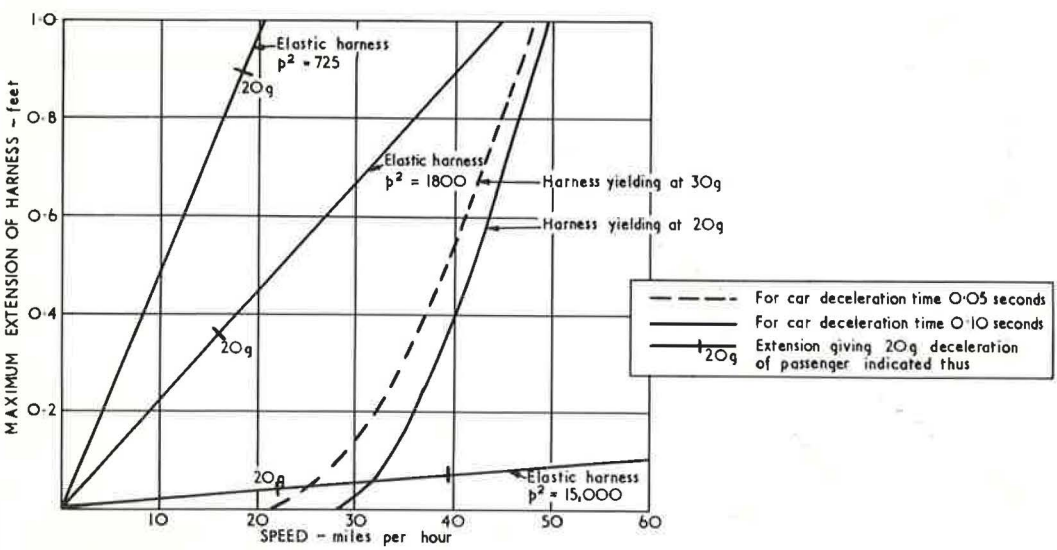

Figure 11. Maximum extensions of yielding harnesses compared with those of elastic harnesses over range of speeds (passenger decelerations obtained by multiplying extensions by appropriate p^2).

ACKNOWLEDGMENTS

This paper describes work carried out as part of the program of the Road Research Board of the Department of Scientific and Industrial Research, United Kingdom, and is published by permission of the Director of Road Research.

REFERENCES

1. Moreland, J. D., Proc., Symposium on Biomechanics, Institution of Mechanical Engineers, London, pp. 33-6 (1959).
2. Ryan, J. J., and BeVier, W., "Safety Devices for Ground Vehicles." U. S. Department of Health, Education, and Welfare (Sept. 1960).
3. Severy, D. M., Mathewson, J. H., and Siegel, A. W., "Automobile Head-On Collisions, Series II." SAE Trans., 67:238-62 (1959).
4. Moore, R. L., and Christie, A. W., "The Design of Lamp Columns for Roads with Few Pedestrians." Light and Lighting, 53:330-4 (1960).

Appendix

The symbols used in this report are defined as follows:

M = mass of vehicle;
V = initial velocity;
m = mass of passenger;
k = stiffness of linear spring representing seat harness;
x = coordinate of anchorage of seat harness with respect to a fixed external point;
y = coordinate of a particular point of passenger with respect to same fixed external point;
t = time measured from instant of first impact;
τ = duration of deceleration of car;
x_0 and y_0 = values of x and y at $t = 0$;
S = stretch of harness;
S_τ = stretch of harness at time $t = \tau$;
V_τ = velocity of passenger at time $t = \tau$;
Y_τ = value of y at time $t = \tau$.

Constant Deceleration of Vehicle

If the vehicle is decelerated with a constant deceleration A, instantaneously applied at $t = 0$, then the movement of the seat anchorage,

$$x - x_0 = Vt - \frac{At^2}{2} \tag{1}$$

The equation for the movement of the passenger is

$$m\frac{d^2y}{dt^2} + k\left[(y - y_0) - (x - x_0)\right] = 0 \tag{2}$$

Substituting for $(x - x_0)$ from Eq. 1,

$$\frac{d^2y}{dt^2} + p^2y = p^2\left(y_0 - \frac{At^2}{2} + Vt\right) \tag{15}$$

in which

$p^2 = k/m$.

The solution of this equation, satisfying the initial conditions that $t = 0$, $y = y_0$, and $dy/dt = V$ is

$$y - y_0 = -\frac{At^2}{2} + Vt + \frac{A}{p^2}(1 - \cos pt) \tag{3}$$

The stretch of the harness,

$$S = (y - y_0) - (x - x_0)$$

$$= \frac{A}{p^2}(1 - \cos pt) \tag{4}$$

or expressed nondimensionally,

$$\frac{p^2 S}{A} = (1 - \cos pt) \tag{5}$$

p^2S is the deceleration of the passenger, so that p^2S/A is the ratio of his deceleration to that of the vehicle.

This equation describes the behavior of the system during the period $0 \leq t \leq \tau$, where τ is the duration of the deceleration. If τ is greater than π/p, the maximum deceleration of the passenger is twice that of the car; but when $\tau < \pi/p$, a separate calculation has to be made for $t > \tau$, to obtain the maximum value of the stretch of the harness.

Movement of Passenger When $t > \tau$

The following equation gives the movement of the passenger in the period when $t > \tau$; that is, after the car has come to rest:

$$m\frac{d^2y}{dt^2} + k(y - y_\tau + S_\tau) = 0$$

or

$$\frac{d^2y}{dt^2} + p^2y = p^2(y_\tau - S_\tau) \tag{16}$$

The initial conditions now are that at $t = \tau$, $y = y_\tau$, and $\frac{dy}{dt} = V_\tau = \frac{A}{p}\sin p\tau$, the solution is

$$y - y_\tau = \frac{V_\tau}{p}\sin p(t - \tau) - S_\tau\left[1 - \cos p(t - \tau)\right] \tag{17}$$

This has its maximum when

$$\tan p(t - \tau) = \frac{V_\tau}{pS_\tau} \tag{18}$$

The maximum total stretch of the harness is, therefore,

$$S_{max} = (y - y_\tau)_{max} + S_\tau = \sqrt{\frac{V_\tau^2}{p^2} + S_\tau^2} \tag{19}$$

Substituting for V_τ and S_τ gives

$$S_{max} = \frac{A}{p^2}\sqrt{2(1 - \cos p\tau)} \tag{20}$$

or

$$\frac{p^2 S_{max}}{A} = \sqrt{2(1 - \cos p\tau)} \tag{21}$$

Sine Wave Deceleration

If the deceleration time curve for the car has the form of a sine wave, lasting for one-half a period (that is, for a time $\tau = \pi/\omega$ with maximum deceleration A, then $d^2x/dt^2 = -A \sin \omega t$, for $0 \leq t \leq \frac{\tau}{\omega}$, and $d^2x/dt^2 = 0$, for other times.

With the initial conditions that at $t = 0$, $x = x_0$, and $dx/dt = V$,

$$x - x_0 = \frac{A}{\omega^2} \sin \omega t + \left(V - \frac{A}{\omega}\right) t \tag{8}$$

Putting Eq. 8 into Eq. 2,

$$\frac{d^2y}{dt^2} + p^2 y = p^2 \left[y_0 + \left(V - \frac{A}{\omega}\right) t + \frac{A}{\omega^2} \sin \omega t \right] \tag{22}$$

The solution of Eq. 22, for the same initial conditions as before (i.e., for $t = 0$, $y = y_0$, and $dy/dt = V$), is

$$y - y_0 = \left(V - \frac{A}{\omega}\right) t - \frac{A}{p^2 - \omega^2} \left(\frac{\omega}{p} \sin pt - \frac{p^2}{\omega^2} \sin \omega t\right) \tag{9}$$

The stretch of the harness is

$$S = -\frac{A}{p^2 - \omega^2} \left(\frac{\omega}{p} \sin pt - \sin \omega t\right) \tag{10}$$

and the magnification factor is

$$\frac{p^2 S}{A} = -\frac{p^2}{p^2 - \omega^2} \left(\frac{\omega}{p} \sin pt - \sin \omega t\right) \tag{11}$$

in which A is the maximum deceleration of the car.

After the car has stopped (i.e., for $t > \tau$, when $\tau = \pi/\omega$, the passenger may still be moving forward, and his deceleration may still go on increasing for some time. The analysis given in the preceding section again applies as given in Eq. 19.

In this case, from Eq. 9, by differentiation, and Eq. 10, for $t = \tau = \pi/\omega$.

$$V_\tau = -\frac{A}{p^2 - \omega^2} \left(1 + \cos \frac{p\pi}{\omega}\right) \tag{23}$$

and

$$S_\tau = -\frac{A}{p^2 - \omega^2} \frac{\omega}{p} \sin p \frac{\pi}{\omega} \tag{24}$$

Substituting in Eq. 19,

$$S_{max} = \frac{A\omega}{p\,(p^2 - \omega^2)} \sqrt{2\,(1 + \cos p\tau)} \tag{25}$$

and

$$\frac{p^2 S_{max}}{A} = \frac{p\,\omega}{p^2 - \omega^2} \sqrt{2\,(1 + \cos p\tau)} \tag{26}$$